

2023

MSc. Thesis



Kefu Shen
TU Delft
11/20/2023

MSc Thesis

3D Fiber Reinforced Concrete Printing of Houses in Wujiazhuang, China

By

Kefu Shen

To obtain the degree of Master of Science
In Civil engineering, track Building Engineering
at the Delft University of Technology,
to be defended publicly on November 30, 2023 at 13:30

Student Number: 5296099

Thesis Committee: **Ass. Prof. Dr. (Mariana) M.A. Popescu**
Dr.ir.H.R. (Roel)Schipper
Ass. Prof. Dr. B. (Branko) Šavija



Preface

Starting my master's program at TU Delft has been an amazing experience, and looking back on it now, I still feel that time has flown by and I have a lot of feelings. In the first year of my master's program, I first learned about the application of 3D printing in building construction and felt that this technology was very innovative and had good prospects for the future, so I prioritized this direction in my graduation project, and ultimately, I gained more knowledge and mastered more research methodology and logic of thinking through this research.

In general, this research was not particularly smooth, especially in the absence of relevant tutorials and most of the research work was done in software. However, with the help of tutors, classmates, and the software staff, I was able to complete the study. I believe that the difficulties I encountered in this research are not without their significance, as they helped me to develop a positive mindset to think of solutions in the face of difficulties, and to learn from them in order to avoid the same problems in the next time.

I would like to thank the three committee members, namely Ass. Prof. Dr. (Mariana) M.A. Popescu, Dr.ir.H.R. (Roel)Schipper, and Ass. Prof. Dr. B. (Branko) Šavija for their help and guidance in completing this study. I would like to thank Dr. ir. H.R. (Roel) Schipper for his weekly follow up and advice, which was very helpful in finalizing the study. Thanks to DIANA support and Francesco Messali's help in using the software, I was able to get the right analysis method.

I would like to thank my family and friends for their encouragement and companionship during my master's study, which gave me more motivation and confidence to complete my research. The time I spent at TU Delft was wonderful, I gained professional knowledge and experienced more cultures as well as landscapes, which will help me in my future life. After completing my master's degree, I am also confident enough to face the next opportunities and challenges that come my way as I embark on the next step of my career.

Kefu Shen
November 2023

Summary

Nowadays, with the rapid development of 3D printing technology, more and more applications of this technology can be seen in daily life, and architecture is one of the important directions. There are already a lot of creative buildings completed by 3D printing in the world, and many of them have already been put into use. One of the big challenges of this technology is that since the properties of freshly extruded concrete are not high enough, it becomes necessary to use reinforcement strategies to make the concrete meet the requirements of 3D printing. One of the common reinforcement strategies is achieved by adding fibers to the concrete.

In this study, through finite element modeling and analysis of a 3D concrete printed farmhouse located in Wujiazhuang, China, the whole process of 3D printing of the farmhouse, as well as the internal forces of the structure when it enters into use after the printing is completed was analyzed, and the effect of the application of fiber reinforced concrete in the whole process of 3D printing, as well as the optimization strategy was shown in detail.

The literature study summarizes the current state of development of additive manufacturing and 3D printing, as well as the different types classified through the process; introduces FEM and describes its application in 3D printing; describes the process of making fiber reinforced concrete and its advantages over the material properties of normal concrete; reveals the changes in material properties of materials used for 3D printing in the early stages; and describes the field situation of the Wujiazhuang farmhouse and the printing process.

The deformation and stress distribution of the whole structure under the use state had been analyzed by linear static analysis in finite element software, and the material distribution of the structure had been preliminarily determined. After that, the whole printing process of the structure was analyzed by stage and structural nonlinear analysis, and the key issues such as how to simulate the truss structure wall and what parameters will affect the number of printable layers of the structure were analyzed by building multiple models. Finally, the material distribution and printing solution of the structure were given.

The results given were further modified by continuing to reduce the deformation of the structure to meet the code requirements for the displacement of the formwork structure. Several methods were given to minimize the deformation to meet the code requirements from two different perspectives: the geometry of the structure and the material properties.

The reliability of the modeling in this study and the accuracy of the results were verified by using finite element software modeling to analyze a 3D printing model from a paper and comparing the results. The conclusions of this study and the possible applications of the conclusions in 3D printing were finally given, as well as possible directions for future follow-up research.

Contents

Preface	i
Summary	iii
1 Introduction	1
1.1 Typical projects	1
1.2 Challenge	3
2 State of the Art	7
2.1 Introduction	7
2.2 Additive Manufacturing and 3DCP	8
2.3 FEM	13
2.4 Fiber Reinforcement Concrete	15
2.5 Early age and hardening behavior of 3DCP	21
2.6 Information about the 3D Printed Building in Wujiazhuang	26
3 Research Design	33
3.1 Problem Statement	33
3.2 Research Objective	33
3.3 Research Question	34
3.4 Methodology	34
3.4.1 Literature study	34
3.4.2 Simplification and model set-up	34
3.4.3 Construction process optimization	35
4 Validation	37
5 Numerical Modelling	43
5.1 Introduction	43
5.2 Analysis of the entire structure during the use phase	45
5.3 Nonlinear Analysis During the Structural Printing Phase	50
5.3.1 Parameter study	54
5.3.2 Wall structure tests	60
5.4 Analysis of the printing process from layer 1 to layer 20	64
5.5 Analysis of the printing process from layer 21 to layer 30	69
5.6 Roof printing and connections	76
6 Discussions	79
6.1 Optimization of computational results in Chapter 5	79
6.2 Discussions and reflections	83
7 Conclusions & Recommendations	85
Bibliography	87
Appendix: Python Scripts	91

1 Introduction

In recent years, architectural 3D printing has developed very rapidly. The manufacturing process is constantly evolving and becoming more and more widely used around the world. The principle of 3D printing is the construction of layered structures, in which three-dimensional components are printed from a digital model. This emerging digital fabrication brings more opportunities as well as challenges to the construction industry. The technology is in the early stages of maturity, so there are no standardized procedures available to evaluate.

Currently, there are three types of concrete 3D printers used for construction printing, namely gantry, robotic and crane. Gantry and crane printers have the advantage of being easily scalable in size. In comparison, robots are often fixed in size and difficult to scale, but robots have their own advantages in that speed and degrees of freedom allow them to perform many tasks that a gantry printer may not be able to do. Therefore, if the design of the printed object does not require any complexity, gantry printers may be more suitable than robotic printers because robots are more costly and the payload on the robotic arm is usually lower than that of a gantry printer.

1.1 Typical projects

Project Milestone

The Milestone project consists of a series of five 3D-printed houses in the Netherlands, located in Eindhoven's Meerhoven district, which the Eindhoven Municipality and the Technical University of Eindhoven (TU Eindhoven) expressed an interest in constructing during the Dutch Design Week 2016. The City Hall and Eindhoven University of Technology, as well as several companies (Van Wijnen, Saint-Gobain Weber Beamix, Vesteda, and Witteveen + Bos), entered a partnership to complete the entire project. The first building opened in 2021 and is currently occupied.



Figure 1: Project Milestone's First 3D Printed House (Ranjit, 2022)

As shown in the figure above, the first building of the Milestone project is a single-story dwelling with an area of approximately 100 square meters. For the structural aspect of the building, the area is enclosed by multiple 3D printed concrete wall elements that are curved in-plane and out-of-plane and are all used for load-bearing purposes, so that traditional steel-reinforced poured concrete is not used internally.

For the material side of the building, a model of the project Milestone was printed using a commercially available 3D printed mortar (Weber 3D 145-2). The mortar consists of Portland cement (CEM I 52.5 R), siliceous aggregate with a maximum particle size of 1 mm, limestone filler, additives, rheology modifiers and a small amount of short polypropylene (PP) fibers to control plastic shrinkage (Wolfs et al., 2023).

Tecla in Italy

Tecla is an innovative 3D printed home building, developed by Massimo Moretti in collaboration with WASP, that draws inspiration from ceramic bees, printed in 2020. The house consists of two modules up to 4.2 m high, with an area of approximately 60 m³, and was constructed in 200 hours of printing time. The project is characterized by the use of locally sourced natural materials and is as eco-friendly as possible.



Figure 2: Aerial view of Tecla house (Corazza, 2021)

For materials, it consists of local soil with water, rice husk fibers and binders. The thermal insulation filling material consists of rice husk and straw from rice cultivation waste. The composition of the mixture and the filling of the walls were optimized according to the local climate. The early stages of construction are the excavation and mixing phase, in which the

excavator digs up the local soil, which is then analyzed and mixed with water and additives.

The world's longest 3d printed bridge

The world's longest and largest concrete 3D bicycle bridge, with a length of 29 meters, was printed layer by layer in a concrete printing factory and realized by the architectural group BAM. The complete freedom of the architects, who were not limited by materials or traditional processes such as concrete formwork, was a novelty of the project.

The project used parametric design with the aim of giving the bridge more freedom in its geometry. Once printed at the factory, each section was moved to the site and then assembled for pre-stressing for the 8 September 2021 inauguration.



Figure 3: The 3D-printed concrete bicycle bridge in Nijmegen. (Municipality of Nijmegen, 2021)

1.2 Challenge

The material used mostly for architectural 3D printing is concrete (3DCP), as concrete (or mortar) has fresh properties that make it very suitable for extrusion through a nozzle, controlled by a printing robot. In construction industry, several examples of how 3DCP can be applied to realize full-scale buildings, building components or bridges have already been demonstrated over the past years. However, much of this work has a highly experimental character, are demonstrators of academic efforts, or have a limited scale. Challenges that are addressed by the scientific community are (among others):

1. the accurate strength and safety prediction of the printed buildings, in a way that is comparable to the way this is done for regular concrete by the use of building codes,
2. the robotic production process, where preliminary failure of printed concrete before hardening can occur due to stability loss or compressive failure,
3. the geometric limitations and opportunities of robotic printing, which are very different from a more traditional concrete construction process,
4. the process from design to production, which is very different from the conventional

- design process for reinforced concrete,
5. the influence on detailing and connections.

This thesis will mainly focus on the first and second challenge, and at some points also address the other three challenges.

It is commonly acknowledged that concrete has lower tensile strength than compressive strength, which is problematic for most structural applications. In regular (cast) concrete, this is solved by the inclusion of reinforcement steel, pre- or post-tensioning steel, or the addition of steel or plastic fibers to the fresh mixture. It is not straightforward to translate these conventional strengthening methods to 3DCP. Therefore, one of the challenges, already addressed by many other researchers, is the reinforcement strategy most suitable for the 3D printing construction process. Several reinforcement strategies have been proposed in recent years, and one of them is fiber reinforced concrete. Short fibers are added to the concrete matrix providing post-cracking tensile and stress-bridging capacity across the cracks (Regli et al., 2016). However, because of the layering technology inherent to 3DCP (and to AM in general), it is obvious that the improved tensile strength by adding fibers is not necessarily beneficial in the direction perpendicular to the interfaces between layers. The interface strength is lower, as extruded fibers do not bridge the interface, but are only improving the properties within the filament extrusion dimensions. This would potentially lead to structural problems in the end, as inhomogeneity in material characteristics can lead to failure on weak spots. This could already occur during printing, as well as after hardening, after applying dead and live loads on the structure, or as a result of shrinkage or other effects that lead to tensile stresses.

Apart from the use of a robotic arm and the layered application of concrete, the further construction process is also an important factor. Different construction strategies will have influence on the distribution of stresses in the component, for example, the introduction of a crane to lift and move 3D-printed objects during construction also temporarily increases the load at specific locations of those components, which should also be taken into account. As explained before, in those positions of the structure where tensile stresses are expected, it can be beneficial to use fiber reinforced concrete.

This study will investigate whether the stresses in and deformations of a 3D-printed object can be calculated for a number of crucial stages in the construction process, starting with printing, but also including the effects of dead and live loads after hardening, and taking into account the material properties of concrete with or without fibers. The study aims to provide a better understanding of where in the structure the improved material properties by addition of fibers are necessary, and where these improved properties are not strictly needed, for example no tensile stresses are to be expected in any of the construction or life-cycle stages.

To this end, this study will investigate in detail the case of a real 3D printed building in China. The building is located in Wujiazhuang, it was completed in 2021 and already occupied. The building was designed and printed on site by a team led by Professor Xu from the faculty of Architecture at Tsinghua University. This building is a brand-new attempt to 3D print homes in

China and is therefore of great significance.

By using the Finite Element Method (FEM) to determine the internal force distribution of the building in various stages, under the premise of a given printing path and comprehensively considering the impact of possible construction processes during the construction process, the optimal solution for the construction is finally determined.

2 State of the Art

2.1 Introduction

In the following I will describe which aspects of the current state of research I will refer to and the role that these aspects have had on this study as well as their impact.

The first is an introduction to additive manufacturing as well as 3D concrete printing, which has been developing rapidly in recent years and is gradually finding applications in building fabrication. This thesis will briefly introduce the different types and methods of additive manufacturing and apply them to the case study that will be analyzed in this study.

This is followed by the current state of research in FEM and its integration with building construction, especially with the 3D printed building construction process. Due to the current lack of standards and criteria to judge 3D printing technology, FEM has become one of the most important methods to judge the performance of 3D concrete-printed buildings. A brief introduction of FEM and its connection to 3D fiber reinforced concrete printing will be given. I will also describe the FEM software DIANA used in this study and explain the basis for the selection of the software.

Then there is the important factor that is integral to 3D printed buildings, which is the material. The properties of the material will have a decisive impact on whether the 3D printing can be completed and how the printed building will perform. Therefore, different relevant literature will be extracted and different material ratios and their effects on material properties will be investigated. In this context the focus will be on material properties that have a significant impact on 3D printing, such as extrudability and printability.

This is followed by an introduction to the mechanical properties of 3DCP in the early stages as well as after hardening. It is also important to understand the trends in material properties as time increases and the effects that different material ratios can have. And the most common ways in which structures fail during 3D printing and the mechanisms will also be explained. This is also a key factor to focus on during the subsequent FEM analysis, as the causes of structural failure must be understood before the structure can be adjusted and re-analyzed in a targeted manner.

Finally, there is a brief description of the Wujiazhuang site case, which will be analyzed in this study. This section contains the local climatic conditions, the type of buildings and structures, the site construction layout, and the construction methods, some of which will also be used in the finite element analysis, and some of which will be changed or simplified.

2.2 Additive Manufacturing and 3DCP

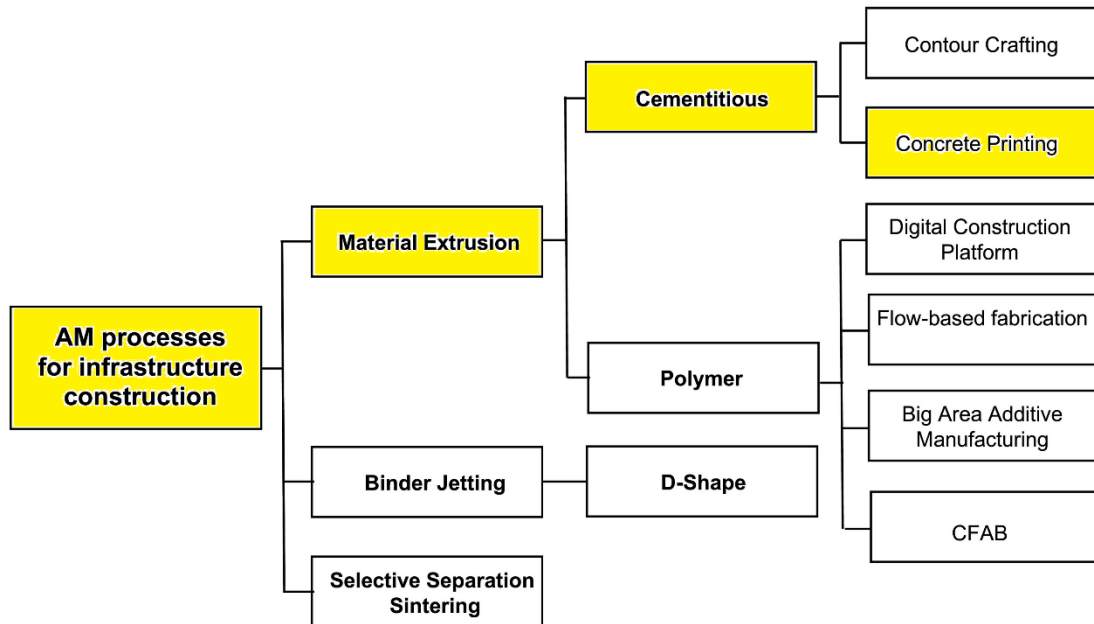


Figure 4: A process classification framework for architectural AM processes (Buswell et al., 2020)

The figure above shows the different fabrication processes for additive manufacturing, which mainly include material extrusion, binder jetting, and selective separation sintering. The most common of these is material extrusion, which can be divided into cementitious and polymer materials. The category to be used in this study is the one marked in the yellow box, i.e., concrete printing. The materials used in the studied cases are normal concrete as well as fiber reinforced concrete, both in extruded form.

One of the most important changes of additive manufacturing (AM) compared to conventional manufacturing, is that it explicitly identifies manufacturing as a computational process that allows manufacturing artifacts of unprecedented complexity but does not tolerate ambiguities in assumed models and representations (Regli et al., 2016).

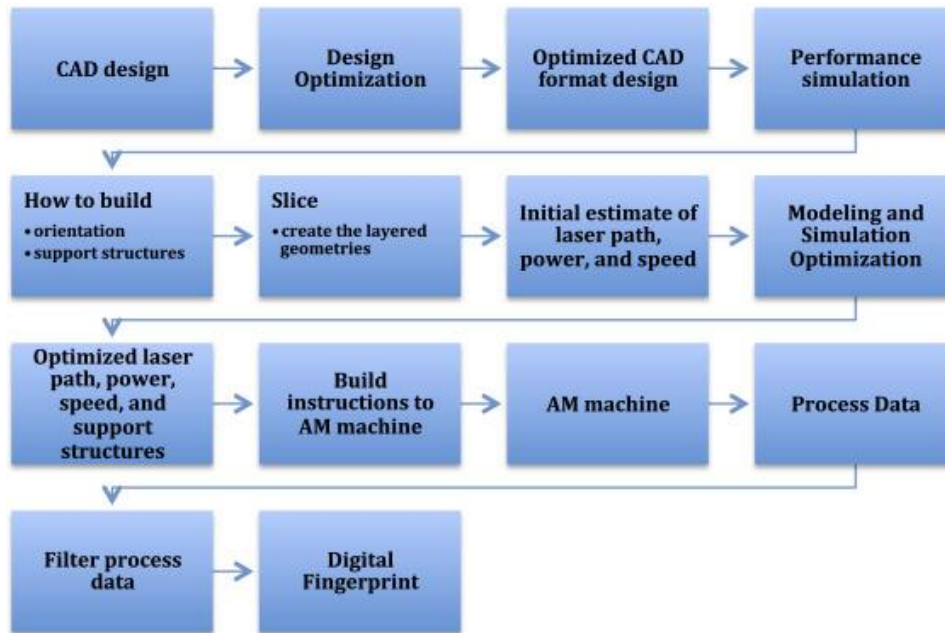


Figure 5: The path from designed model to manufacturing (Regli et al., 2016)

Figure 5 above shows a typical path of AM from design to production. The first step is the CAD design, which includes the preliminary design of the building geometry as well as the internal structure, and optimization based on the test performance to obtain the design in CAD optimized format. After entering the printing process, the first step is to set up the temporary or permanent supports that may be needed as well as the direction of the print, followed by the characteristics of 3D printing, i.e., layering, and the initial estimation of a number of print-related parameters, such as the print speed and printhead-related attributes, followed by a finite element analysis of the printing process, in which the parameters need to be adjusted continuously in accordance with the stage-by-stage results of the analysis in order to ensure the accuracy and reliability of the print. The optimized structure and the various printing parameters are then fed into the AM machine, where the data is processed and filtered for final printing.

This study will also be based on the above process. It can be seen that the most challenging part of the above process is the finite element analysis of the structural printing process, as it requires constant adjustment of various parameters and multiple analyses to obtain an optimized structure and parameters.

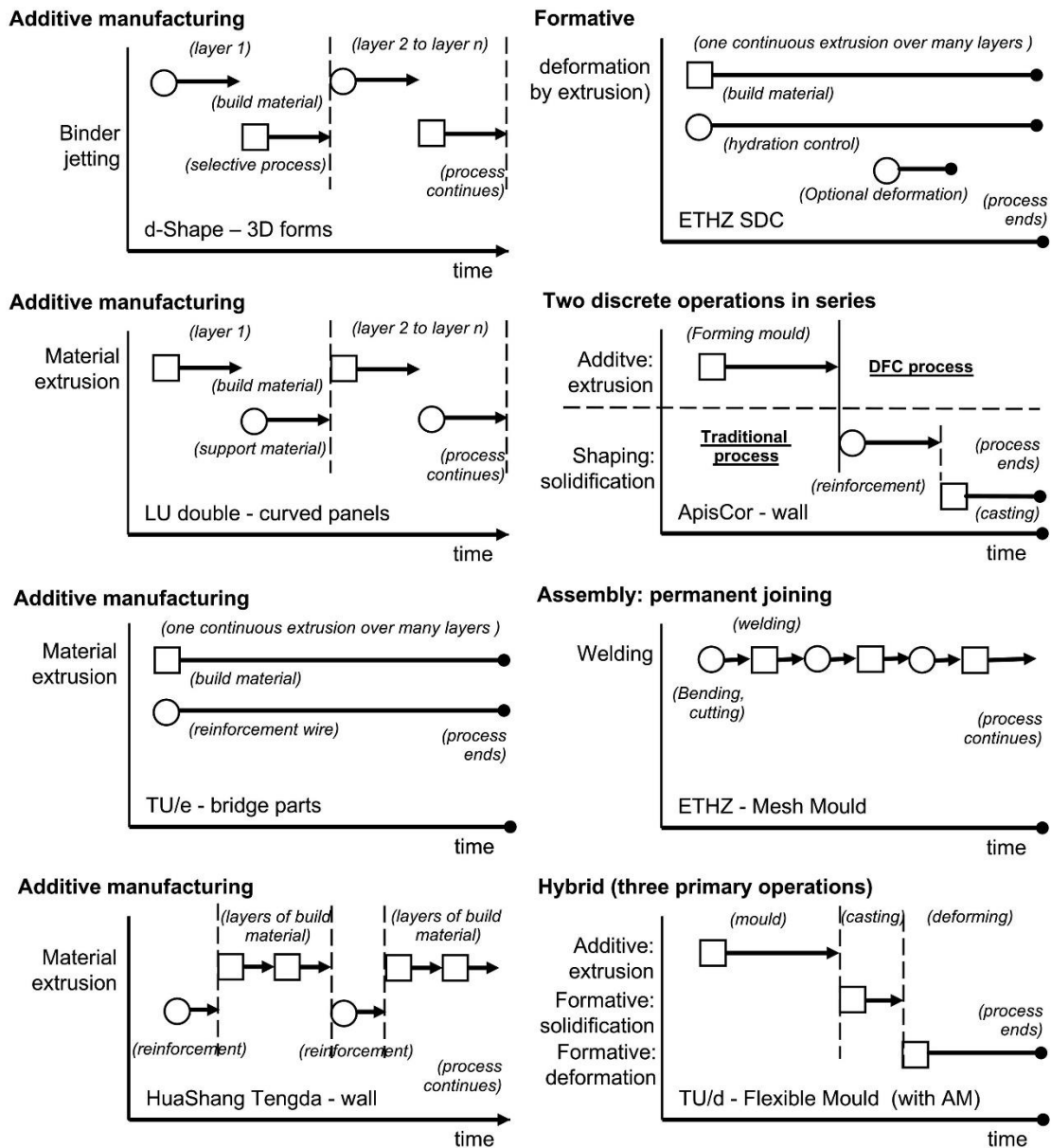


Figure 6: Flowcharts of eight different projects illustrating the interaction of primary operations (denoted by squares) and sub-processes (denoted by circles) in time (Buswell et al., 2020)

The figure above reveals the temporal interactions of the main operations and sub-processes in the different process flows by showing the DFC flows for eight different projects around the world, which also include processes such as the addition of temporary supports. The eight projects are divided into material extrusion, binder jetting, additive extrusion, and hybrid of several types.

For the cases used in this study, the best fit with the eight flowcharts above is the third and fourth in the left column, which are the TU/e bridge project and the Huashang Tengda project. The basic printing process for the case used in this study is that the two printers print the structural walls uninterruptedly, and when printing areas that need to be reinforced with fiber reinforced concrete, the nozzles of the printers extrude a different material, i.e., fiber reinforced concrete., thus allowing the structural weaknesses analyzed in the previous phase to be

strengthened.

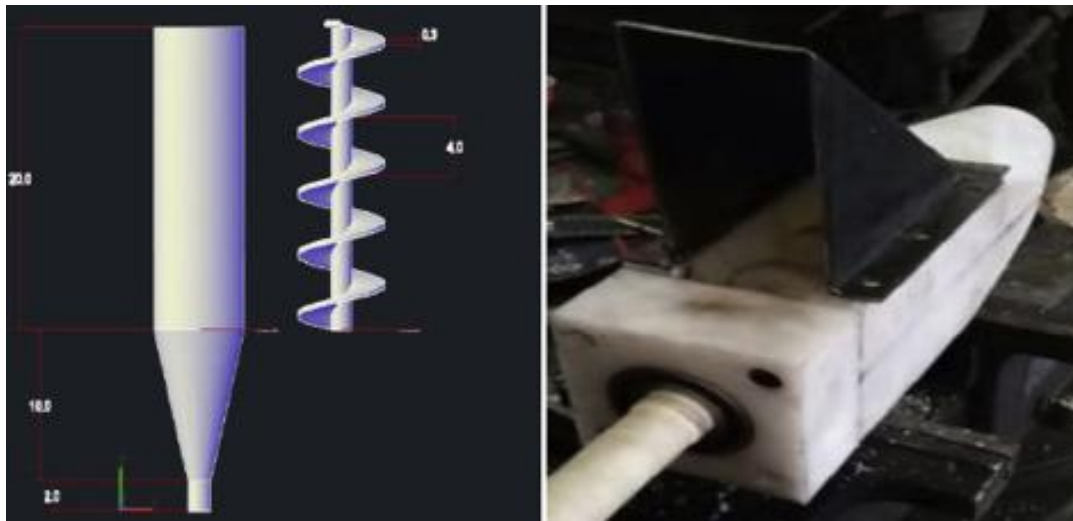


Figure 7: A CAD representation of the screw and the nozzle and the fabricated nozzle (Zeina et al., 2019)

In the 3D printing process, not only the material parameters of the concrete are very important, but also the design of the nozzle should not be neglected. Zeina et al (2019) tested different nozzle diameters and found that the concrete mix ratio as well as the material properties also had a strong relationship with the nozzle diameter. A balanced relationship must be maintained between the speed of the machine and the extrusion rate of the concrete mix from the nozzle tip. Otherwise, the printing resolution would be greatly impacted; if the linear horizontal speed is larger than the extrusion rate, the extruded filaments would be too thin and might even exhibit some ruptures. On the other hand, if the printing rate is too slow, more material than what is necessary would be deposited resulting in thick concrete layers. Zeina got into an optimum mix that was suitable for 3D printing for the given scale. This mix consisted of 125 g of cement, 80 g sand, and 160 g fine aggregates with a w/c ratio of 0.39. In addition, the mix included 1 mL of accelerator and 0.625 mL of retarder.

Xu et al (2019) focused on and developed nozzle design, where he developed a variable size nozzle type by studying four key process parameters including nozzle size, nozzle travel speed, material extrusion rate, and tool path radius of curvature.

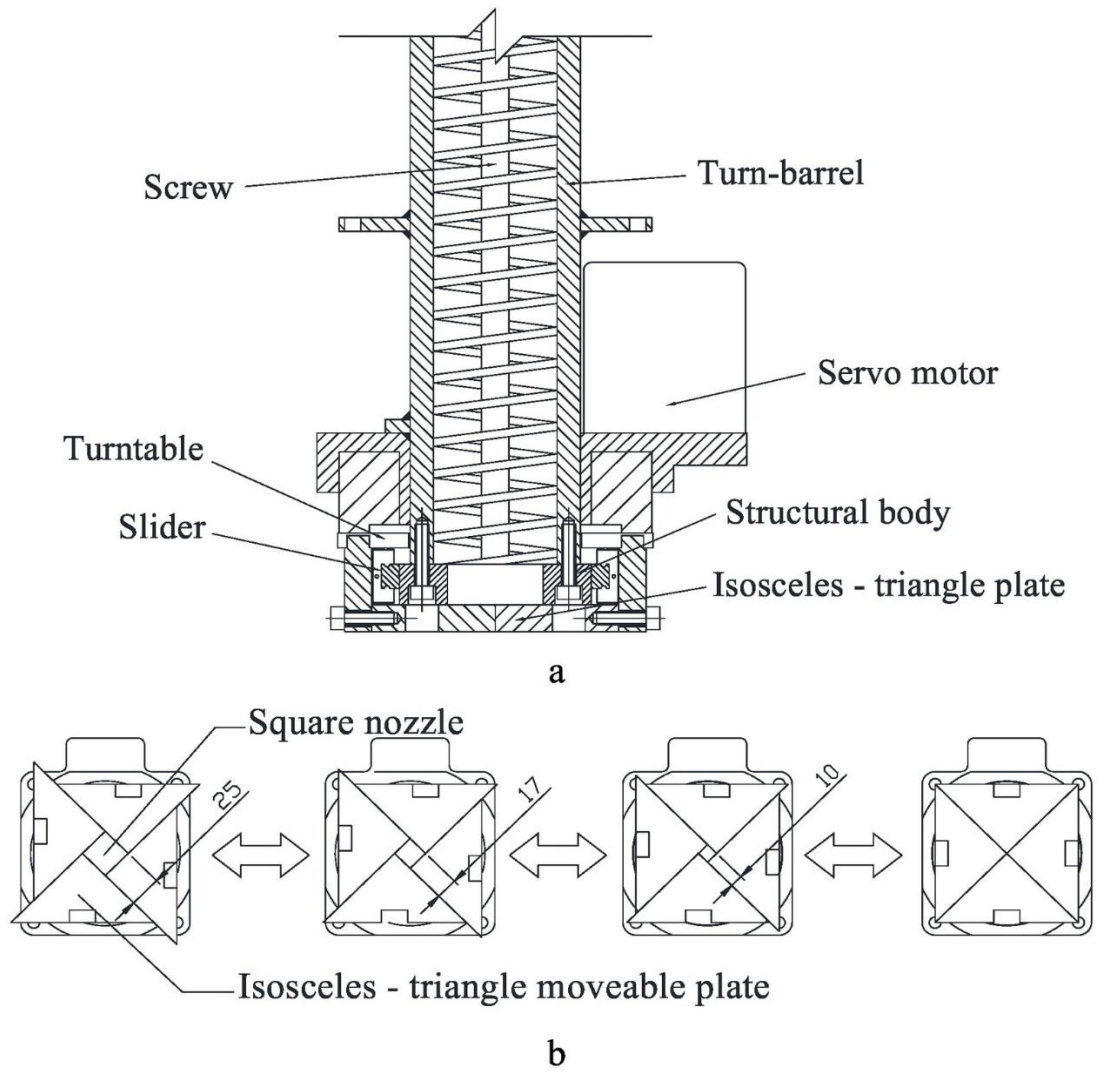


Figure 8: Design of the nozzle - varying module, (a) Vertical section; (b) Bottom view of the variable - size square nozzle. (Xu et al., 2019)

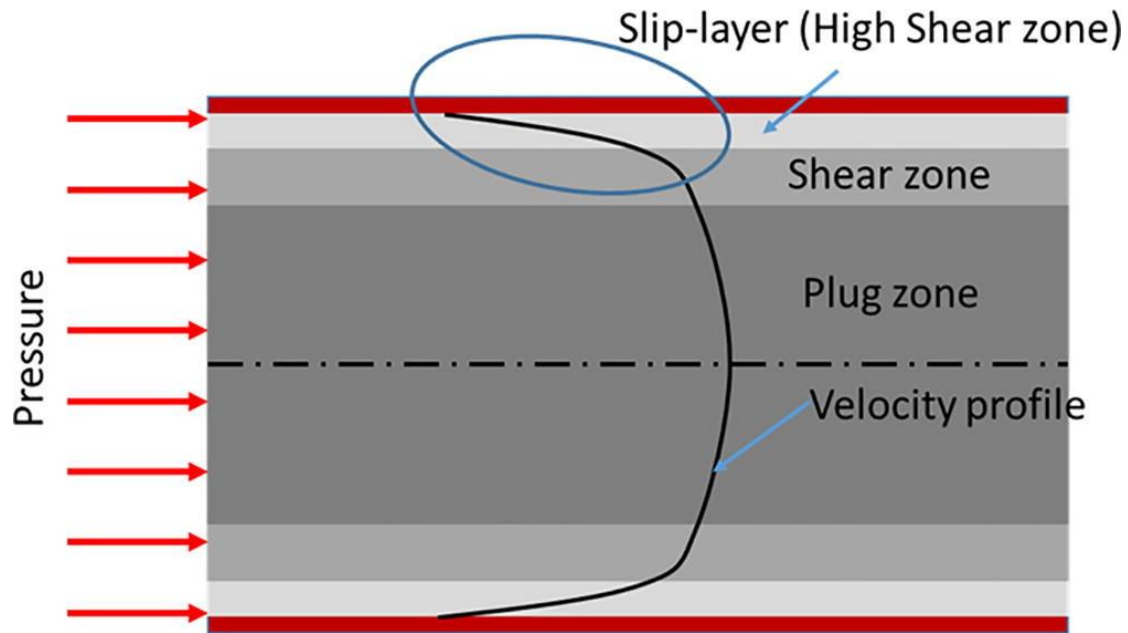


Figure 9: Distribution of velocity along the cross-section of the pipe (Khan, 2020)

Khan (2020) proposed the formation of lubrication layer during concrete pumping. Most of the velocity is developed in the lubrication layer which is seen near the wall. However, the uncontrolled segregation may lead to poor quality of the mix extruded as filament. This may influence the hardened properties of the printed specimen. As the lubrication layer will contain mostly paste, it could lead to formation of shrinkage cracks, reducing the durability of the printed concrete.

2.3 FEM

FEM is the use of mathematical approximations to simulate real physical systems (geometry and loading conditions). Finite element analysis is the substitution of simpler problems for complex ones before solving them. It views the solution domain as consisting of several small interconnected sub-domains called finite elements, assumes a suitable approximate solution for each element, and then deduces a solution to the problem by solving for the domain's total satisfaction condition. Because the actual problem is replaced by a simpler one, this solution is not an exact solution, but an approximate one. Since most practical problems are difficult to obtain the exact solution, and finite elements not only high computational accuracy, but also can adapt to a variety of complex shapes, and thus become a well-established means of engineering analysis.

In the terms of 3DCP, FEM is usually used to analyze the internal stresses of the object and it can make predictions if there will be possible failures during the printing process or after

hardening. Research done by Wolfs and Suiker (2019) proved that the parametric model provides a useful research and design tool for the prediction of structural failure during extrusion-based 3D printing. The model can be applied to explore the influence of the individual printing process parameters quickly and systematically on the failure response of 3D-printed walls, which can be translated to directives regarding the optimization of material usage and printing time.

FEM has also been applied in analyzing the aspect of fiber reinforced concrete. Majko et al (2019) carried out an assessment of different options available for creating long fiber composite models for 3D printing. The analysis is done through a finite element analysis software ADINA, the main objective is to analyze the geometrical constraints added to the structure by the long fibers and the role of the fibers in the structure subjected to load type, during the modeling process, the presence of the fibers is simulated by using reinforcing bars instead. These models were reinforced using long aramid, carbon, and glass fibers. The goal was to analyze geometry constraints of fiber addition into the structure. Three different situations were taken into consideration. The first case uses axisymmetric 2D elements and axisymmetric truss elements. The second case is modelling of reinforced composite with 3D truss elements and planar 2D solid elements. The last case uses 3D truss elements and 3D solid elements.

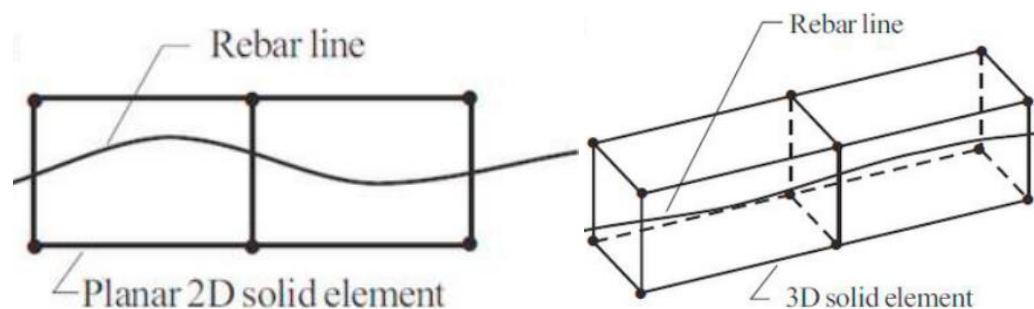


Figure 10: a) Rebar in axisymmetric truss; b) Rebar in 3D truss (Majko et al., 2019)

During the finite element analysis, the fundamental structural principles on which digitally fabricated elements are based do not differ from those of conventional cast or pre-cast RC structures. However, it is necessary to consider that models may need to be adjusted because of the difference in the construction process and its influence on the material properties. Some of the differences include:

1. Reduced bond strength between layers.
2. Anisotropy.
3. Printing path and sequence.
4. Concrete interaction with fibers.

It is used in the previous software simulation that rebars could replace the fibers in the calculation and analysis. From a practical point of view, it could be interesting to understand if

the pre-existing models, developed for the calculation of the bearing capacity of traditional RC elements, would be able to give reliable responses also for elements manufactured with digital fabrication construction techniques. In this regard, to determine the capacity of a structural element, it is first necessary to verify if the hypotheses of available models, are valid also in the case of digitally fabricated elements. For the evaluation of the ultimate moment capacity of reinforced or pre-stressed concrete cross-sections, the following assumptions are considered:

1. Plane sections remain plane.
2. Strain in bonded reinforcement or bonded pre-stressing tendons is the same as that in the surrounding concrete.
3. The tensile strength of the concrete is ignored.
4. Stresses in the concrete in compression are derived from the design stress/strain relationship given in Eurocode 2.
5. Stresses in the reinforcing or pre-stressing steel are derived from the design curves in Eurocode 2.
6. Initial strain in pre-stressing tendons is considered when assessing the stresses in the tendons.

In this study, FEM software will be applied to simulate the building performance, it still needed to be analyzed if the assumptions before are still applicable in certain situations. On the choice of finite element analysis software, the more popular software are Abaqus, ANSYS, Diana and so on. I finally chose to use Diana to complete the whole case analysis and optimization process. The main reason for this is that Diana is relatively easy to use and is more commonly used in the Netherlands, which makes it easier to seek help when encountering problems or issues, such as Diana support or experts within the faculty. There is also a course on the subject, which makes it less difficult to learn on my own.

The functionality of Diana is well defined, and in the case analyzed in this study, the more challenging parts are the structural slicing, the simulation of structural objects geometries, and the nonlinear analysis with the addition of a time parameter. Diana is powerful enough in all three parts to perform the required analyses well.

2.4 Fiber Reinforcement Concrete

As mentioned in the introduction, fibers could be added to the concrete in order to increase the strength so that the component could bear the local tensile stress during the transport or construction process. There are mainly two types of manufacturing method, one of them is extrusion and another is spraying. We will focus on extrusion printing in this thesis.

While extrusion is applied, short fibers added to the concrete matrix could provide post-cracking tensile and stress-bridging capacity across the cracks. This solution provides strong fiber alignment in the printing direction, which could increase the fiber reinforcement effectiveness. For spraying, either short pumpable fibers or longer ones can be added and sprayed together

with the concrete (RILEM, 2021). The difference between the two methods is not only the length of the fibers, but also the degree of controllability. When spraying is applied, fiber alignment is less controllable than when applied with extrusion production. However, spraying is possible to provide fiber reinforcement in any direction of the structural element.



Figure 11: Fiber reinforced concrete after testing (Ataalla, 2018)

In the concept and design of the fiber reinforced concrete, both the compatibility of the fibers with the printing equipment in terms of size and stiffness and the influence of the fibers on the rheology of the concrete should be considered. So sometimes it is necessary to check the maximum number of fibers that can be added without losing printability.

An example that can illustrate the effect of adding fibers on concrete performance is an experiment done by Soltan and Li (2018). They consider printability as the combination of extrudability (the ability of the mixture to pass through a printing system) and buildability (the ability of a mixture to remain stable after deposition and during printing). They tested a total of five mixtures, all of which contained 2% polyvinyl alcohol (PVA) fibers by volume and differed only in the ratio of cement to fly ash or in the amount of water; the fourth mixture, which had the best all-around performance, was chosen as an example. They compared the structural mechanical properties of the samples produced by the two processes, both of which were made of identical materials (both fourth mixture), the first one with fibers oriented along the loading axis and 3D printed, and the second one cast. The figures below compare the tensile strength and strain capacity of the two samples.

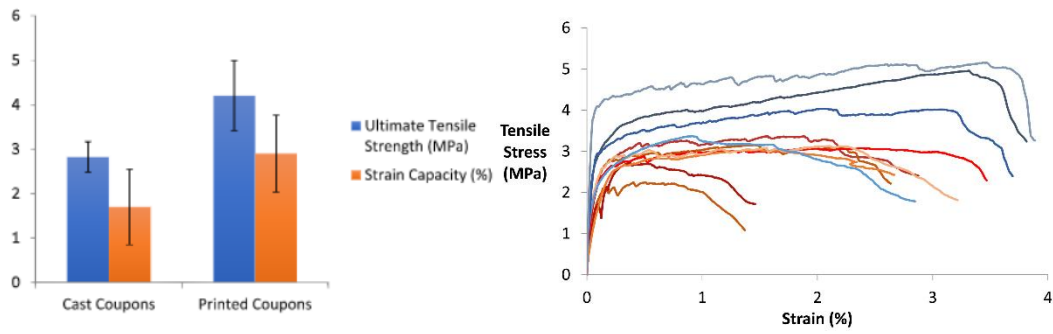


Figure 12: The comparison of tensile strength and strain capacity, blue curves represent printed samples, red curves represent casted samples (Soltan & Li, 2018)

It can be seen that the samples fabricated by printing have higher ultimate tensile strength as well as strain capacity than the casted samples, probably due to the higher degree of alignment of fibers in the tensile direction, which withstands higher tensile forces.

This experiment also gives the indication that it is possible that adding fibers could be a solution during construction phase, and that the effect of fibers in printed concrete can even be higher than in cast concrete. Fibers could be added to the printed mixture while passing points on the printing path where the expected stresses significantly increase. Subsequent analysis should also be taken to prove if it is enough by only adding fibers.

The benefits of fibers mainly arise after cracking and the material behavior is usually translated by a tensile stress to crack opening or to strain. This will depend on multiple variables, such as fiber type, geometry and content, fiber matrix bond strength and fiber distribution and orientation, in particular the fiber's orientation regarding an active crack plane.

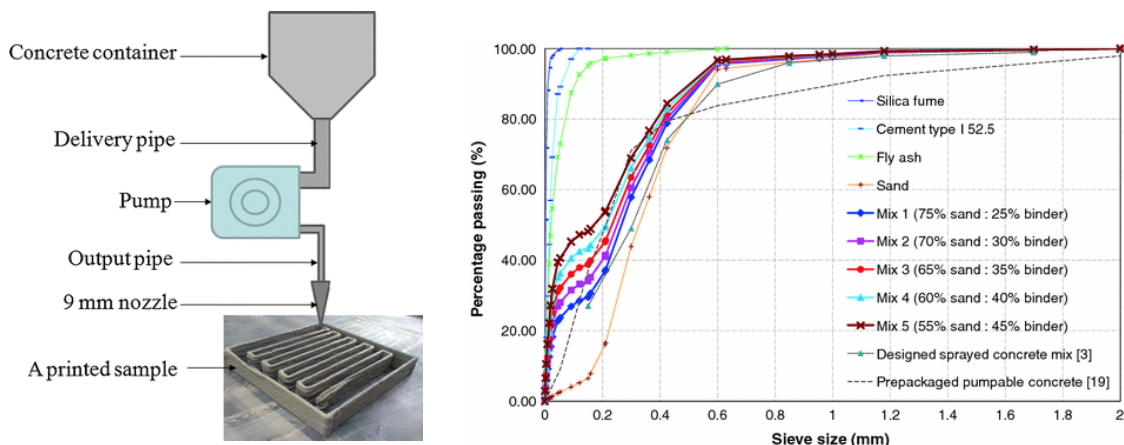


Figure 13: a) 3D printing process concrete delivery system; b) Percentage passing for different sand/binder proportions (Le et al., 2012)

The above figure illustrates the transportation of concrete in the 3D printing process. Le et al (2012) tested the best concrete ratio using a nozzle with a size of 9mm as shown above, with the main purpose of satisfying the extrudability as well as the printability of the concrete. Le found through tests that the fourth type of 3D printed concrete has the best extrudability. He then used this proportioned mixture to test important metrics such as compatibility. The extrudability tests showed that Mix 4 (water–binder ratio of 0.26) was best suited to printing freeform components, which had a 60:40 sand/binder ratio, comprising 70% cement, 20% fly ash and 10% silica fume, plus 1.2 kg/m³ micro polypropylene fibers. This mix also needed 1% superplasticizer and 0.5% retarder to attain an optimum workability of 0.55 kPa shear strength, an optimum open time of up to 100 min and the ability to build many layers with various filament groups.

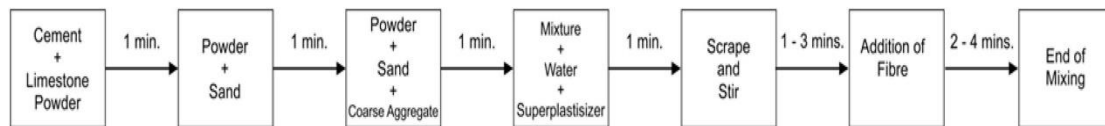


Figure 14: Process of adding fibers to concrete (Awolusi et al., 2019)

A 20-L capacity Hobart planetary mixer was used. The dry materials (binder and sands) were first mixed for 5 min. Approximately three quarters of the water was then added to the mixture and mixed for 5 min. At this point, HRWRA was mixed with the rest of the water and slowly added to the mixture. The mixing was carried on for another 9 min until a good rheology was achieved for facilitating homogeneous fibers dispersion. Then, the steel fibers were gradually added and mixed for 10 min. Finally, the VMA was added and mixed until a printable consistency was achieved. The mixing time was approximately 30 min. Visual assessment by the authors confirmed the absence of fiber segregation in the fresh mixture.

Table 1: Characteristics of PVA fibers (Sun et al., 2022)

Length (mm)	Diameter (µm)	Tensile strength (MPa)	Elongation (%)	Elastic modulus (GPa)	Density (g·cm ⁻³)
9	31	1600	7	43	1.3

Table 2: Comparison of common concrete and 3D printed concrete (Sun et al., 2022)

	Common concrete	3D-printed concrete
2-h compressive strength	–	15–28 MPa [3]
1-day compressive strength	–	35–47 MPa [3]
Coarse aggregate	4.75–90 mm [6]	NA
Fluidity	100–220 mm [7]	170–190 mm [8]
Thixotropy	NA	With
Initial setting time	2–3 h	10–100 min [8], [9]
Final setting time	10–24 h [10]	60–180 min

Sun et al (2022) experimentally tested the mechanical properties of 3D printed concrete incorporating PVA fibers. In addition to cement, cementitious materials and aggregates, retarders were added to the material to regulate the setting time, as well as superplasticizer to improve the flow of the concrete.

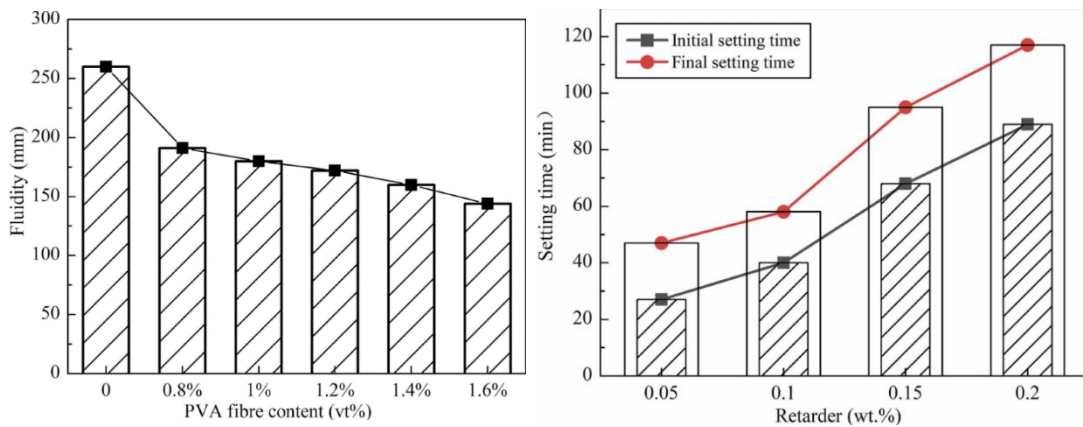


Figure 15: a) Effects of PVA fibers on mixture fluidity; b) Effect of retarder on mixture setting time (Sun et al., 2022)

Asakawa et al (2022) found that printed components using AM-based 3DCP systems inevitably contain discontinuous interlayers, such as cold joints in concrete structures. The presence of such defects can lead to strength degradation in the printed structure. Furthermore, the introduction of steel reinforcement as a general reinforced concrete structure in AM-based 3DCP systems is challenging. Therefore, they developed an automatic metal fiber sandwich reinforcement system for AM-based base compression structures. A prototype of the automatic metal fiber implantation system was built. Specimens were obtained and mechanical tests were carried out to confirm the reinforcing effect of the metal fibers. The reinforcement of the metal

fibers was also used to improve the mechanical properties of the printed specimens.

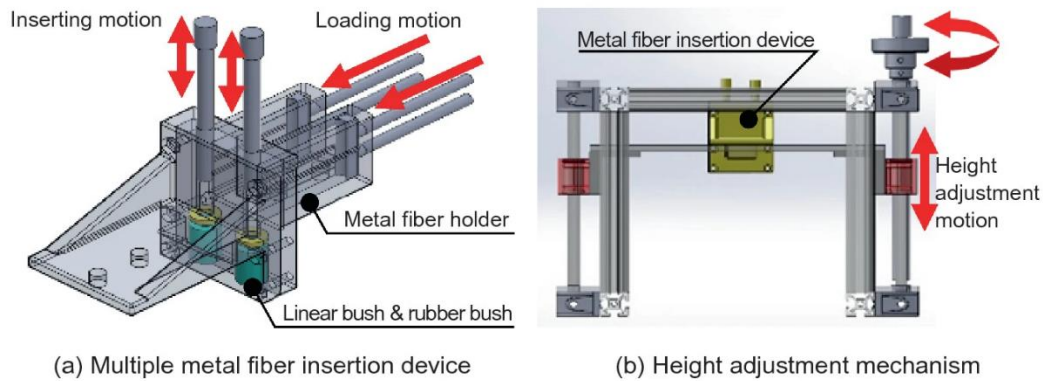


Figure 16: Multiple metal fiber insertion device (Asakawa et al., 2022)

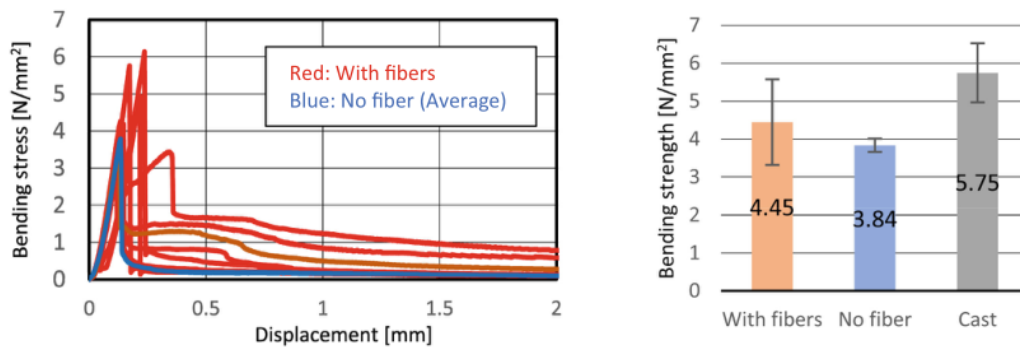


Figure 17: The bending test results (Left) and the average bending strength (Right) (Asakawa et al., 2022)

From the above figure, it can be seen that the insertion of metal fibers using the proposed insertion device helps to increase the bending strength, but the reinforcement effect is limited. The probable reason for this is that only a minimum amount of simple metal fibers were applied, and due to the limited amount of reinforcement, their strength is less than that of the cast samples.

Arunothayan et al (2021) introduced a new type of printing material, which is UHPFRC (Ultra High-Performance Fiber Reinforced Concrete). They investigated the effect of three key factors, fiber volume fraction, nozzle size, and printing speed, on the frequency of fiber orientation angle. There are three meaningful conclusions: The fiber orientation distribution in the printed UHPFRC specimens is identical for different Cartesian print speeds; In printed filaments, fibers closer to the nozzle walls aligned more towards the printing direction than the fibers close to the center of the nozzle. This difference in alignment was significant in larger nozzles, which shows the existence of a low-sheared flow at the center of larger nozzles; The preferential alignment of fibers in the printing direction enhanced the flexural performance of the UHPFRC specimens in that direction.

Yang et al (2022) developed a new 3D printed Ultra High-Performance Fiber Reinforced Concrete (3DP-UHPFRC). They mainly tested the effect of adding 1% volume fraction of steel fibers to the mixture on the mechanical properties. The results showed that the elastic modulus of the specimens without steel fibers was slightly lower than that of the specimens with steel fibers, indicating that the addition of steel fibers increased the modulus of elasticity. Moreover, the differences in the elastic modulus of the specimens with different fiber lengths and under different loading conditions were extremely small, indicating that the fiber length and loading method do not have a significant effect on the elastic modulus. They also found that 3DP-UHPFRC prepared with 1 vol% 6 mm steel fibers is more suitable for construction than 3DP-UHPFRC prepared with 1 vol% 10 mm steel fibers, i.e., some aspects of performance will be better.

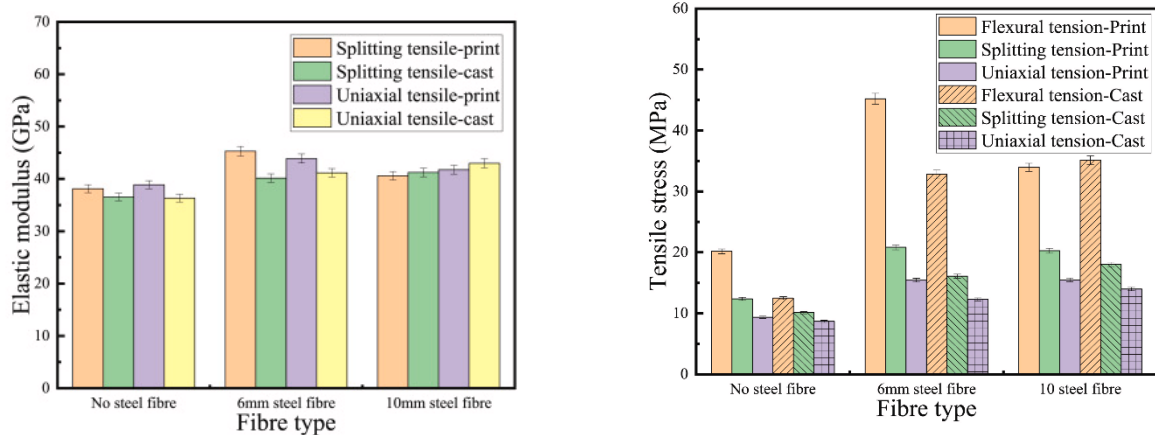


Figure 18: Comparison of the performance of mixtures (no fibers) with mixtures with 6 mm and 10 mm steel fibers added, respectively (Yang et al., 2022)

2.5 Early age and hardening behavior of 3DCP

Wolfs et al (2018) tested how concrete properties change during the 3D printing process (from being pumped out to hardening) and noted that the critical damage layer may not occur in the layer with the highest load-bearing capacity, but rather in the layer with the least stability. In the designed experiments, the changes in each material property of concrete were tested by uniaxial unconfined compression test and direct shear test respectively for a period of 90 minutes starting from the time when concrete was extruded, and concrete specimens were selected at five time points within 90 minutes to perform each of these two tests on the specimens. It can be seen from the figure below that both the unconfined compressive strength and Young's modulus increase with time. The printing process was then simulated using the finite element software Abaqus by printing cylinders and stacking them layer by layer at a given

printing rate and finally analyzing the number of layers that were damaged, while the final cause of damage was basically a combination of instability and material yielding.

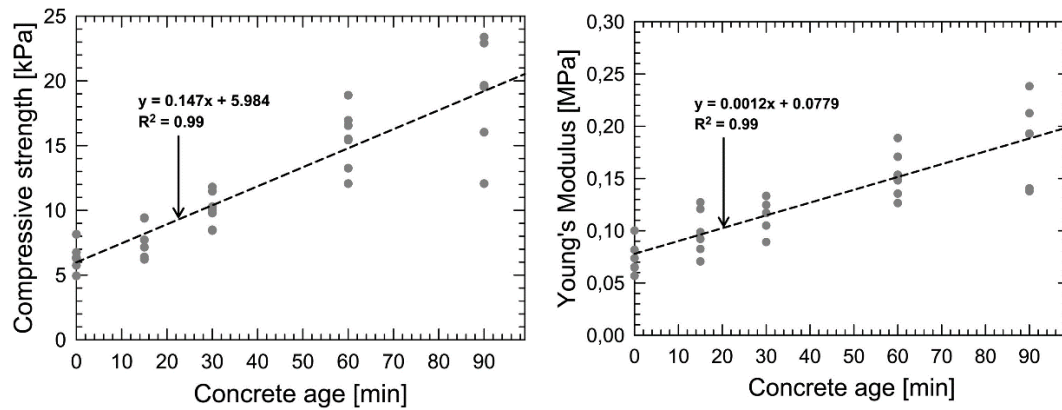


Figure 19: Compression strength development (left) and Young's modulus development (right) from compression testing for up to 90 minutes (Wolfs et al., 2018)

From the above figure, it can be seen that the concrete compressive strength and Young's modulus increase linearly with time from 90 minutes after the extrusion of the material, a linear function will also be used to describe this relationship in this study.

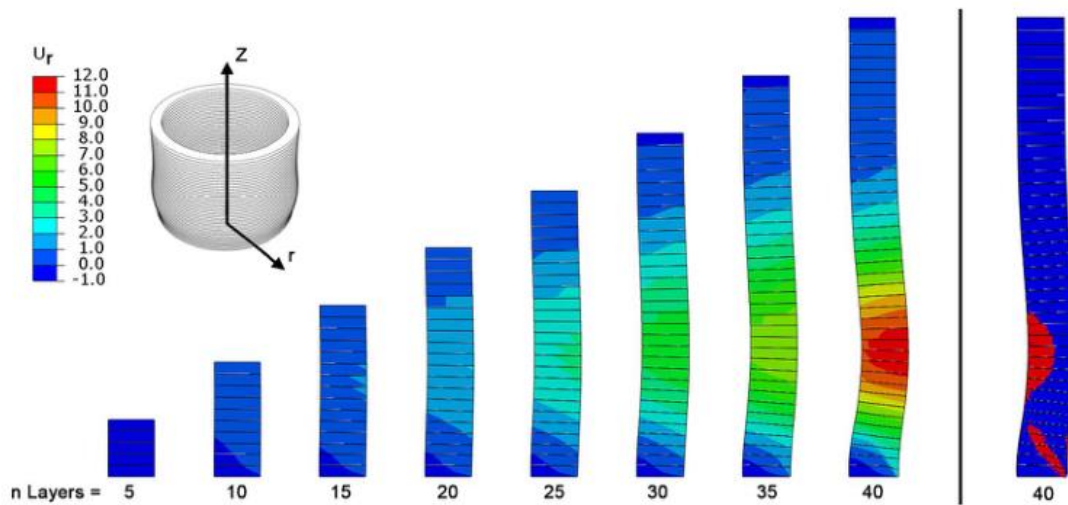


Figure 20: Numerical results of an axisymmetric modelled cylinder (Wolfs et al., 2018)

Wolfs et al (2018) use a mixture of Portland cement (CEM I 52.5 R), siliceous aggregate with a maximum particle size of 1 mm, limestone filler, additives, rheology modifiers and a small amount of polypropylene (PP) fibers as the material for experiments. Compressive strength, Young's modulus and density were derived from the uniaxial unconfined compression test, while shear strength and density were derived from the direct shear test.

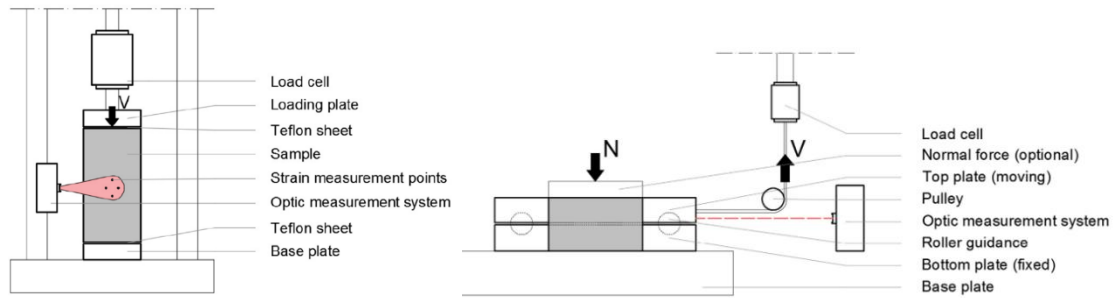


Figure 21: a) uniaxial unconfined compression test; b) direct shear test (Wolfs et al., 2018)

In J. Mink's thesis (2019), some parameters of normal concrete and fiber reinforced concrete were compared in terms of their indices, the main ones being compressive strength, Young's modulus, and Poisson's ratio. The average compressive strength of fiber reinforced concrete in the fresh state (0 min) was seven times greater than that of normal concrete, and the average compressive strength in the final state was nearly twice that of normal concrete. For Young's modulus, the fiber reinforced concrete is nearly ten times larger than normal concrete in the fresh state and approximately twice as large after 180 minutes (final state). The Poisson's ratio of fiber reinforced concrete, on the other hand, was always smaller than that of normal concrete during the experiment. Both mixtures had the same amount of materials and ratios except whether or not fibers were added. When analyzing the results, it can be noticed that fiber reinforced concrete has a sharp rise in properties at the beginning of material extrusion, which may be caused by the addition of fibers making the material set faster.

Table 3: Unconfined compressive strength of concrete without added fibers and Young's modulus with time (Mink, 2019)

Time (min)	Compressive Strength σ_y (kPa)			Young's Modulus E (kPa)		
	μ_{σ_y}	σ_{σ_y}	RSD	μ_E	σ_E	RSD
n = 3						
0	6.14	1.23	20%	74.53	15.49	21%
15	9.05	3.80	42%	91.28	45.23	49%
30	9.82	3.14	32%	97.39	35.98	36%
60	32.58	14.92	45%	343.07	142.32	41%
90	108.65	34.62	32%	1428.14	460.22	32%
120	120.28	17.30	14%	2181.16	377.06	17%
180	232.32	23.47	10%	7261.83	1193.74	16%

Table 4: Unconfined compressive strength of concrete with added fibers and Young's modulus with time (Mink, 2019)

Time (min)	Compressive Strength σ_y (kPa)			Young's Modulus E (kPa)		
	μ_{σ_y}	σ_{σ_y}	RSD	μ_E	σ_E	RSD
n = 5						
0	44.17	9.71	22%	770.73	199.15	25%
15	52.05	8.33	16%	933.24	168.48	18%
30	65.82	21.72	33%	1259.72	548.31	43%
60	108.54	10.85	10%	1830.56	232.71	13%
90	164.96	21.85	13%	3258.65	433.97	13%
120	270.79	40.39	15%	7661.89	3036.20	40%
180	420.32	53.63	13%	16325.73	2448.86	15%

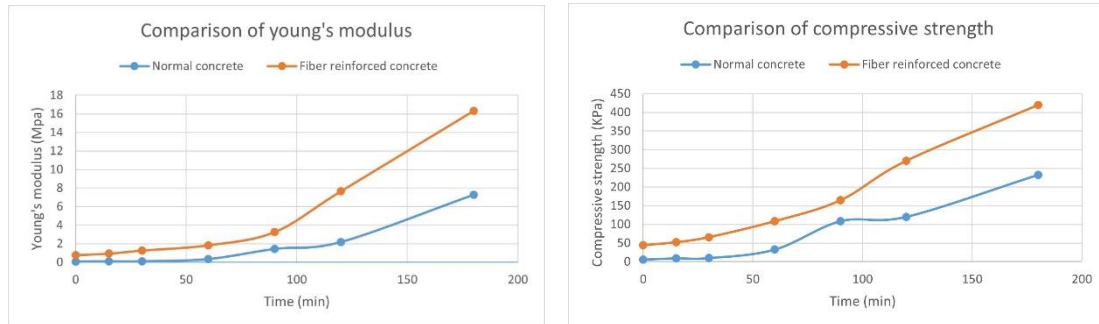


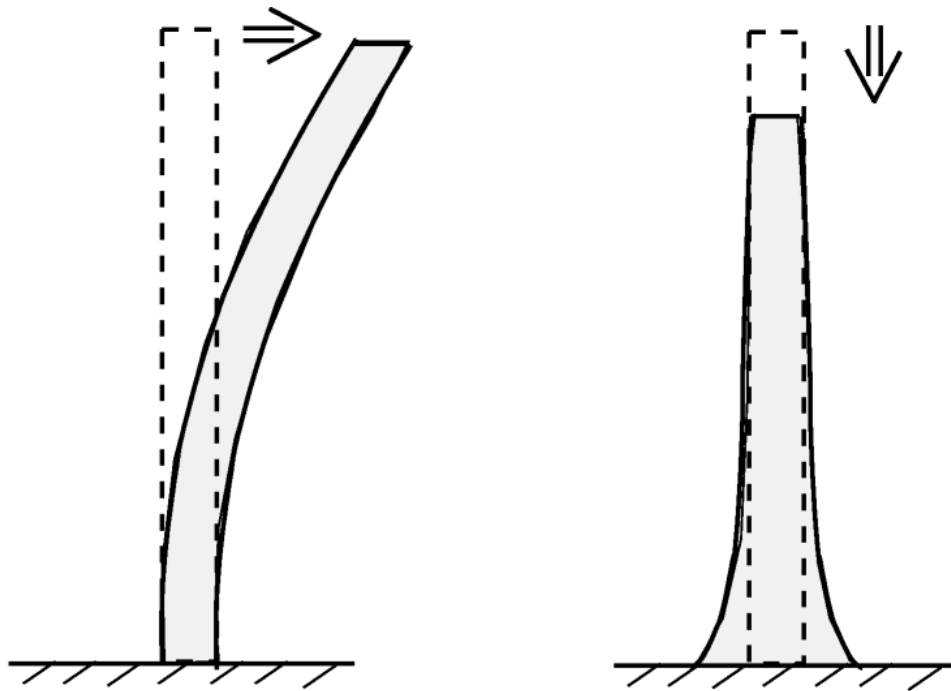
Figure 22: Comparison of Young's modulus and compressive strength of normal and fiber reinforced concrete, reproduced from Table 3 and Table 4.

Through the study of the above literature, it can be found that fiber reinforced concrete has obvious performance advantages over normal concrete in the process of 3D printing. These performance advantages will serve well when printing for buildings, for example, when printing for more stress concentrated areas such as windows and doors, the use of fiber reinforced concrete may be a good choice.

Printability of 3DCP, as well as extrudability and buildability, which are closely related to rheological properties, and fresh mechanical properties are important factors to be considered in the early stages of 3DCP. 3DCP needs to satisfy printability, and it has higher requirements for rheology and hydration than normal concrete. Printability is considered to be the ability of fresh 3DCP to be continuously extruded and built up with acceptable deformations prior to solidification, and it consists of extrudability and buildability (Hou et al., 2021).

Extrudability is defined as the ability to deliver fresh concrete as a continuous filament to the nozzles in the hopper of the extruder (Le et al., 2012). In the extrusion process, 3DCP is required to be extruded uniformly and continuously without any blockage, cracks and segregation (El Cheikh et al., 2017). At the pump, a relatively soft material that is easy to pump needs to be used, and at the nozzle, a hard material is needed so it won't sag or deform. Concrete is a mixture, consisting of particles of various sizes, shapes, and densities, so careful and optimized mixture design is required to ensure good extrudability (Paul et al., 2018).

Buildability is used to evaluate the ability of a fresh 3DCP to support its own weight as well as the load of the overlying concrete without collapsing during the printing process. 3DCP must be able to keep its shape deformation within a controlled range after extrusion. The layer thickness is generally set very small to limit the initial gravitational stresses to control the deformation (Roussel, 2018).



Elastic buckling

Plastic collapse

Figure 23: a) elastic buckling; b) plastic collapse (Wolfs & Suiker, 2019)

The elastic buckling mechanism reflects failure caused by a loss of geometrical stability, while plastic collapse is characterized by the maximum stress reaching the material yield strength. Suiker (2022) developed a finite element model to test the effect of vertical displacement of layers on structural failure during 3D printing. It is demonstrated that the effect of vertical wall deformations on the prediction of failure by elastic buckling typically is minor, so that for this failure mechanism this contribution may be left out of consideration.

2.6 Information about the 3D Printed Building in

Wujiashuang

The starting point of this study in Wujiashuang, China is based on a concrete farmhouse built by Tsinghua University. The project covers an area of 106 square meters, and its shape adopted the form of local traditional cave dwellings.

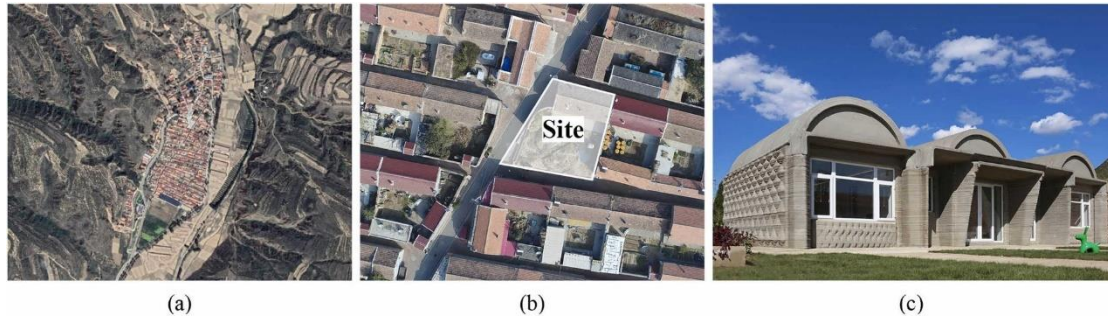
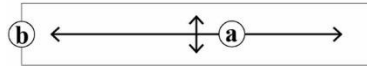


Figure 24: a) Area conditions as seen by Google Maps; b) Overhead view of construction site; c) The completed 3D printed farmhouse (Xu et al., 2022)

As the figure shown above, the road and site around the building construction site is narrow, if the factory prefabricated and then transported to the 3D printing site for assembly will be very inconvenient and will consume a lot of manpower and material resources. Therefore, the construction team chose to transport the printing equipment to the site for on-site printing. As for the weather conditions, the region has a large temperature difference between day and night during the 3D printing period, which has a higher requirement for the stability of the printing material.

Legend

Robot tracks:



(a) Robot's moving direction(s)

(b) Track bed

Production area:

- (1) In-situ printing zone
- (2) Site preprinting zone
- (3) Water supply
- (4) Garbage collection area
- (5) Material stacking area
- (6) Electricity supply

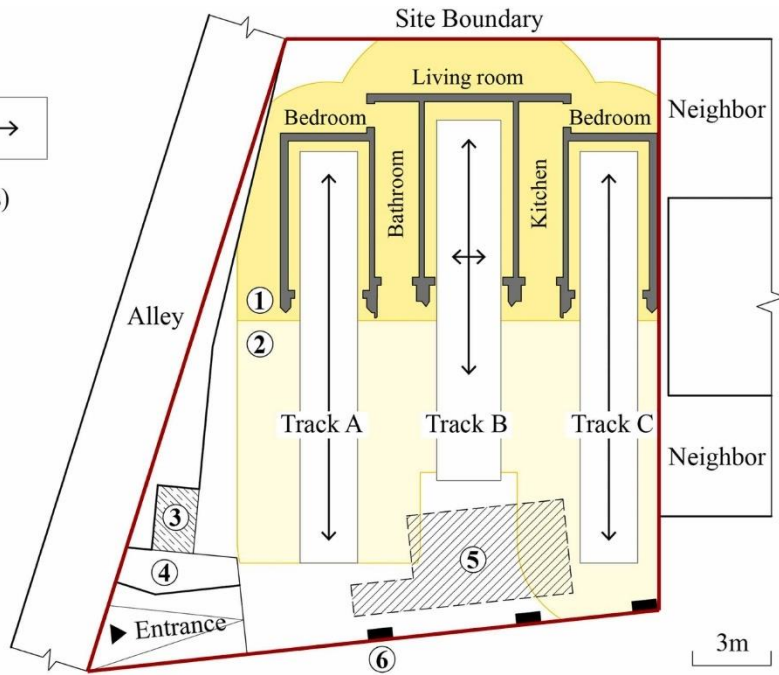
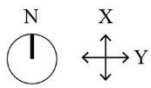


Figure 25: Construction site production area design (Xu et al., 2022)

The construction site is about 24m long and 22m wide, with an area of about 410 square meters. As can be seen from the layout of the construction site, there are a total of three printing devices on the construction site, of which the middle printer needs to move in both the X and Y axes to print, while the next two printers only need to move in the X direction to meet printing needs. The flexibility of the construction site printing design is to use part of the print track as a preprinting zone. The advantage of this design is the flexibility to print objects in the preprinting zone that cannot be printed as intended due to unforeseen circumstances, such as modifying the print path or repairing the printing device. There is also a dedicated area for rehydrating the concrete to avoid premature drying and cracking.



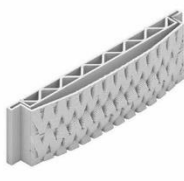


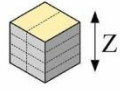
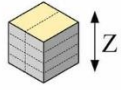
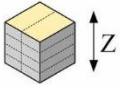
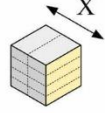
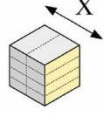
Foundation Trench	Structural Wall	Decorative Wall	Arch Roof	Flat Roof
				
Printing Direction				
Horizontal	Horizontal	Horizontal	Vertical	Vertical
Loading Direction				
				
Printing Environment				
Factory preprinting	In-situ printing	Site preprinting	Site preprinting	Site preprinting

Figure 26: Types of components that need to be printed for the 3D printing process (Xu et al., 2022)

For this project, a special composition of fiber reinforced concrete was developed which can meet the requirements of both structural strength and printability. The concrete consists of Sulphur-aluminous cement (SAC), sand, polyvinyl alcohol (PVA) fiber, water, and multiple additives including a retarder, thickener, water reducer, and early strength agent. Two types of sand are used with particle diameters of 0.2-0.4mm and 0.4-0.7mm (XU et al., 2020).

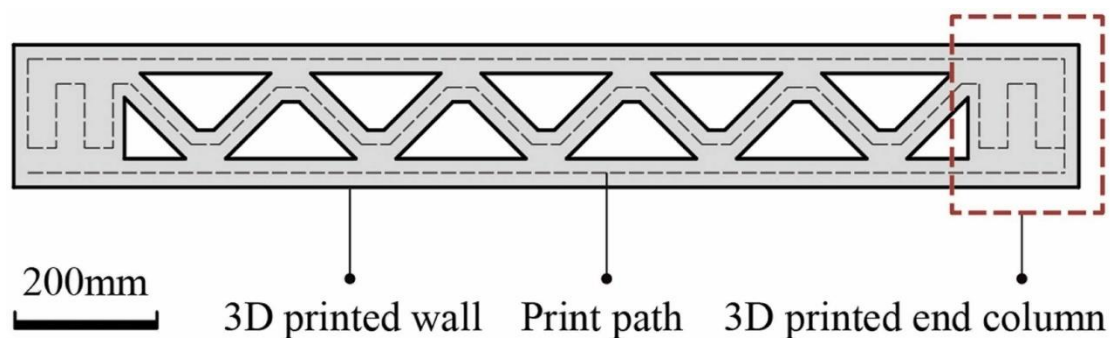


Figure 27: 3D printed walls (Xu et al., 2022)

The above diagram shows the basic construction and print path of a structural wall. Since the corner locations are under more pressure, the choice was made to set the columns at the corners to be solid.

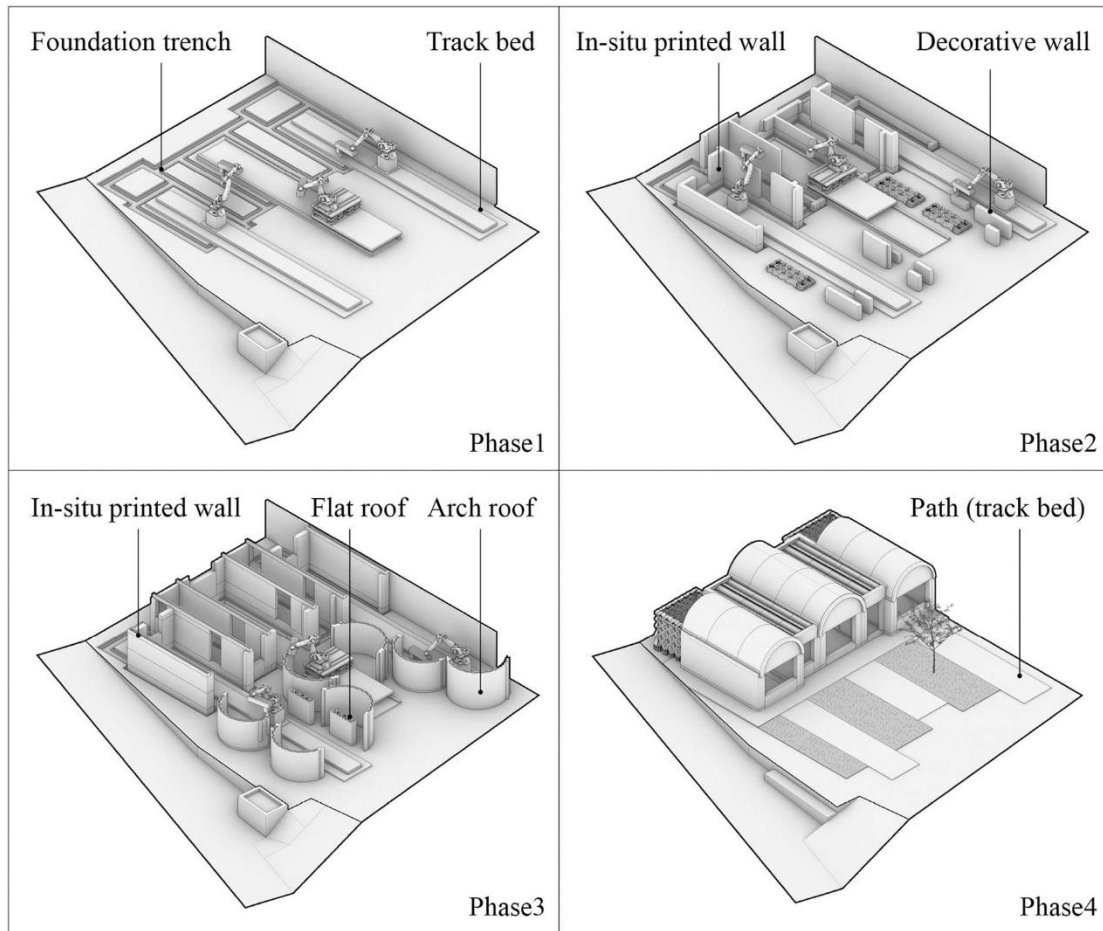


Figure 28: Four stages of 3D printing for this project (Xu et al., 2022)

The first stage is the 3D printing and assembly of the foundation, a two-part process that begins with prefabrication of the foundation trench assembly at the factory and then transported to the site for assembly with the robotic arm once completed. Then the second and third stages are the on-site printing of the structural walls and roof, respectively. After printing the components, all of them are lifted and placed in the right position. Finally, there is the decoration work.

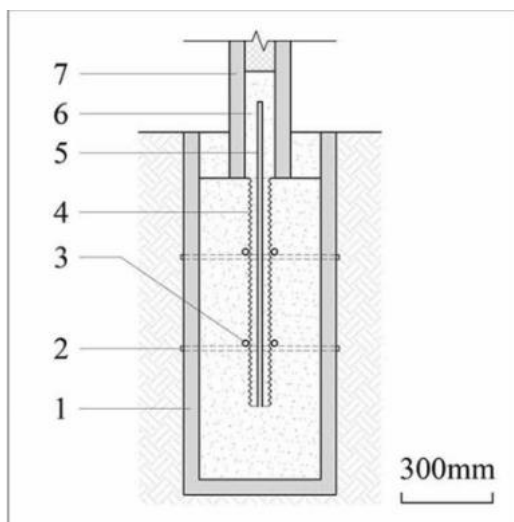


Figure 29: a) Connection details of foundation and wall; b) Diagram of the living room after printing (Xu et al., 2022)

It shows that the concrete foundation trench was printed in factory, and it was lifted and placed on site. Fiber reinforced plastic rebars are placed in X, Y and Z directions, where the X-direction reinforcement was pre-inserted, mainly because the concrete was not fully solidified during the printing of the component. When transported to the site for construction, workers only need to tie the reinforcement in the Y direction to connect all the horizontal reinforcement.



Figure 30: a) Southwest view of the project; b) Floor plan of the project (Xu et al., 2022)

The width of the printing head of the robotic arm is 40mm, and the arch roof, flat roof and wall are all truss-type wall panels with chords and webs of 40mm thickness. The approximate manufacturing process is the arch plate, and the flat plate are printed on the ground first, and then the wall is printed to the bottom elevation of the roof. Finally, the arch plate, the flat plate and the wall are connected through special nodes to ensure the integrity of the structure.

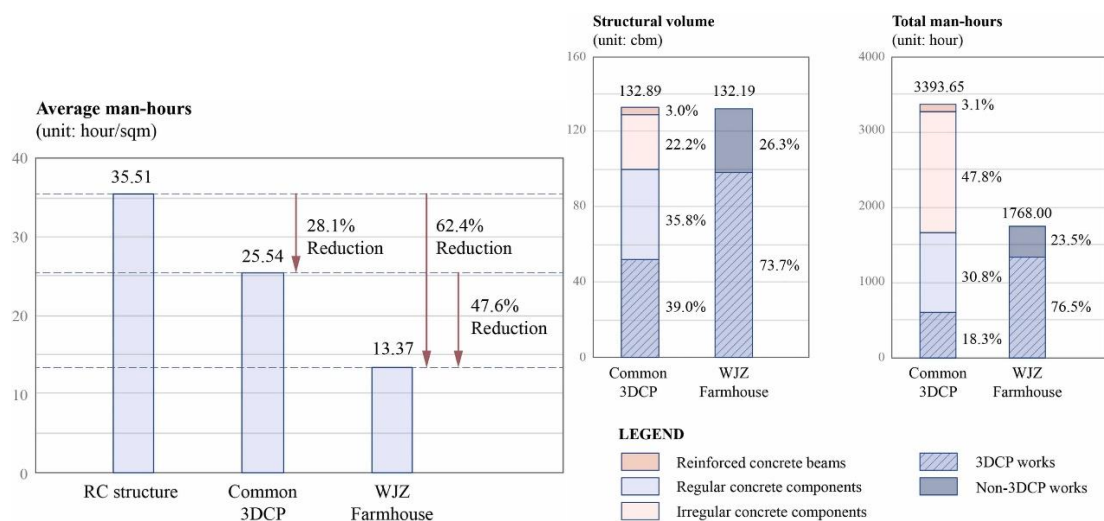


Figure 31: a) Comparison of man-hours in different situations; b) Comparison of structural volume and

man-hours distribution (Xu et al., 2022)

Another highlight of the project is that it saves more manpower compared to traditional 3D printing technology processes. Manpower can be saved through the previously mentioned workflow. The specific details are also reflected in the diagram.

In order to facilitate the analysis, one of the three similar structures can be selected for finite element analysis in this study. Although more detailed and comprehensive drawings cannot be found, some data can also be assumed, and special attention should be paid to the internal forces of the arch structure. The internal forces that may appear in the arch structure during or after the construction process are more complicated.

Through researching and studying the literature, I have learned about the classification of additive manufacturing and 3DCP as well as the different manufacturing processes; the combination of finite element analysis and 3DCP as well as the application examples, different kinds of finite element analysis software; the process of making fiber reinforced concrete, the mix ratio design of the mixtures, the design of the printing nozzles, and the effect of different types of fibers on the mechanical properties of the concrete; and the differences in the properties of the fiber reinforced concrete and the ordinary concrete in the early stages and after hardening, where the properties of the early stage are more complex and critical (printability, buildability, and the mechanical properties), and the failure mechanisms that exist in the printing process.

This study will attempt a time-dependent nonlinear analysis that simulates the architectural 3D printing process by applying a common type of reinforcement for 3D printing materials (adding fibers) to the 3D printing scene and exploring its effects. This study will investigate how this type of reinforcement improves the process of architectural 3D printing, using finite element analysis to predict if the print will be successful and how to optimize the printing process.

3 Research Design

3.1 Problem Statement

In the current stage of digital fabrication, especially that of building construction, and in the scope of 3D printing using fiber reinforced concrete, several problems that have not been fully studied may occur during the construction or transport phase. These problems are due to lack of preparation, lack of selection and analysis of material, and lack of software simulation. Some situations during the construction or transportation will cause sudden and sharp increase in internal stresses, which could lead to local failures. During the literature research in the previous chapter, it was found that most of the studies on fiber reinforced concrete applied to architectural 3D printing have explored the material itself, i.e., continuously varying the material mix ratio or fiber properties (type, length, content) and testing the early properties and properties after hardening of the different mixtures, but very few studies have combined the material properties and the actual architectural 3D printing process with finite element analysis to accurately predict the printing process of 3D fiber reinforced concrete printing.

3.2 Research Objective

This study will combine finite element analysis and 3D fiber reinforced concrete printing with a case study of a 3D printed farmhouse located in Wujiazhuang, China. There are two main objectives of this study, the first is the 3D fiber reinforced concrete printing aspect. This study will analyze the whole process of 3D printing of the building and the state after the printing is completed and put into use, analyze the deformation and stress distribution of the structure during the printing process through the stages, add fibers to the structural materials at the failure positions or weaker ones (which may fail in the subsequent printing process), and optimize the solution of adding fibers in the feedback loop. Through this process, the effect of adding fibers to 3D printed materials on the whole 3D printing process will be studied, and the strategy of adding fibers and optimization in the printing process will be obtained, which can provide a reference for the subsequent 3D fiber reinforced concrete printing. And the second is in finite element analysis of 3D printed structures (not limited to fiber reinforced concrete). This study can also give the simulation method of 3D printed structural components in the process of finite element analysis as well as the adjustment strategy of structural failure in the process of analysis, and the strategy of how to effectively reduce the computation time, which will provide reference for the subsequent use of finite element method to analyze the 3D building printing.

3.3 Research Question

Main question:

How to simulate, analyze and optimize the final structure and the whole process of 3D fiber reinforced concrete printing for a simple building using Finite Element Method (FEM), taking into account the hardening behavior of a 3D printed and where needed also fiber reinforced concrete mixture?

Sub questions:

- 1) What was the geometry and construction method of the house in the case study?
- 2) What are the material properties of 3D-printed concrete after mixing, during printing and during and after hardening?
- 3) How can time-dependent behavior of material be modelled correctly with FEA?
- 4) In analyzing 3D printing of buildings using FEM, how to determine the failure mechanism of the structure and how to adjust the structural solution?
- 5) What is the effect of local addition of fibers on the material properties and on the total structure?

3.4 Methodology

3.4.1 Literature study

Literature study could address the first and second sub questions mentioned earlier. The first question is related to the case and can be solved by studying the literature related to the case to understand the geometry of the building and the construction methods on site. The second question is related to 3D printed materials, and many studies have revealed the changes in the properties of 3D printed concrete at different stages, as well as the comparison of the various properties of fiber reinforced concrete with those of normal concrete. In addition to this, literature or tutorials related to finite element analysis will be studied, and since this study will use DIANA for modeling and analysis, tutorials related to the use of DIANA as well as materials from the course CIE 5148 will be studied.

3.4.2 Simplification and model set-up

Before building the finite element model, some conditions in the real situation need to be simplified. The first is the large diurnal variation of the construction site temperature, which will be disregarded in the finite element analysis. The second is the design of the foundation. The actual situation is that the foundation trench is pre-supported in the factory and transported to the site for lifting, but the foundation will not be considered in the modeling, and only the ground

support will be put in. Lastly, the seismic design was done for the structure, but it was not considered in the FEM modeling process.

Once the simplification is completed, first a model of the complete structure in the use stage will be created, followed by a complete model of the printing process. Slicing will be used in this process, and to completely simulate the entire printing process, multiple models will need to be created and optimized, which will need to be combined with the results of the finite element analysis and adjusted in time.

3.4.3 Construction process optimization

After the completion of the modeling, the finite element method will be used to completely analyze the printing process of the entire building, thus requiring a focus on the optimization of the construction process.

Before proceeding with the development of the workflow, the timeline of the analyzed building production is analyzed and briefly described. The first is the design phase, followed by the construction phase, which is the printing phase, starting from the printing phase as the first day, where the main part of the building will be printed, but not the roof. On the 10th day, the concrete of the building body has been hardened to a certain extent, and the roof is assembled at this time. On the 28th day after the roof is assembled, the building is ready for the initial use phase.



Figure 32: Timeline of building production

After introducing the timeline, the workflow is described below. This study starts with the analysis of the building in its use phase, so the first step is to perform a structural static analysis of the building, use fiber reinforced concrete in the parts with large deformations thus reducing the deformation of the building and providing assurance of the safety of the building during its use. The final result of this process is a preliminary fiber concrete distribution solution.

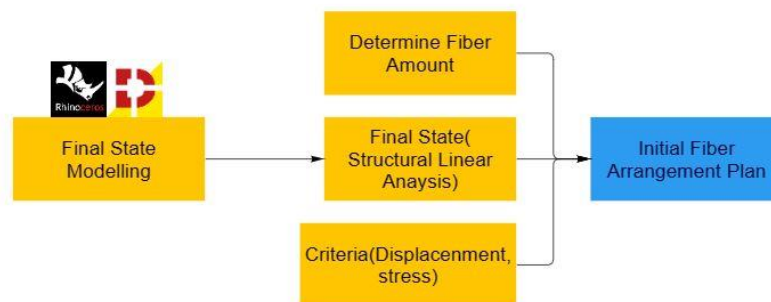


Figure 33: Analysis of structure in use phase

After obtaining the initial distribution solution of the fiber concrete, the analysis proceeds to the building printing phase, in which the main part of the building is printed, but with the roof removed. The dynamic analysis of the printing process of the main body of the building is performed in DIANA, i.e., the analysis of each printed layer is performed. The main body of the building is layered, and a nonlinear and stability analysis is performed to verify that the building will not collapse during the printing process. If the initial solution results in the building collapsing, the initial solution needs to be adjusted, i.e., the distribution of the fiber concrete needs to be changed. After the change, the finite element analysis described above is continued until the analysis indicates that the structure meets the requirements. The result of this process is an optimized distribution solution for the fiber concrete.

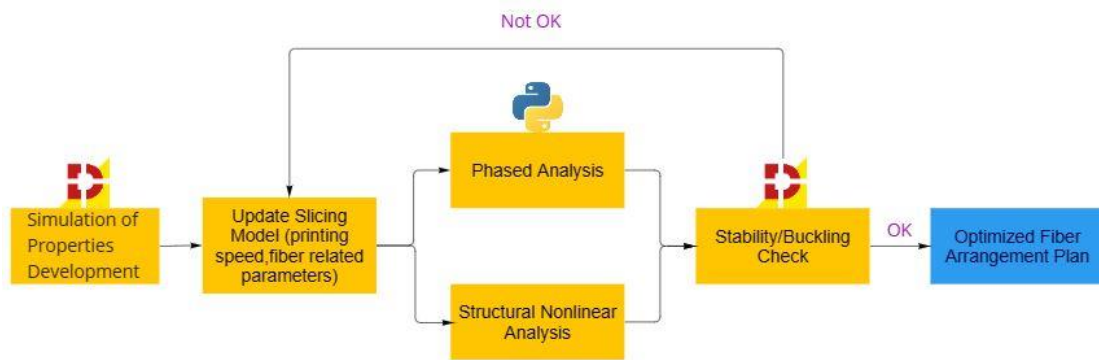


Figure 34: Analysis of main structure during printing phase

After obtaining the optimized fiber concrete distribution solution, it also means that the main part of the building has been successfully printed. The next stage is the roof assembly. First, the roof section is divided into 2 smaller objects to be installed and assembled separately. If the analysis reveals that it will cause local instability or collapse, the roof division method or the fiber concrete distribution will be changed until the analysis yields the required results. At this point, the final roof assembly and fiber concrete distribution plan can be derived.

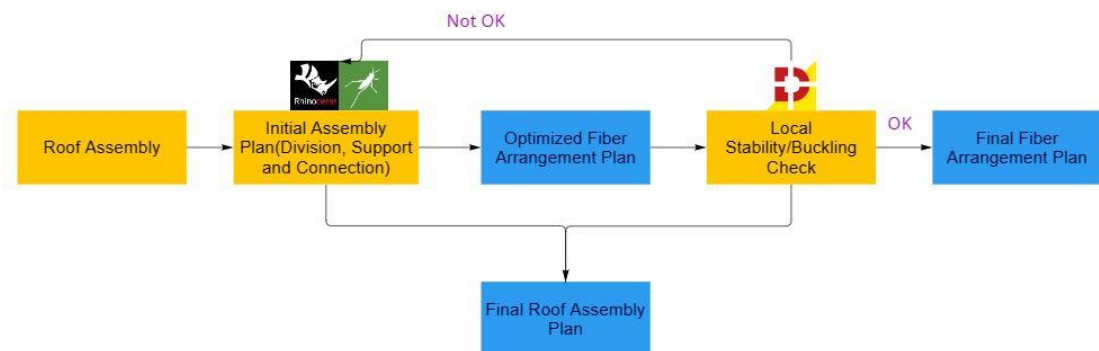


Figure 35: Analysis of roof in printing phase

4 Validation

This chapter will refer to another 3D concrete printing related paper. Wolfs et al (2018) measured the properties of concrete used for 3D printing and analyzed the 3D printing process of a 40-layer cylinder using finite element software. This study will take the same parameters and analyze them numerically with different software and compare the results.

Regarding the material aspects, as already mentioned in Chapter 2, the Young's modulus, tensile strength, and compressive strength of the concrete specimens were measured by uniaxial unconfined compression test and direct shear test, respectively, as the variation of Young's modulus, tensile strength, and compressive strength with time over a 90-minute period of time after the concrete was extruded.

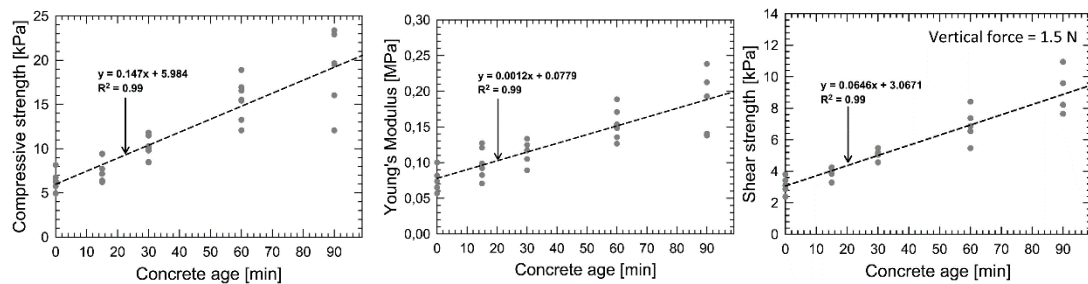


Figure 36: Compressive strength development (left) and Young's modulus development (middle) up to 90 min derived from the compression tests; Shear strength development (right) up to 90 min derived from the direct shear tests. (Wolfs et al., 2018)

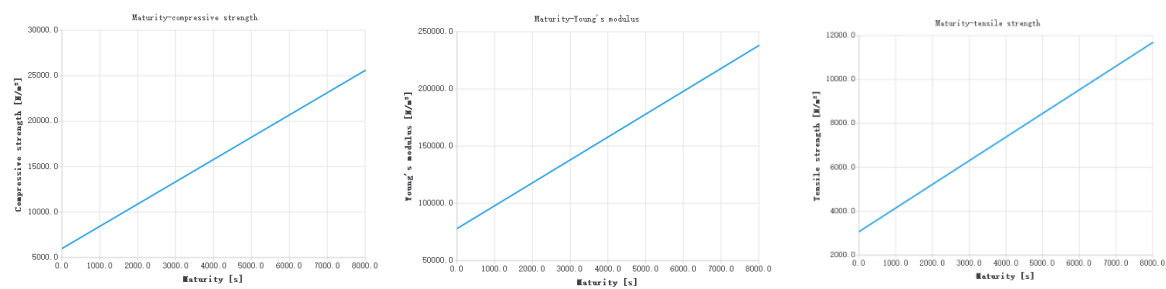


Figure 37: Compressive strength (left), Young's modulus (middle), and tensile strength (right) over Time Set in DIANA.

According to the parameters used in the experiment by Wolfs et al, the printing process was modelled for a layered cylinder with a heart line radius of 250 mm, a thickness of 40 mm, and a layer height of 10 mm (Wolfs et al, 2018). The printing speed was set as 5000 mm per minute (83 mm per second). For the density of concrete, 2070 kg/m³ was used in the experiments.

Three different material properties were analyzed to investigate the effects of the relatively large dispersion of material properties during printing. Experimentally derived average values as well as upper and lower bounds for the strength and stiffness parameters were used. The relative standard deviation of the experimental strength and stiffness values was about 17.5% of the corresponding average values. Therefore, the values were used as reduced and increased values of the average values to obtain estimates of the upper and lower bounds of the failure deformation modes.

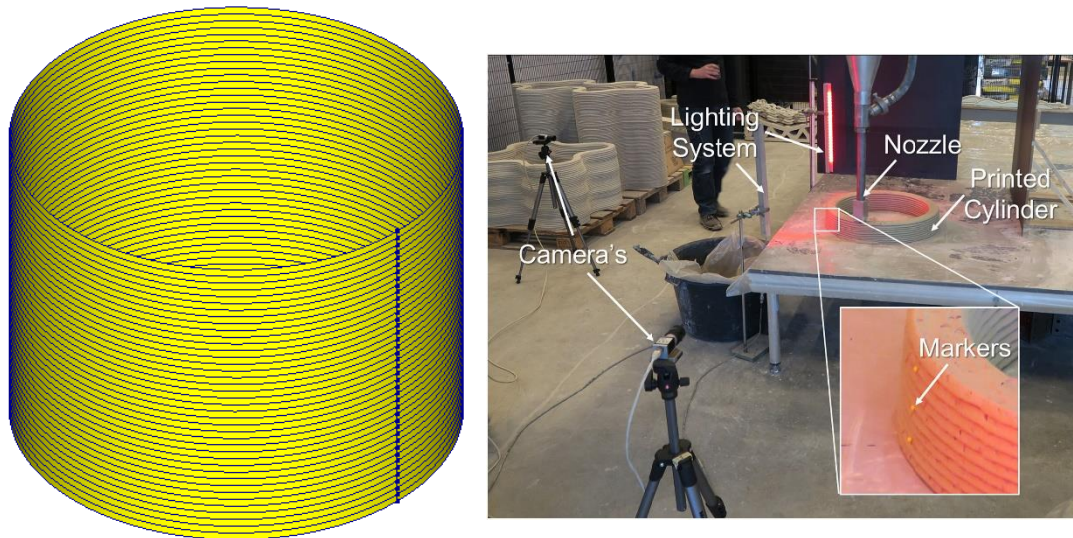


Figure 38: Modeled (left) and lab-printed cylinder (right) (Wolfs et al., 2018)

For support, only the role of ground support was considered, i.e., limiting movement in three directions without limiting rotation. For loading, only self-weight was considered since the state during printing was analyzed. The following is a calculation of the printing time for each layer. For the first test, the average material properties were used.

$$T = 3.14 \times 0.5 \div 0.083 = 19 \text{ s}$$

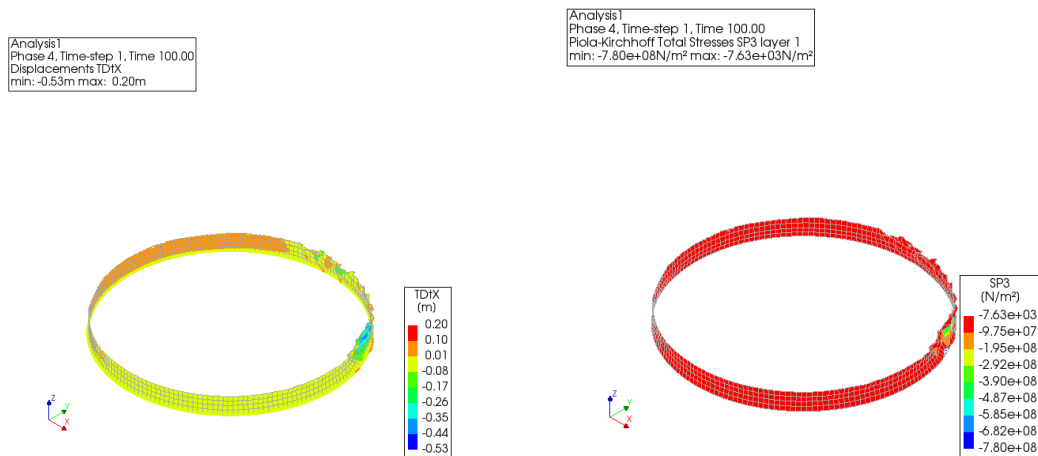


Figure 39: Deformation and stress distribution of the structure when printed to the maximum number of layers.

As can be seen from the results above, the structure was only able to successfully print 3 layers and would collapse on the 4th layer due to the large deformation of the structure. This result is clearly different from Wolfs et al (2018) who found that cylinders could be successfully printed up to 40 layers during their experiments.

Since the material properties were the same as those derived from the experimental tests, and the structure was of similar shape, the loads were only self-weight. Therefore, the only possible reason for such different results could be the method of support. Due to the small size of the cylinder and the fact that the printing process took place in the laboratory and not in the field, the support could have been limited not only to movement in three directions but also to rotation, so the support was changed in the software to limit movement in three directions and to limit rotation in two directions (X and Y directions).

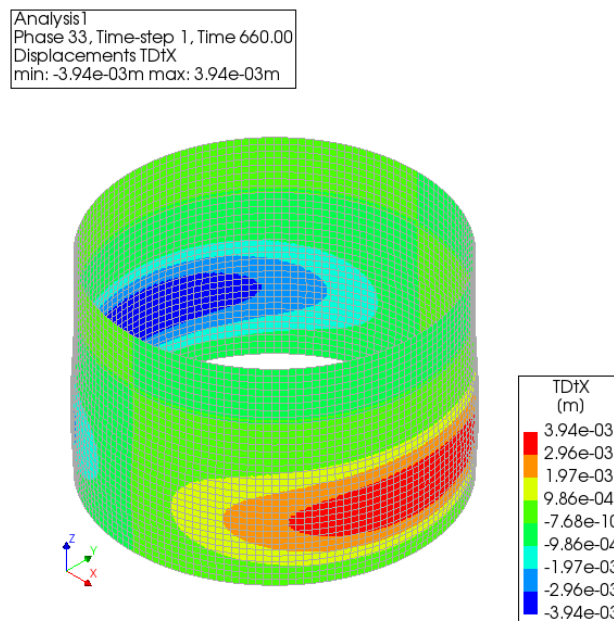


Figure 40: Deformation of the cylinder when printed to the maximum number of layers as analyzed by DIANA (average)

As shown in the figure above, the structure was printed to the 33rd layer when using the average material properties. Since in the referenced literature only the structural deformation plots using the lower bound material properties were given, in order to compare the structural deformations in different software, the following modeling analysis using the lower bound material was also done.

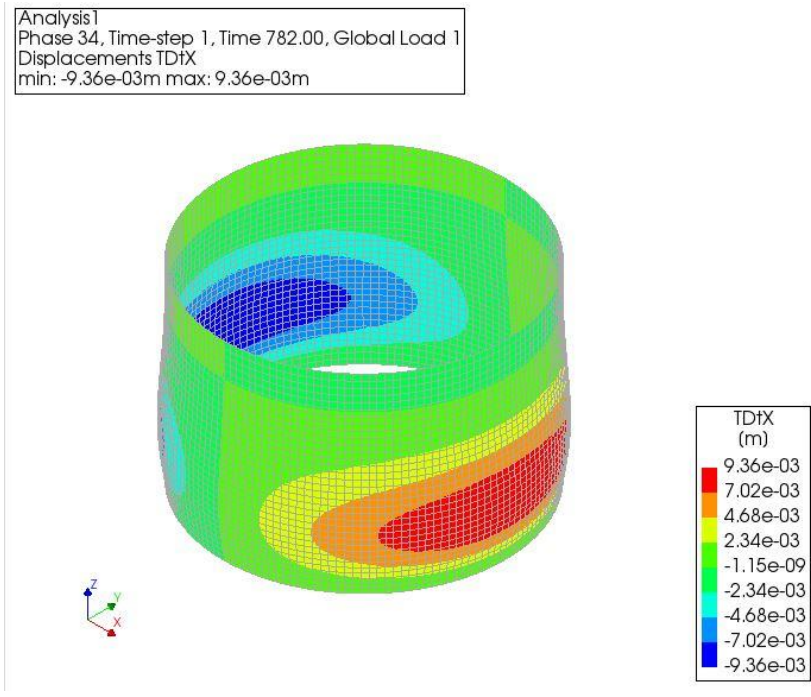


Figure 41: Deformation of the cylinder when printed to the maximum number of layers as analyzed by DIANA (lower bound)

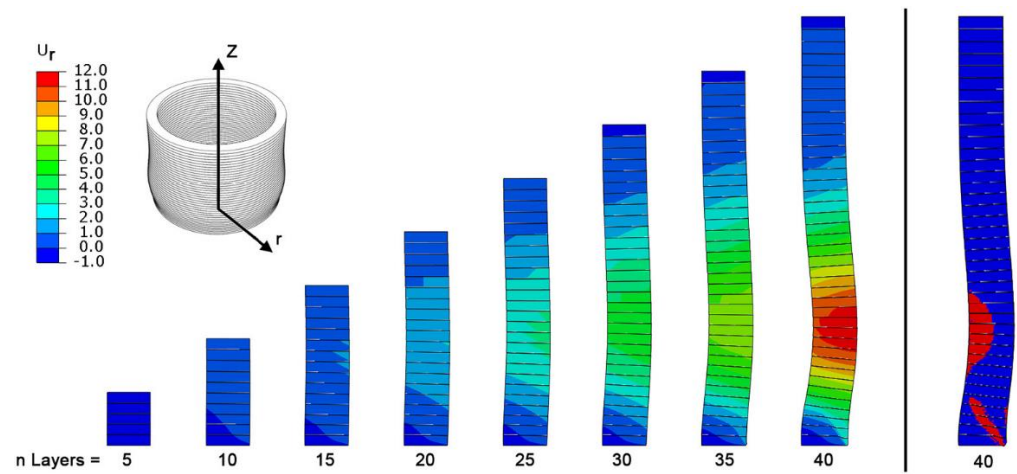


Figure 42: Deformation of the cylinder when printed to 40 layers as analyzed by Abaqus using lower bound material properties (Wolfs et al., 2018)

From the comparison results of the above two figures, the cylinder in the printing to the 40th layer of the deformation of the largest position were found in the 10th to the 20th layer of the place between, and respectively, about 9.36 mm and 12mm. Although the values were slightly different, the overall deformation of the structure was relatively similar. It is possible that the difference in maximum deformation between the two software analyses was due to the difference in mesh size or some specific parameters in the analysis.

Table 5: Summary of failure-deformation results (Wolfs et al., 2018)

		Number of layers	Max. radial deformation [mm]		
			Layer 23	Layer 26	Layer 29
μ	29	10,3	12,7	15,3	
σ	2,4	2,2	2,7	2,2	
RSD	8%	21%	21%	14%	

Table 6: Summary of numerical results for the lower bound, average, and upper bound analyses (Wolfs et al., 2018)

Analysis	Number of layers	Max. radial deformation before failure [mm]
Lower bound	40	11,0
Average	46	13,89
Upper bound	53	13,05

Table 7: Summary of numerical results for the lower bound and average analyses in DIANA

Analysis	Number of layers	Max. radial deformation (mm)
Lower bound	34	9.36
Average	33	3.94

It can be noticed from the three tables above that the model built in DIANA using the lower bound material properties was closer to the results obtained from the actual experiments in terms of the number of printed layers, but in terms of the structural deformation, the model still analyzed a smaller value of deformation than the actual situation.

Based on the comparison of the results produced by the two software, the error is basically within the acceptable range. Since the dimensions of the cylinder and the printing time for each layer were not given in detail in the paper, these were my own calculations. Therefore, the similarity of the results showed that the model built in DIANA was reliable.

5 Numerical Modelling

5.1 Introduction

In this chapter, a number of models will be built in DIANA and subjected to different analyses to meet the requirements of the building at different stages of the process from the start of the printing process to the use stage of the building. There are three analysis methods that will be used in the DIANA analysis, which are linear static analysis, nonlinear combined phase analysis, and stability analysis.

Table 8: Comparison of 3 different analyses

	Analysis 1	Analysis 2	Analysis 3
Type	Linear static	Phased nonlinear	Stability
Material	Concrete (linear)	Concrete (nonlinear)	Concrete (nonlinear)
Load	Gravity and live load	Gravity	Gravity
Main results	Displacement, Stress, strain	Displacement, Stress, strain	Buckling value
Stage	Use	Printing	Printing

Analysis 1 is relatively simple and is mainly used when the structure has been printed and is already in use, so it is important to consider not only the self-weight but also the live loads that occur during use. For the materials, the state of the materials is relatively stable, so the values of the various material properties will no longer change. Through this analysis, it is possible to determine whether the structure can meet the requirements of the code in its final state.

Analysis 2 uses a combination of phase analysis and structural nonlinear analysis. The main purpose of the combination of these two analyses is to perform a structural nonlinear analysis on the existing printed finished structure for each additional layer printed, starting from the first layer. In this way, the printing status of the structure can be accurately determined to each layer, so that the printability of the structure can be judged more accurately and provide a basis for subsequent optimization analysis. On the material side, since this analysis is used to analyze the structural printing process, it is particularly important that the material properties change over time.

Analysis 3, like Analysis 2, is similarly used during the printing of the analyzed structure. However, they focus on different aspects; Analysis 3 is more concerned with the stability of the structure. Therefore, Analysis 3 gives a buckling value. The buckling value is the factor of safety

against buckling or the ratio of the buckling loads to the applied loads.

Table 9: Interpretation of possible buckling values, (SolidWorks Help, 2012)

BLF Value (factor of safety)	Buckling Status	Notes
$1 < \text{BLF}$	Buckling not predicted	The applied loads are less than the estimated critical loads. Buckling is not expected.
$0 < \text{BLF} < 1$	Buckling predicted	The applied loads exceed the estimated critical loads. Buckling is expected.
$\text{BLF} = 1$	Buckling predicted	The applied loads are exactly equal to the estimated critical loads. Buckling is expected.
$\text{BLF} = -1$	Buckling not predicted	The buckling occurs when the directions of the applied loads are all reversed. For example, if a bar is under tensile load, the BLF should be negative. The bar will never buckle.
$-1 < \text{BLF} < 0$	Buckling not predicted	Buckling is predicted if you reverse all loads.
$\text{BLF} < -1$	Buckling not predicted	Buckling is not expected even if you reverse all loads.

In the structural nonlinear analysis, some parameters that have an important impact on the printability of the structure will be set, such as the print time of each layer. Parameters that also affect the time required for the analysis are set, such as the number of iterations, the type of structural nonlinearity and more detailed options therein, as well as the option to calculate the analysis and view the results.

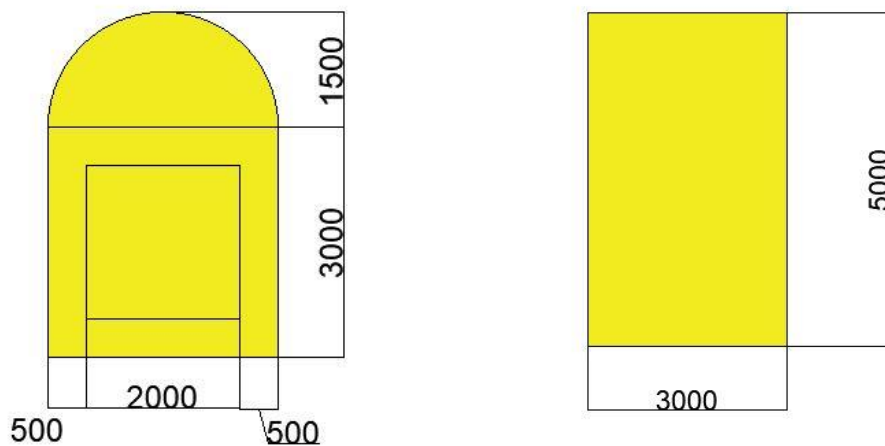


Figure 43: Size of the house

5.2 Analysis of the entire structure during the use phase



Figure 44: 3 parts of the printed farmhouse (RIC Technology, 2022)

The model of the 3D printed building in Wujiazhuang was established in DIANA. Considering that the original building had three roughly identical parts, only one of these parts was selected in the modelling process, and the analysis of the three different parts could be achieved subsequently by changing the boundary conditions of the part. When modeling the roof of the structure, since it is a gable roof, the roof was first modeled in Rhino 7, and then the file was imported into Diana to finally complete the modeling of the entire structure.

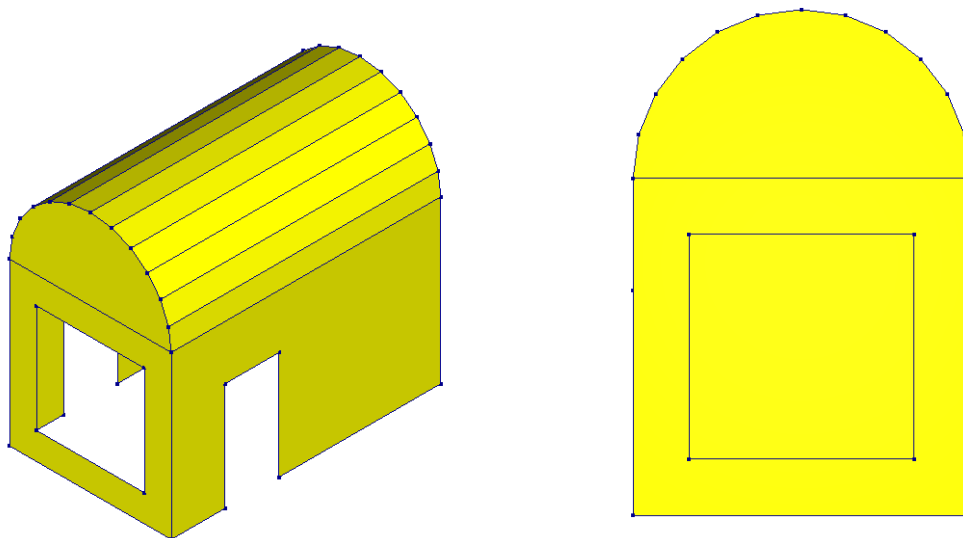


Figure 45: Modelling of building in the final state

First of all, C30 concrete was used for the whole structure to try to see whether normal concrete

can meet the specification requirements under self-weight and live loads, and the material properties were directly utilized in the DIANA database.

Table 10: C30 concrete properties in DIANA database

C30	
Young's modulus	$3.35 \times 10^{10} \text{ N/m}^2$
Poisson ratio	0.2
Density	2350 Kg/m^3
Compressive strength	$3.8 \times 10^7 \text{ N/m}^2$

Boundary conditions at the bottom are basically the same, i.e., they restrict movement in the x, y and z directions, but not rotation, which is also more in line with the situation of the bottom support in practical engineering. This type of support also simulates the support of the foundation for the structure in the actual case and will be widely used for the bottom support of the subsequently built models.

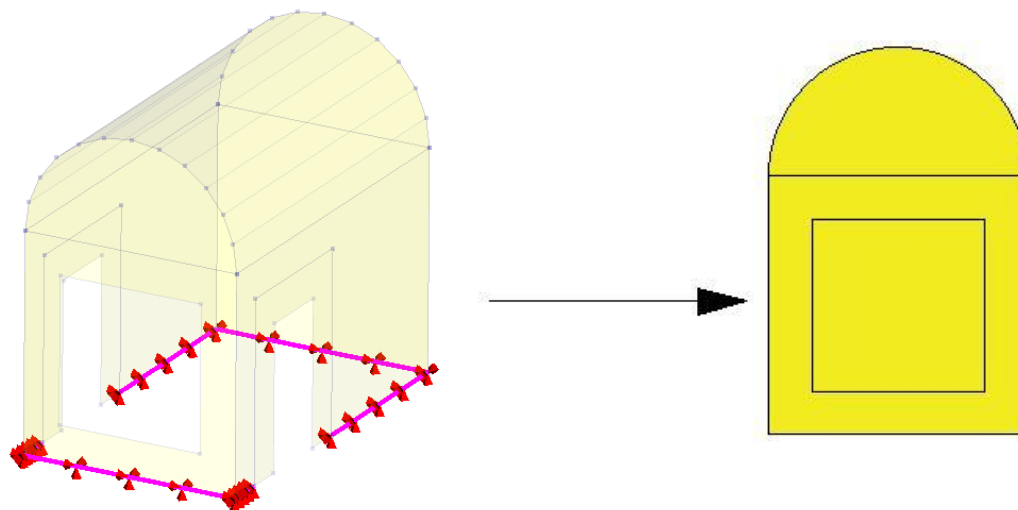


Figure 46: a) Foundation supports in Diana; b) Wind direction.

When applying loads, only wind loads, self-weight, and a combination of these two loads were considered in the initial stages. In total, the two load patterns (gravity and combination of gravity and wind load) simulate the main loads that the structure will be subjected to at the 3D printing site. The following wind loads are calculated.

Basic wind velocity is 27m/s, and basic velocity pressure is 0.46 KN/m². The formula to calculate the wind pressure on external surfaces is:

$$W_e = q_p \times c_{pe}$$

q_p is the peak velocity pressure and c_{pe} is the external pressure coefficient.

For the building where wind loads are to be calculated, $b=5m$, $d=h=3m$.

$$e = \min(b, 2h) = \min(5, 2 \times 3) = 5m$$

$$e > d$$

Table 11: Recommended values of external pressure coefficients for vertical walls of rectangular plan buildings

Zone	A		B		C		D		E	
	$c_{pe,10}$	$c_{pe,1}$	$c_{pe,10}$	$c_{pe,1}$	$c_{pe,10}$	$c_{pe,1}$	$c_{pe,10}$	$c_{pe,1}$	$c_{pe,10}$	$c_{pe,1}$
5	-1,2	-1,4	-0,8	-1,1	-0,5		+0,8	+1,0	-0,7	
1	-1,2	-1,4	-0,8	-1,1	-0,5		+0,8	+1,0	-0,5	
$\leq 0,25$	-1,2	-1,4	-0,8	-1,1	-0,5		+0,7	+1,0	-0,3	

Zone A:

$$-1.2 \times 0.46 = 0.55 \text{ KN/m}^2$$

Zone B:

$$-0.8 \times 0.46 = -0.37 \text{ KN/m}^2$$

Zone D:

$$0.8 \times 0.46 = 0.37 \text{ KN/m}^2$$

Zone E:

$$0.5 \times 0.46 = 0.23 \text{ KN/m}^2$$

A simplification is made here by considering zone A and B together, both considered as loads in zone A.

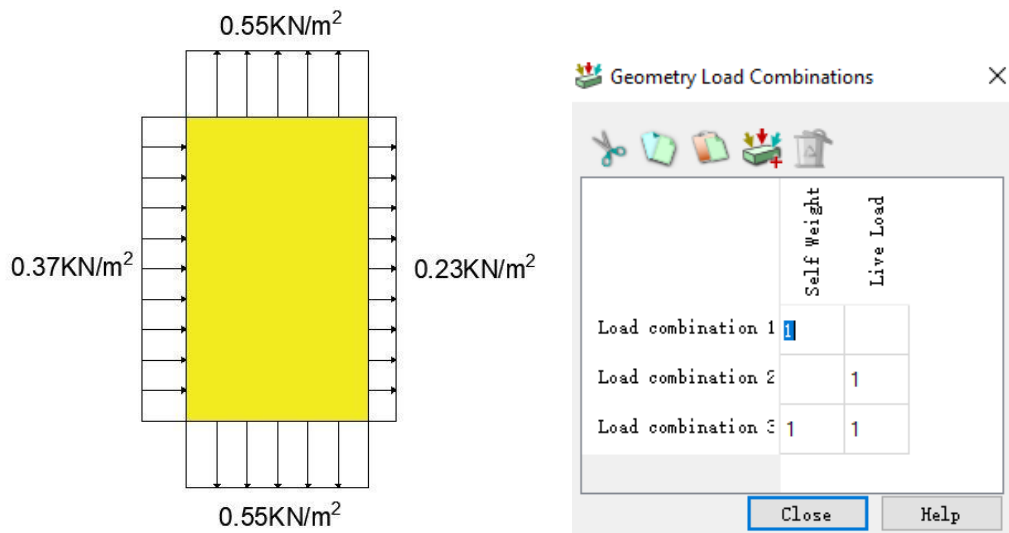


Figure 47: a) The magnitude and direction of wind loads; b) Load combinations.

The final step before running the analysis is meshing. Since the edges are not straight, the semi-circular front elevation grid is subdivided more densely, and the subdivided grid changes at the windows and doors of the building.

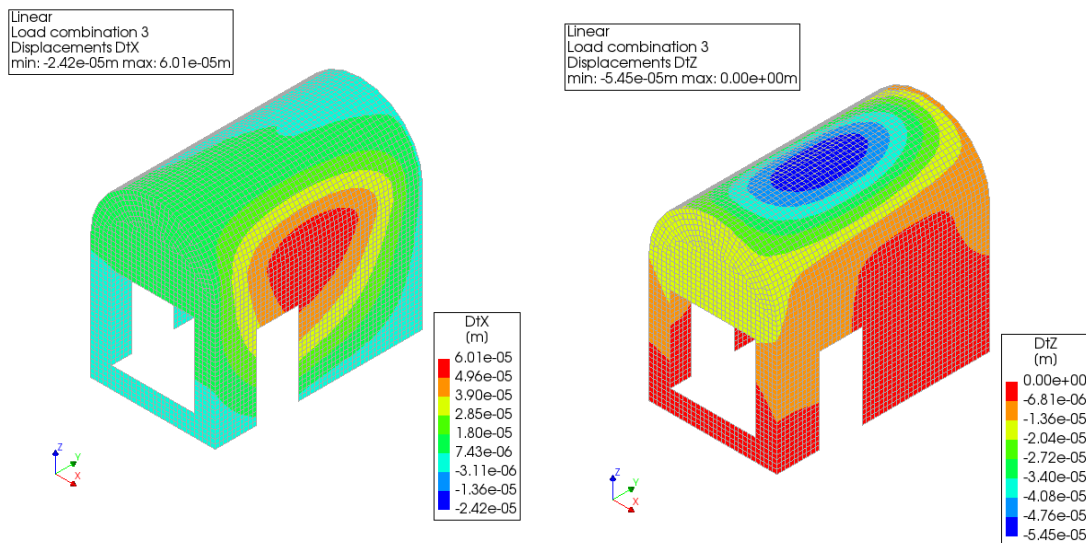


Figure 48: Deformation under self weight and wind load (combination 3)

Here only the deformation of the structure in X and Z direction is chosen because the displacement in Y direction is less compared to X direction. From the above figure, it can be seen that the maximum displacement in the X direction is about 0.06 mm, which occurs at the roof above the door on the leeward side, and the maximum displacement in the Z direction is about 0.05 mm, which occurs right in the center of the roof. It can be seen that the maximum displacements all meet the code requirements.

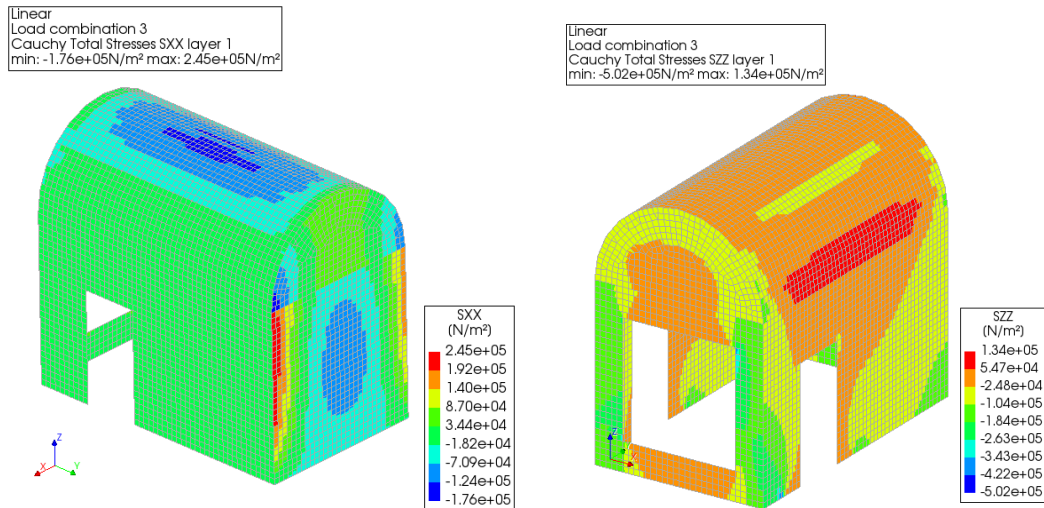


Figure 49: a) Cauchy total stresses (SXX) where the maximum tensile stress occurred; b) Cauchy total stresses (SZZ) where the maximum compressive stress occurred.

The two diagrams above show where the maximum tensile and maximum compressive stresses occur during the service phase. Stress (Sxx) is the force per unit area acting in the x direction on a plane perpendicular to the x axis. It can be seen that the maximum structural tensile stress is located between the back and side sides of the structure leeward of the wind and is about 0.25 Mpa. while the maximum compressive stress occurs at the corners of the windows as well as at the bottom edge of the structure and is about 0.5 Mpa. Both are less than the tensile and compressive strengths of the material, which satisfy the code requirements.

The linear static analysis was used for the first analysis, and the focus in the results obtained from the analysis was on the deformation and Cauchy total stresses. It can be seen from the figure that for the total stresses, the absolute values of stresses at the window corners of the front façade and at the connection between the side façade and the roof are large, and fiber reinforced concrete can be added to these weak areas during construction. However, it should be noted that this analysis only considers the areas where the structure is stressed under the combination of wind and gravity loads in the steady state and does not consider other loads that may arise during construction, such as the temporary support structure, which may arise and will continue to be analyzed in the subsequent study.

5.3 Nonlinear Analysis During the Structural Printing Phase

After analyzing the complete structure of the first phase, the analysis of the printing process, which is more detailed in structure, begins in the second phase. Before performing the analysis, slicing needed to be done to simulate the effect of 3D layer-by-layer printing, which also makes the analysis results more accurate. In order to simplify the analysis, the height of each layer is set to 0.1m, which may be higher than the layer height of one layer printed in actual 3D printing, and the main purpose is to reduce the calculation time under the premise of guaranteeing the calculation accuracy. Due to the different walls to be printed for certain layers and the possibility of adding temporary supports from printing certain layers, the printing phase of the main body of the structure was divided into two, the printing of the first 20 layers and the printing of the 21st to 30th layers.

The total printing time will be influenced by several factors, such as nozzle size, printing speed and number of printers. According to the research results of Nguyen-Van et al. (2022), different printing speeds will not only cause different printing time, but also different concrete properties, which will lead to different structure stability. Here 70mm/s was taken as the normal printing speed, which was also commonly used in industry. The nozzle size was set as 25mm.

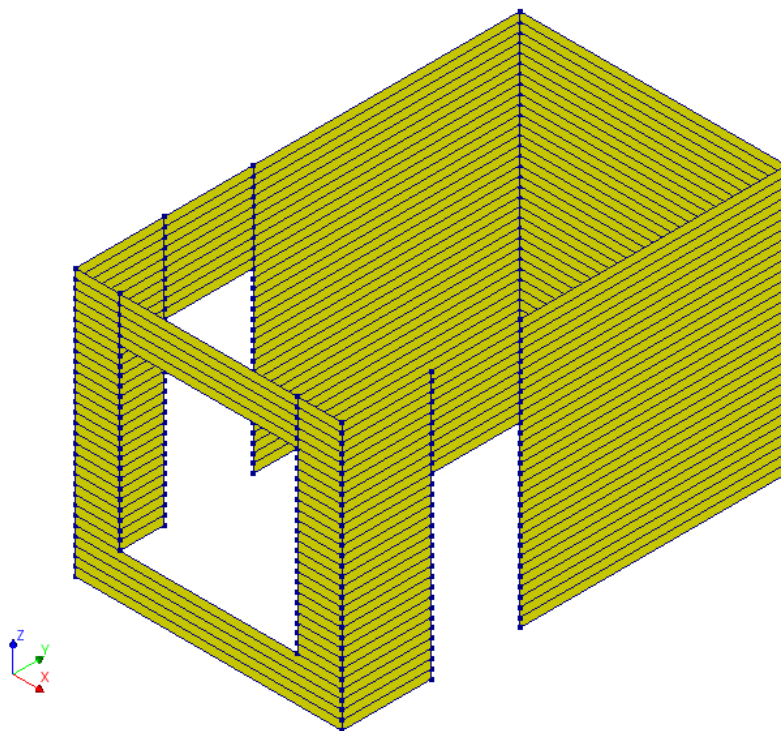


Figure 50: Slicing (0.1m per layer)

As shown in the figure, 0.1m is the height of a layer simulated by the software for calculation, not the height of a layer printed by the printer during the actual 3D printing process. The

simulated layer is the height of the actual printing of four layers. The structural slicing does not include the roof because the roof will also be printed on site and assembled later, and it will be printed in a different direction than the main body of the structure, so only the main body of the structure is layered here. The entire printing process consisted of a total of 30 layers, with the front elevation of the structure left open for windows from the 6th to the 25th layer, and the two sides of the structure left open for doors from the first layer to the 20th layer.

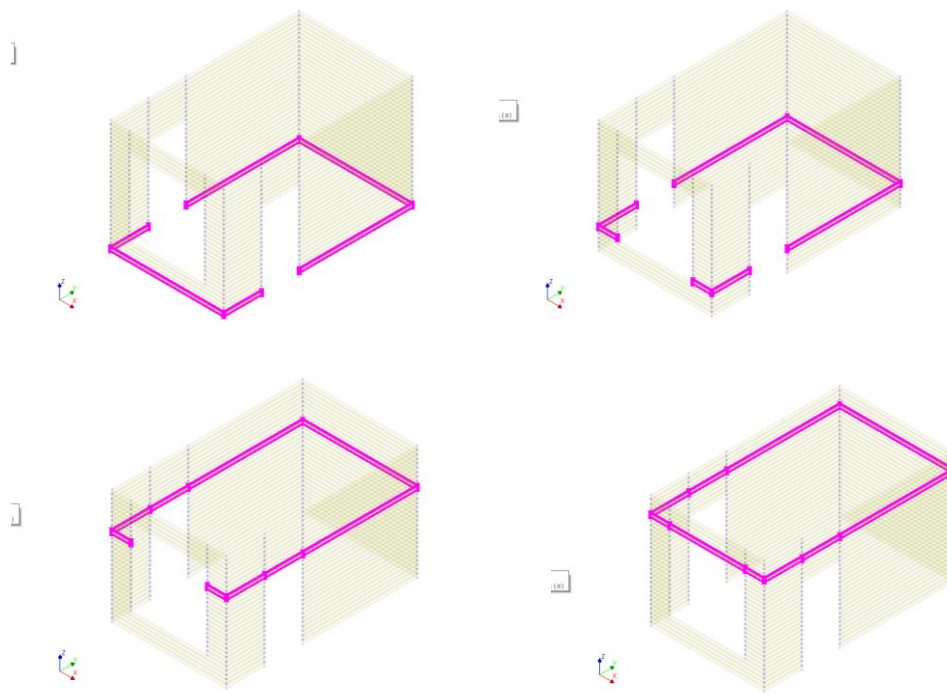


Figure 51: Four types of print building components depending on the number of layers printed, 1 to 5 layers, 6 to 20 layers, 21 to 25 layers and 26 to 30 layers, respectively.

There are two printers working on the whole process of printing and will keep the same printing time for both parts of each layer. As can be seen from the above figure, the structural components printed at certain times are not consecutive, so the two printers will print the components on one side separately.

A stability analysis was first done on the structure (i.e., Analysis 3 as mentioned in the introduction), as stability analysis is relatively simple and less computationally time consuming compared to phased and nonlinear analysis and allows for a quicker initial determination of the maximum number of layers the structure can be printed to.

For the material parameters used in this analysis, since the stability analysis did not introduce a time parameter, the effect of maturity on material properties did not need to be taken into account in this analysis, and therefore the final material parameters used are listed below. The wall thickness was set at 0.1m thick and all wall elements in DIANA were shell elements. The support is the same as in the previous static analysis, so it is not specifically described here.

Since this analysis is the printing stage of the analyzed structure, only self-weight is considered for loading.

Table 12: Concrete (linear) properties

	Young's modulus	Poison's ratio	Mass density
Concrete (linear)	1.8e+07 Pa	0.3	2100 Kg/m ³

Analysis3
Mode 1, Buckling value 0.99739
Displacements D1X
min: -1.00m max: 1.00m

Command console

```
print( "Structure fails when printing layer "+str(n) )
else:
    print( "Structure is stable" )printing layer 1 buckling value = 2.4152
printing layer 2 buckling value = 2.0439
printing layer 3 buckling value = 1.6259
printing layer 4 buckling value = 1.3422
printing layer 5 buckling value = 1.1434
printing layer 6 buckling value = 0.99739
Structure fails when printing layer 6
```

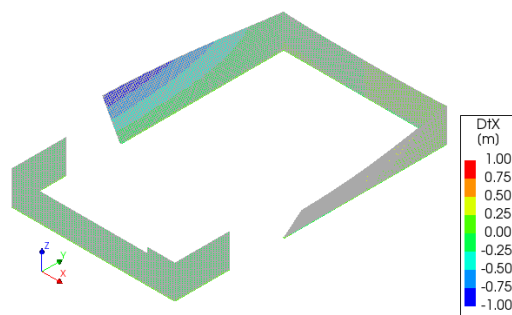


Figure 52: Structural deformation and stability analysis results (buckling value)

The results of the analysis 3 done on the overall structure showed that the structure was only able to successfully print five layers and would start printing the sixth layer with two walls showing significant instability and subsequently collapsing causing the entire analysis to stop. It can also be seen from the above figure that the buckling value decreases with the increase in the number of layers until the 6th layer when the buckling value is less than 1, indicating that the structure will fail at this point.

In order to ensure the accuracy of the analysis, it is not enough to do a stability analysis, but it is also necessary to continue with the phased and nonlinear analysis to obtain more accurate results. Prior to this, only half of the structure was intercepted in order to reduce computational time and because the structure analyzed was symmetric.

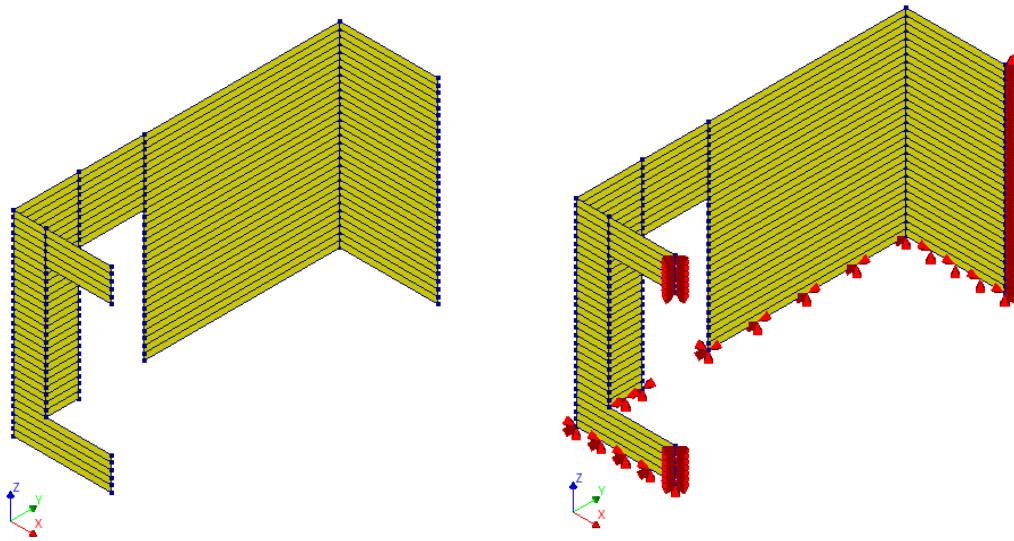


Figure 53: Half of the structure and the supports

Since Analysis 2 introduces a time parameter, it is necessary to consider the effect of maturity on material properties. According to Wolfs et al (2018), set the pattern of different properties of concrete with time as shown below.

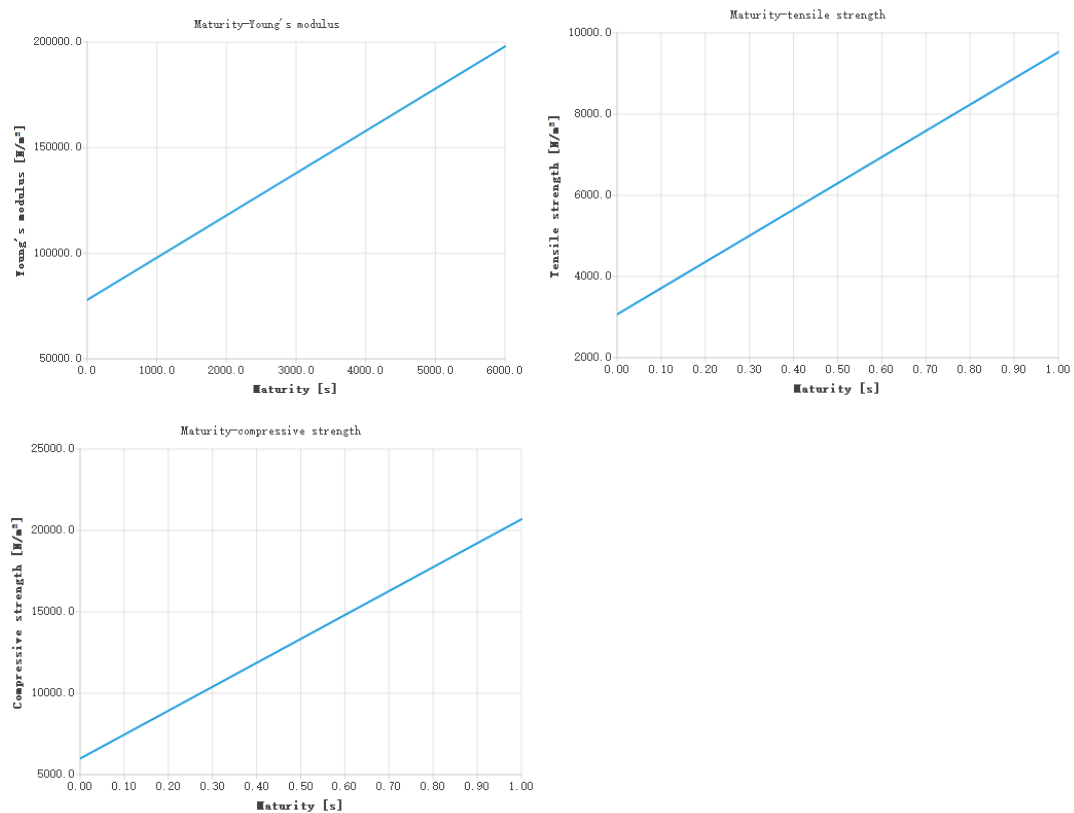


Figure 54: Young's modulus, tensile strength, and compressive strength of early concrete over time.

In terms of the boundary conditions, in addition to the same supports of the simulated foundation as in the previous analysis, boundary supports formed due to the fact that only one half of the structure was taken to simulate the supports formed by the other half of the structure were added. Thus, supports were added at the edges of the symmetric structure to limit the horizontal displacement in that direction, while displacements and rotations in the other directions were unrestricted, and the final supports are shown in figure 53. According to the printing speed and nozzle size, the printing time for each layer was considered to be 3930 seconds. The calculation in detail can be found in 5.4.

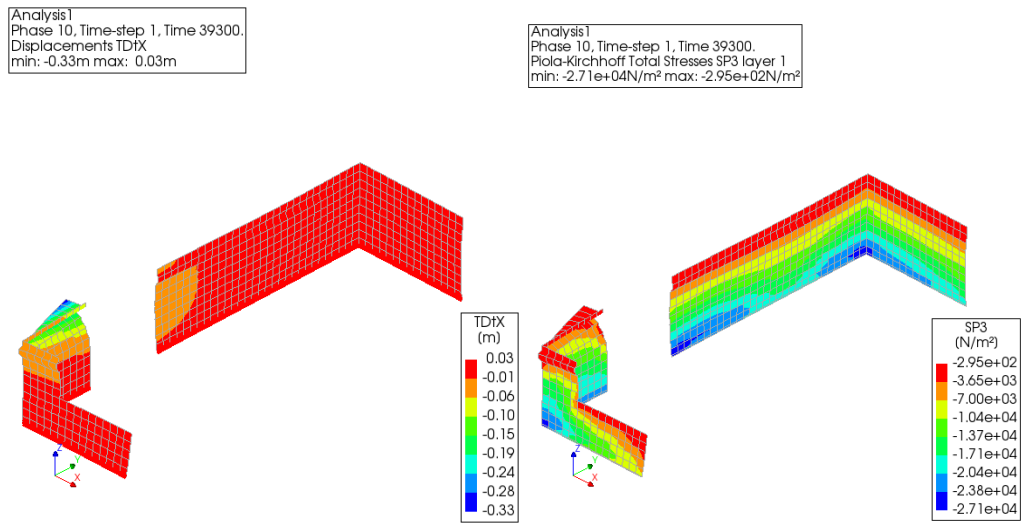


Figure 55: Deformation and stress at the maximum number of printable layers

As can be seen from the figure above, Analysis 2 predicted that the structure will only be successfully printed up to the 10th layer and will collapse when the 11th layer is printed. This result was slightly different from the one obtained in the previous analysis 3 and illustrated the need to perform analysis 2.

Based on the results of the above initial analysis, an analysis of the causes of premature failure during structure printing begins below. Since the results show that the walls that collapsed were on the shorter side of the wall, single walls were analyzed and calculated first to simplify the calculations and to further enhance the understanding of the various parameters that affect the printing process.

5.3.1 Parameter study

The first is the lack of edge support wall stability analysis, since the maximum length of the continuous wall to be printed in the structure analyzed was 3m, 3m was chosen as the length of the wall in the single wall test, and due to the presence of the door, from the first layer to the twentieth layer, the wall will lack support on one side, which also led to the collapse of the wall on both sides due to instability in the printing process. To simplify the analysis, a separate model

with only 3m walls was built for separate analysis. In this analysis, four parameters that have a significant impact on the printability of the structure will be considered separately, the temporary supports, the wall width, the Young's modulus of the material, and the structural print speed. By varying one of them separately, the four parameters will be tested for their contribution to the stability improvement of a single wall.

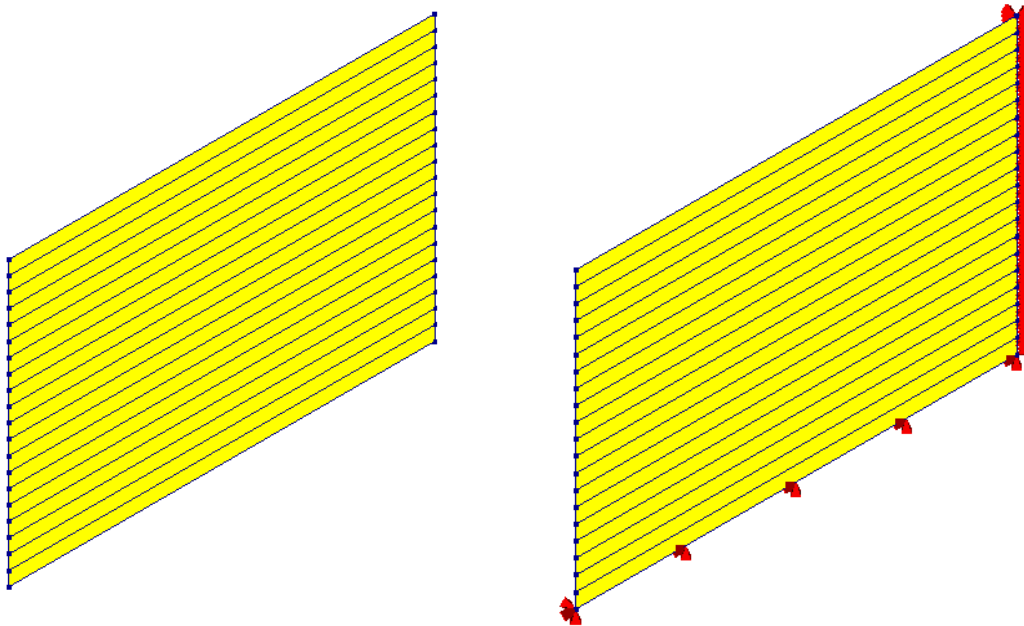


Figure 56: Geometry of single-wall tests and boundary conditions

The materials used for the single wall test were the same as those analyzed previously. As can be seen from the figure above, the boundary conditions used for this test, in addition to the same foundation support as before, were added to simulate the support of the wall on the other side of the wall, and therefore the vertical support was set to limit the horizontal displacement of the wall (in the X and Y directions), while the displacement in the Z direction and the rotation in all three directions were not restricted. The thickness of the wall was also taken as before, as 0.1 m. In the single wall test, only the dead weight was considered, as the analysis was still in the printing phase of the wall. In terms of printing time, since a wall with a length of only 3m was analyzed, the printing time was reduced accordingly and calculated as 60 seconds.

Analysis2
Phase 6, Time-step 1, Time 360.00
Displacements TDtX
min: -1.47e-17m max: 3.54e-15m

Analysis2
Phase 6, Time-step 1, Time 360.00
Piola-Kirchhoff Total Stresses SP2 layer 1
min: -7734.42N/m² max: 3000.00N/m²

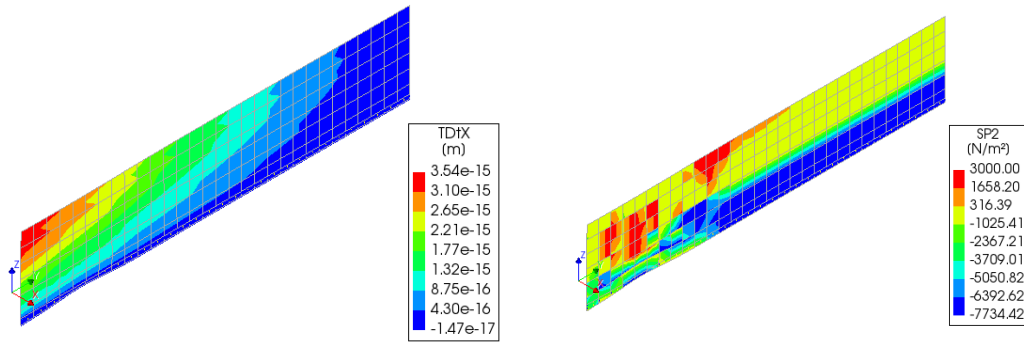


Figure 57: Deformation and stress when printing to the maximum number of layers

Since the deformation of the structure in the X direction was significantly larger than that in the Y direction, only the analytical results of the deformation in the X direction are taken. It can be seen from the above figure that the structure can only be printed up to the 6th layer at the most. This result was the same as the result obtained from the overall structural analysis done before, which can prove that this section of the wall is the main cause of the collapse of the whole structure in the previous analysis, and also proved the accuracy of the prediction of the previous analysis.

The next step will be to change each of the four previously mentioned parameters and again analyze the effect of these four parameters on the maximum number of layers the structure can be printed to. The parameters that will be changed are the presence of temporary supports, increasing the thickness of the wall (from 0.1 m to 0.2 m), increasing the Young's modulus of the material (to three times the original) and using a longer print time (from 60 seconds per layer to 90 seconds per layer). The other three parameters are better understood, the purpose of changing the printing time is to allow more setting time for the concrete, which results in a higher Young's modulus and compressive and tensile strength.

The first parameter is the addition of a temporary support, which appeared as an extra wall that will be printed along with the wall structure. As can be seen in the figure below, this temporary support still limited the displacement of the structure in both the X and Y directions, the same as the other vertical support that was set up previously. All parameters except temporary support remained the same as before.

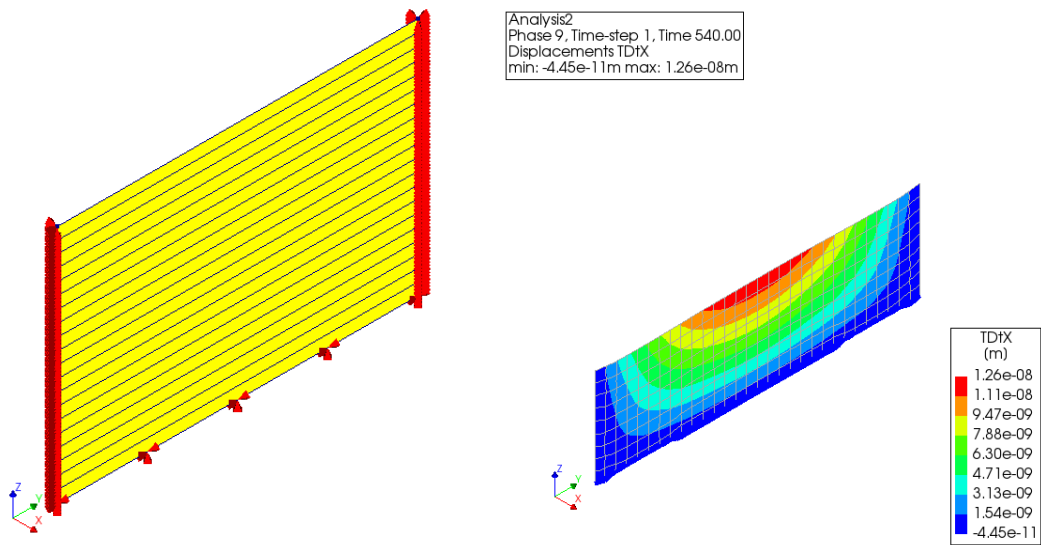


Figure 58: Increased temporary support and maximum number of layers the structure can be printed to

It can be seen from the above figure, the addition of temporary support increased the maximum number of layers that the structure can be printed to layer 9, which is an improvement over the previous one.

The next parameters to be changed are the thickness of the wall and the Young's modulus of the material, respectively. Since the deformation of the structure is the most obvious way to determine whether the structure has failed or not, only the deformation of the structure was taken as a criterion for this analysis.

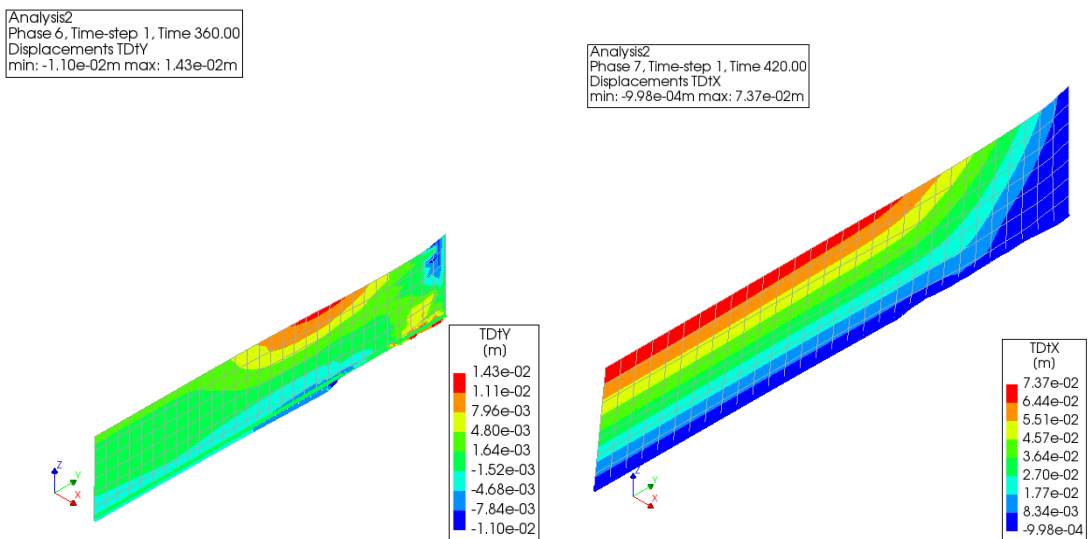


Figure 59: Maximum number of layers that can be printed by varying the structure thickness (Left) and Young's modulus (Right), respectively.

As can be seen from the results shown above, changing the thickness of the structure did not have a significant effect on the maximum number of layers that can be printed to, whereas changing the Young's modulus had some positive effects. From this analysis it can be concluded that Young's modulus plays an important role in controlling the deformation of the structure during the printing process.

The last parameter was to increase the printing time per layer, which was initially chosen to increase from 60 seconds per layer to 90 seconds per layer, thus allowing more time for the material to harden, i.e., to obtain higher strength as well as Young's modulus.

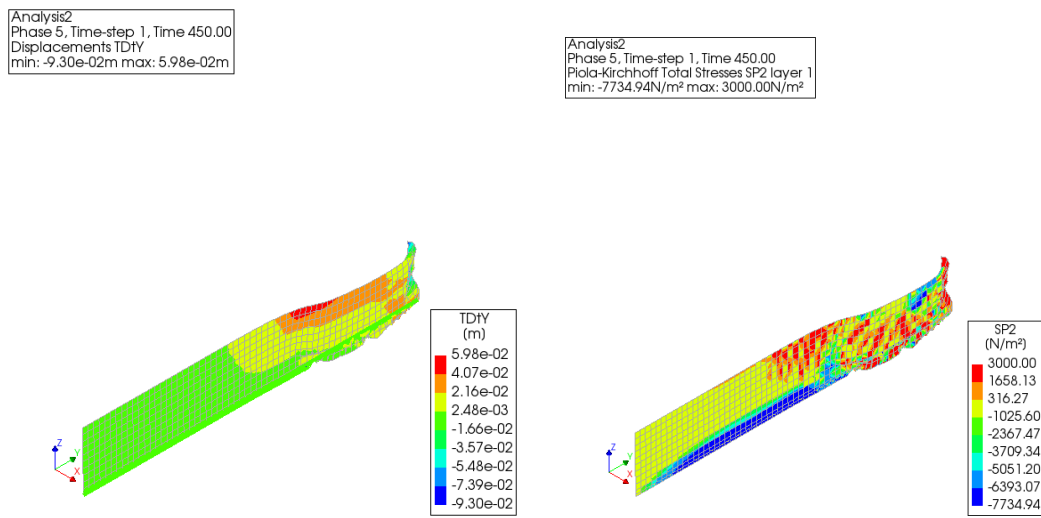


Figure 60: Maximum number of layers that can be printed on the structure after changing the print time and stress distribution.

As can be seen in the figure above, the maximum number of layers that the structure can be printed to is 5 and will deform significantly at the 6th layer printed, causing the structure to collapse. This result was not expected as the material gained higher strength and Young's modulus, and a possible reason for the structure failing to print to a higher number of layers is that the increased print time was not long enough, resulting in the material not increasing its properties enough to support printing to more layers.

Table 13: Parameters affecting the maximum number of layers that can be printed and their effects.

Parameter	The maximum number of layers that can be printed
None	6
Temporary support	9
Thickness	6
Youngs' modulus	7
Printing speed	5

As can be seen from the table, changing the thickness of the structure and increasing the print time had no significant effect on the printability of a single wall, the other two parameters both had some degree of improvement on the printability of the structure, with the temporary addition of horizontal support to the structure having the most obvious effect, in which case the structure can be printed up to the 9th layer. However, it can also be found that even if these parameters are changed, the final effect is not enough to make the structure printable. Therefore, the next research direction became the simulation of structural components in DIANA. In all the tests done before, the walls were set up as shells, but the geometry did not correspond to the shape of the walls in the actual printing process, which could potentially lead to structural failure. In order to determine the effect of this factor, the wall structure was next modeled in DIANA, i.e., trusses were added, and the print performance of this wall was analyzed and tested.

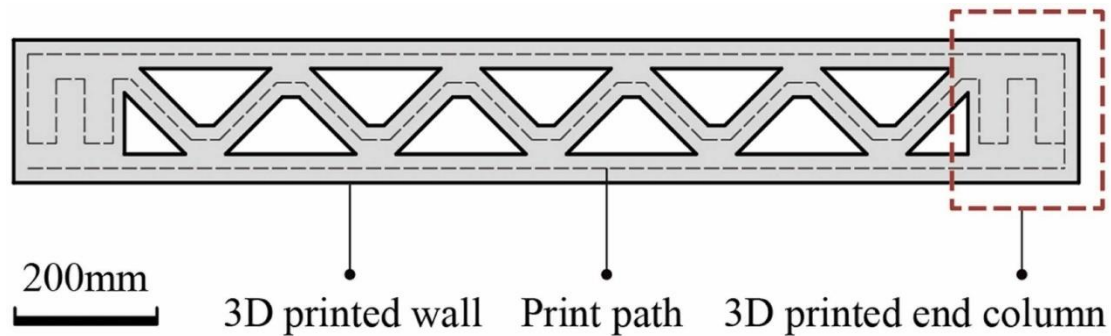


Figure 61: Structural walls printed on site (Xu et al., 2022)

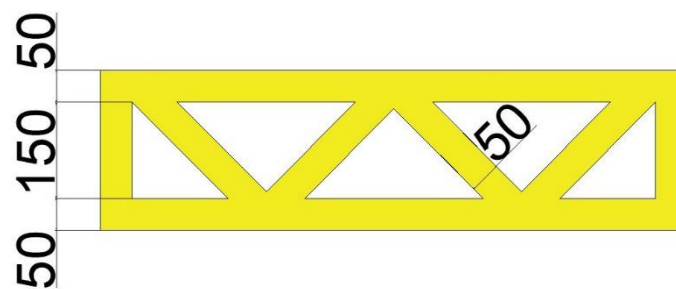


Figure 62: Truss structure wall simulated in DIANA

Before performing the test, there is another parameter that has to do with FEA that may affect the results of the test, which is the mesh size. The mesh size not only affects the accuracy of the calculation, but also the time required for the calculation. When subsequently analyzing complex structures, if the mesh size is set too small, the calculation time can become very long. Therefore, it is first necessary to test the accuracy of the calculation with different mesh sizes. The size of the mesh also has a significant impact on the calculation time and the accuracy of the results, so some tests need to be performed to determine the appropriate size and to reduce the calculation time of the structure.

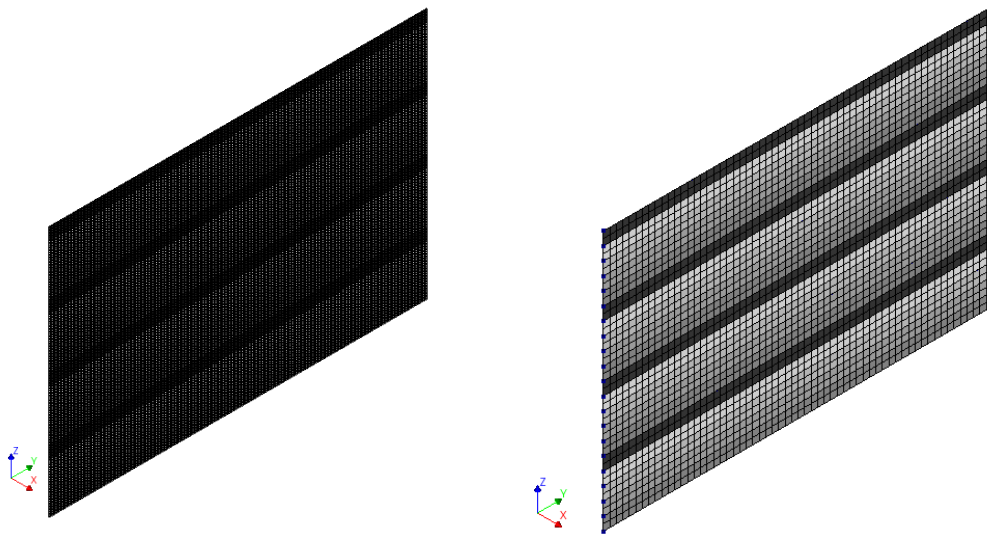


Figure 63: Different mesh sizes

Through testing, it was found that the analysis results were the same when the mesh size was 0.1 m and when the mesh size was smaller, indicating that 0.1 m is an acceptable mesh size and is exactly the same height as the printed layer, which is simpler. Therefore, the 0.1 m mesh size was used for all subsequent analyses.

5.3.2 Wall structure tests

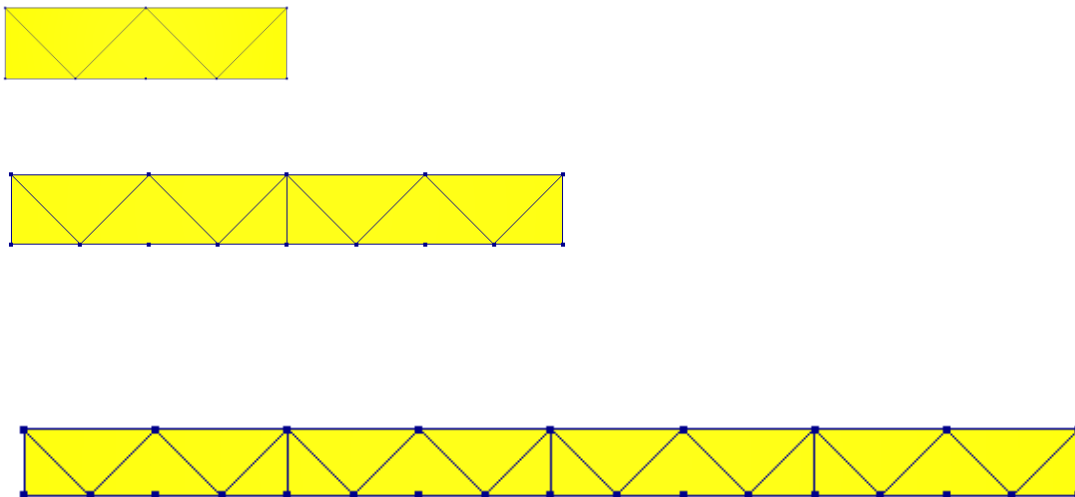


Figure 64: Three different lengths (0.8m, 1.6m, 3.2m) of truss structure walls

Based on the printing speed as well as the nozzle size, the printing time for each layer of each of the three types of walls was calculated as follows.

$$T_1 = (0.8 + 0.2 + 0.8 + 0.2 + 1.13) \times 2 \times 4 \div 0.07 = 360 \text{ s}$$

$$T_2 = (1.6 + 0.2 + 1.6 + 0.2 + 2.26) \times 2 \times 4 \div 0.07 = 670 \text{ s}$$

$$T_3 = (3.2 + 0.2 + 3.2 + 0.2 + 4.52) \times 2 \times 4 \div 0.07 = 1300 \text{ s}$$

Firstly, a wall length of 0.8 m was selected. For the truss structure, the thickness of both the outer wall and the truss is 0.05 m. The spacing of the centerline of the outer wall is 0.2 m, so the thickness of the whole wall is 0.25 m. For shell structure, the thickness of the wall is 0.25m for direct setting. Ensuring the same thickness of both structures, the structural printing performance was tested. For materials, all materials used for the truss walls were the same as those used in several previous analyses. The entire wall is also supported only by the foundation at the bottom, with no other horizontal or vertical support. Only self-weight was considered during the analysis.

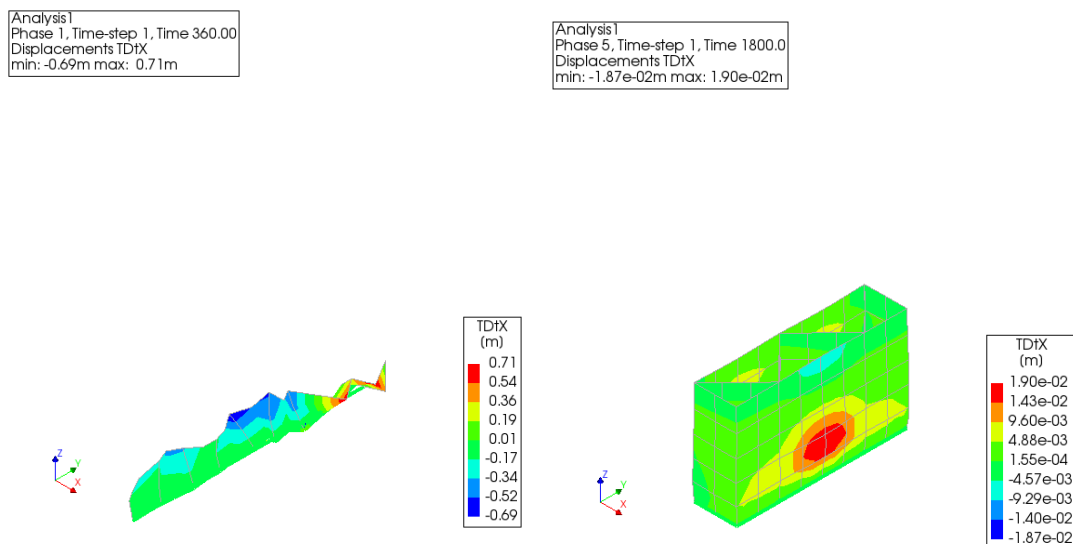


Figure 65: Number of printed layers for different wall structures at a wall length of 0.8 m

From the results shown above, it can be seen that the maximum number of layers that can be printed on the truss structure wall and the shell wall were different. The shell element wall would collapse immediately upon analysis, i.e., it would be essentially inaccessible for 3D printing. This is due to structural instability, and there are two possible reasons for this failure at the first layer of printing, the first is that the calculated single layer height set was high (0.1m), and the structure is unable to print to a height of 0.1m, and the second possible reason is that the shell element did not simulate the actual printed truss structure wall well in DIANA. And for the truss structure wall, it can be successfully printed up to the fifth layer.

In order to further understand the impact of wall length, the truss structure and the shell element

structure with both lengths of 1.6m were selected for comparison. All parameters were the same as in the previous analysis except for the wall length.

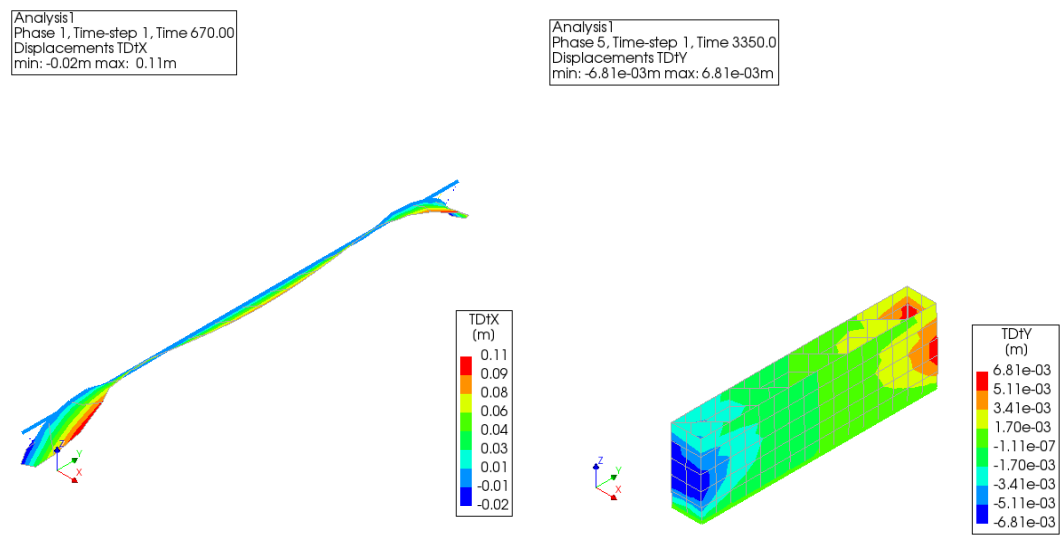


Figure 66: Number of printed layers for different wall structures at a wall length of 1.6 m

From the figure, it can be seen that whether it is a shell structure or a truss structure wall, the results obtained were the same as the previous analysis. Therefore, the length of 3m wall was selected and tested again, 3m wall is also the length of the wall needs to be printed in the actual printing process, so the significance of this test is not only a comparison of the two structures of the wall, but also for the actual analysis carried out after the preparation.

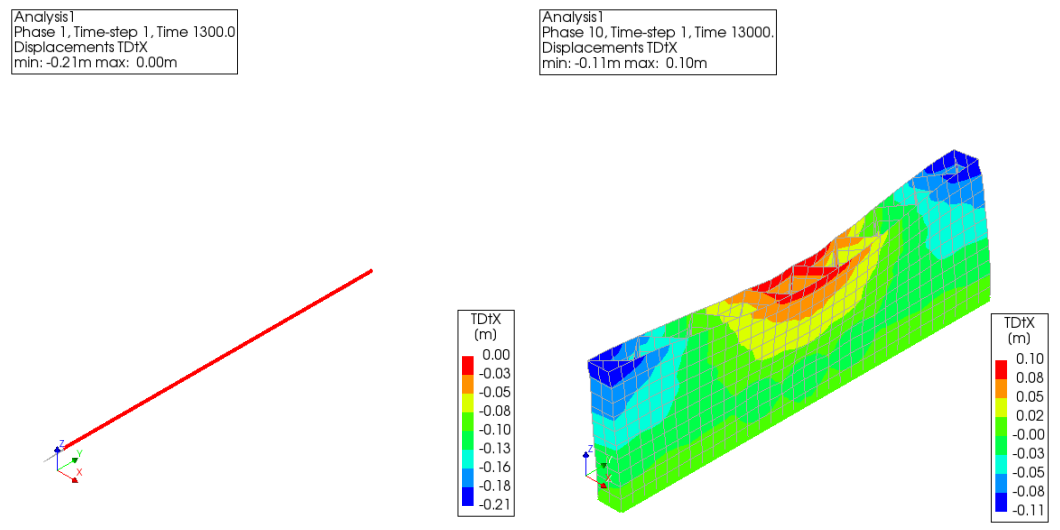


Figure 67: Number of printed layers for different wall structures at a wall length of 3.2 m

As can be seen from the test results, when the length of the printed wall is 3m, the shell unit structure collapsed at the first level, as did the results from the previous two analyses. The truss structure wall, on the other hand, was successfully printed up to the tenth layer, which is a more

significant increase compared to the previous two analyses. This indicates that the stability of the wall increases with the length of the wall within a certain range.

It is concluded that when printing walls of different lengths, the truss structure has a positive effect in terms of stability improvement due to the presence of trusses. Since a wall with a length of 3 m needs to be printed in the actual structure, it can be inferred from the results of the above tests that a truss structure would be a better choice, but still requires horizontal temporary support to avoid instability during the printing process.

Since in all three of the above tests the shell unit wall collapsed when the first layer was printed, which does not correspond to what happens in practice, the following additional test was conducted to test the performance of the shell element wall with horizontal support on one side of the wall.

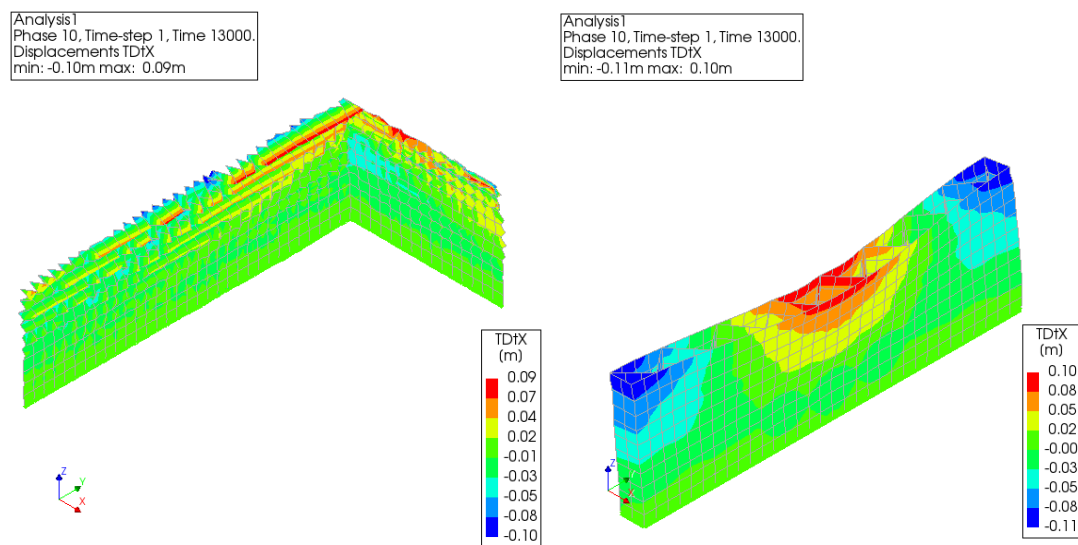


Figure 68: Number of printed layers for different wall structures at a wall length of 3.2 m

As can be seen from the results, the addition of horizontal support results in a shell unit wall that was very similar to a truss structure wall, both in terms of the number of layers that can be successfully printed and the displacement. Therefore, it can be approximated that the results of the shell element after adding the horizontal support and the truss structure wall are the same in DIANA.

5.4 Analysis of the printing process from layer 1 to layer 20

The first step is to model layers 1 to 20, after intercepting the general overall structure, the structure obtained was divided into two parts, at this stage of the analysis only the longer part of the wall was analyzed, because the probability of failure of this section of the wall during the printing process is higher.

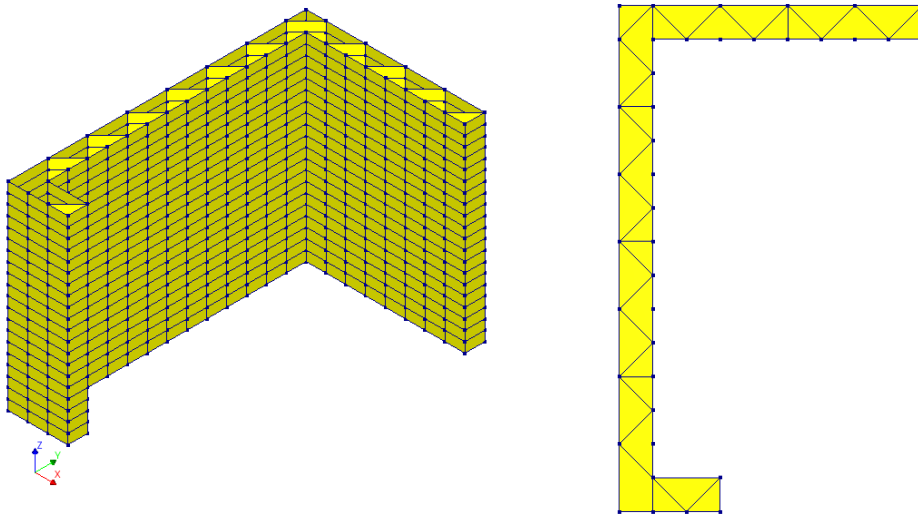


Figure 69: Truss structure wall and the top view

As the picture shown above, the printer will move from inside to outside gradually, and print the inner wall, truss, and external wall respectively. The length of the truss is:

$$L = (1.8 + 2.6 + 0.4) \times 1.414 = 6.8 \text{ m}$$

Therefore, the total printing time for each layer (below 20) is:

$$T = (0.4 + 2.6 + 1.6 + 0.2 + 1.8 + 3 + 0.6 + 0.2 + 6.8) \times 2 \times 2 \times 4 \div 0.07 = 3931 \text{ s}$$

The conclusion is the printing time for each layer (below 20) was considered 3930s.

Stability analysis was done before performing phased and nonlinear analysis. The main reason for this was that the stability analysis was simpler, and it allowed for a preliminary determination of whether the structure would be unstable during the printing process. The final results are shown below.

```

print( "Structure is stable" )printing layer 2 buckling value = 402.61
printing layer 3 buckling value = 277.58
printing layer 4 buckling value = 194.67
printing layer 5 buckling value = 142.16
printing layer 6 buckling value = 107.88
printing layer 7 buckling value = 83.763
printing layer 8 buckling value = 66.27
printing layer 9 buckling value = 53.562
printing layer 10 buckling value = 44.232
printing layer 11 buckling value = 37.286
printing layer 12 buckling value = 32.042
printing layer 13 buckling value = 28.029
printing layer 14 buckling value = 24.915
printing layer 15 buckling value = 22.463
printing layer 16 buckling value = 20.5
printing layer 17 buckling value = 18.897
printing layer 18 buckling value = 17.552
printing layer 19 buckling value = 16.386
printing layer 20 buckling value = 15.335
Structure is stable
\

```

Figure 46: Results of stability analysis

As the figure shown above, all of the buckling values were all greater than 1, the stability of the structure during the whole printing process will not be a problem. Therefore, phased and nonlinear analysis followed. For the boundary conditions, in addition to the foundation supports, supports limiting displacement in the X direction were added at the edges of the structural walls to simulate the effect of the other half of the walls due to the horizontal support effect of the other half of the structure.

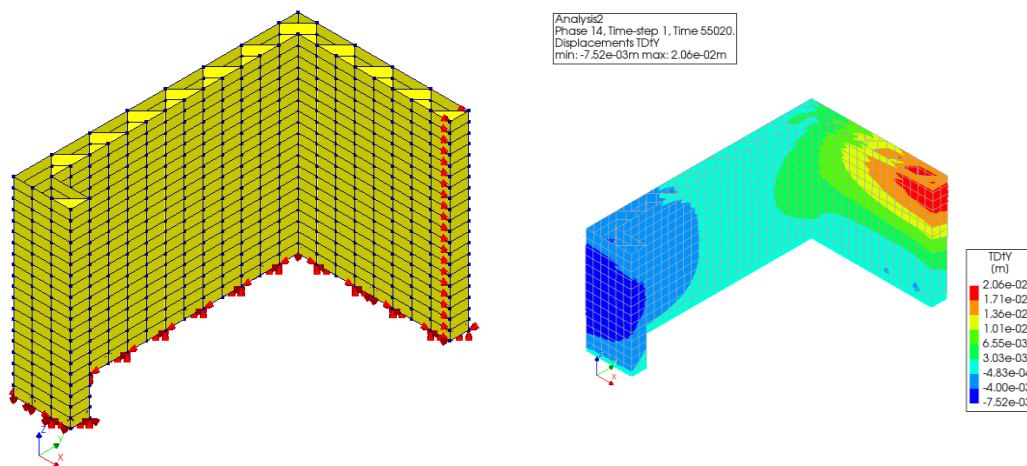


Figure 70: Boundary conditions and maximum number of layers the structure can be printed to

As can be seen from the results shown in the figure above, the structure can be printed up to the 14th layer and will deform significantly and then collapse when the 15th layer is printed. Therefore, it is necessary to change several important parameters that can affect the printing results, according to the conclusion of the previous parameter study. Next, the thickness of the walls and trusses were increased to re-test whether the structure could be printed to a higher

number of layers. However, the results showed that the number of layers that could be printed was the same, indicating that the thickness of the structure did not improve the performance of the structure in this test, this result is the same as the previous conclusion from parameter study. In general, increasing the thickness of the structure improves the stability of the structure, and since the stability tests performed previously showed no problems, these two results suggested that the reason for the structure not printing to higher levels is due to material properties rather than stability.

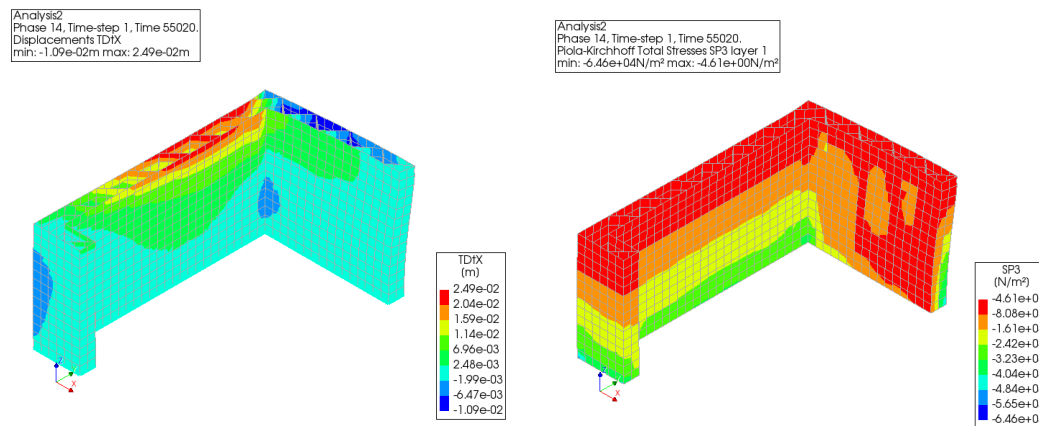


Figure 71: Maximum number of layers the structure can be printed to after changing the compressive and tensile strength of the material and the stress distribution.

In the next step, the tensile and compressive strength of the material was increased and retested. The results remained the same as before, indicating that the failure of the structure was not due to the material somewhere in the structure being unable to withstand the increased tensile or compressive stresses (as shown in the figure above), but rather the failure was caused by excessive deformation somewhere in the structure.

Therefore, fiber reinforced concrete needs to be introduced at this point. According to the conclusions of Mink's thesis (2019), Young's modulus of fiber reinforced concrete will reach 10 times that of ordinary concrete when it is first extruded, and 2 times that of ordinary concrete after 90 minutes. Therefore, the material properties of fiber reinforced concrete are set as follows.

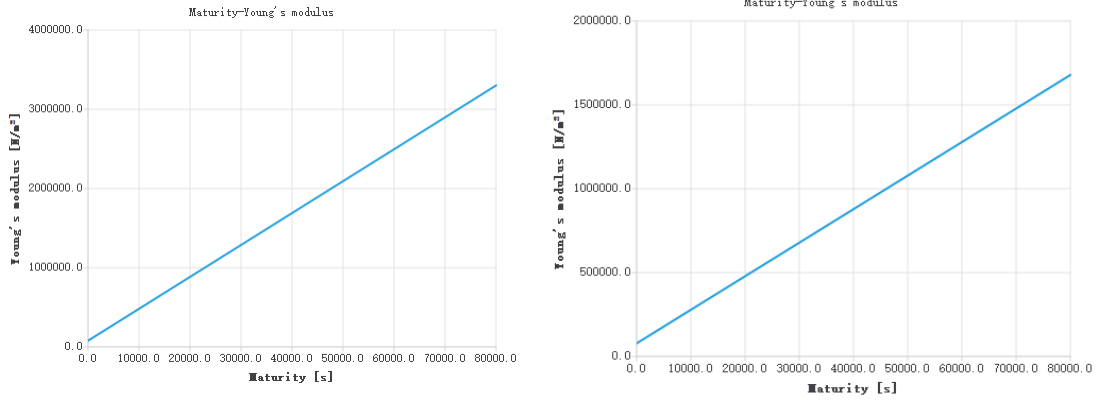


Figure 72: Young's modulus of fiber reinforced concrete (Left) and normal concrete (Right) with time.

After many attempts, i.e., constantly changing the position and amount of added fibers, starting from the 12th layer, the entire layer (including truss) was replaced with fiber reinforced concrete. This material not only increases the tensile and compressive strength, but also increases the Young's modulus at the same time, which are three material parameters that are very important in DIANA modeling. The results showed that the wall with the shorter length on the other side would fail first and collapse at the 15th layer due to excessive deformation in the Y direction, which was not the case in the previous tests.

So, for the last test, only the wall material with the longer length in the Y direction was changed to fiber reinforced concrete, while the other materials in the layer were changed back to the previous plain 3D printed concrete. This time it was finally possible to successfully print up to 20 layers.

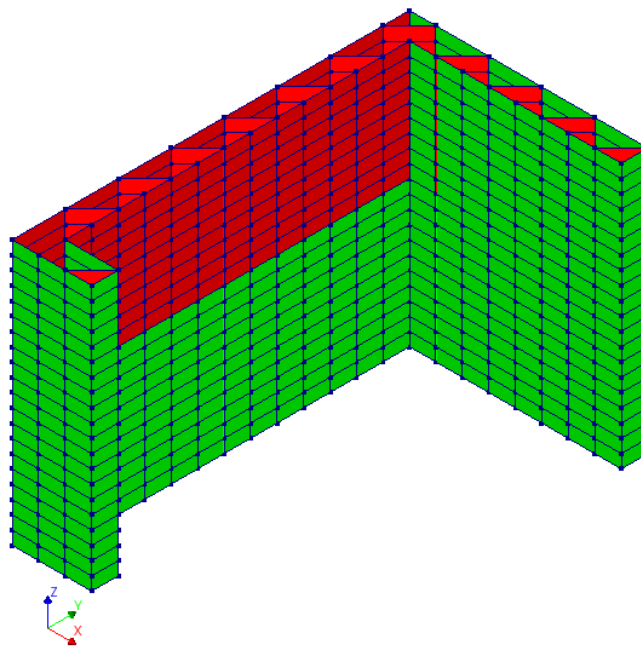


Figure 73: Material distribution of the structure: fiber reinforced concrete (red) and normal concrete (green)

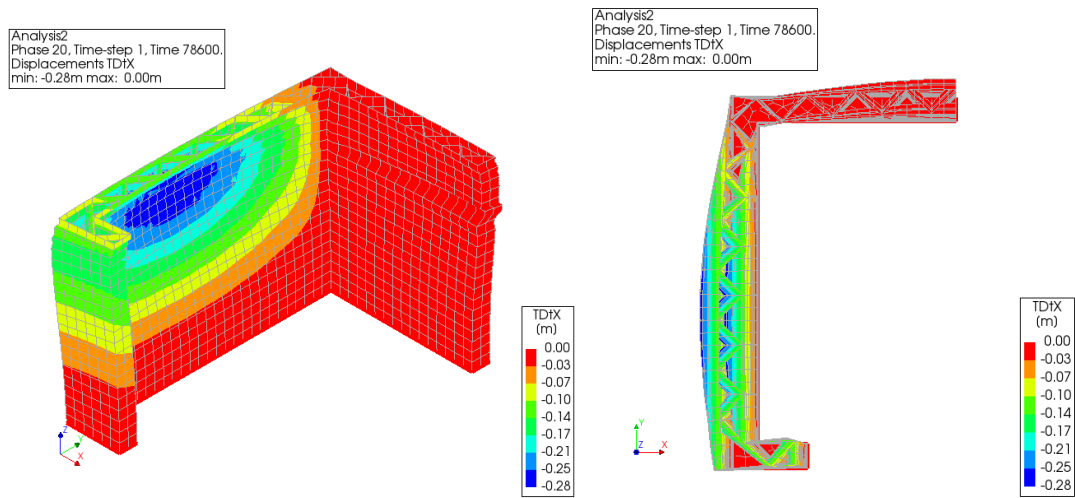


Figure 74: Deformation of the structure when printed to the 20th layer.

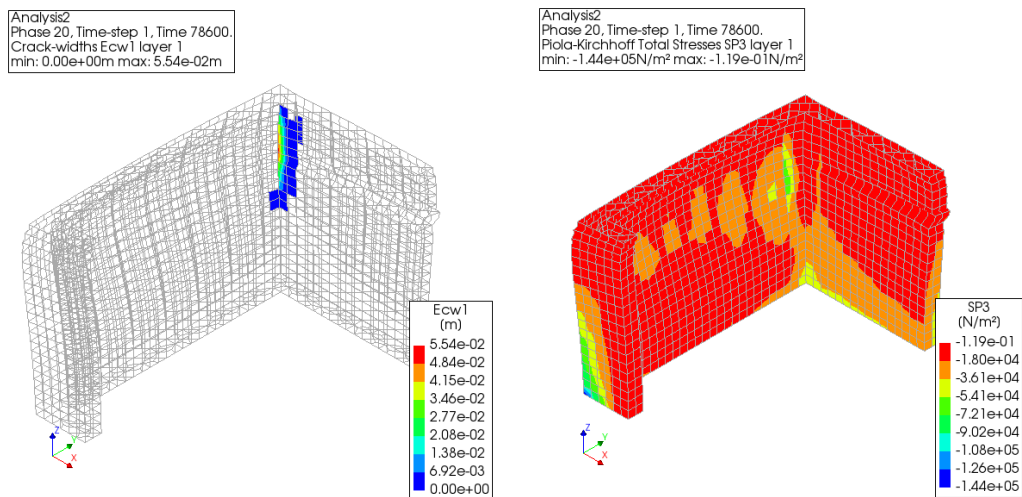


Figure 75: Cracks and stress distribution when printed to the 20th layer.

As can be seen from the above results, DIANA predicted that the structure can already be successfully printed up to the 20th layer. However, from the structural deformation shown in the above figure, it still did not meet the requirements in the code. In terms of cracks, the figure shows that the most likely location for cracks to occur is in the connection between the two longer walls, starting at about the 10th layer, and the width of the cracks is about 5cm, which is also relatively large. Further optimization of the material distribution will be done in the next chapter "Discussion". Regarding the stresses, it can be seen that the maximum stresses were also less than the corresponding strengths of the materials, so the stresses meet the code requirements. After the above analysis it can be concluded that the first 20 layers of the building can be successfully printed.

5.5 Analysis of the printing process from layer 21 to layer 30

The next stage of the printing process was the twenty-first through the thirtieth layers of the building, which was more challenging than the previous stage because the walls above the windows and doors needed to be printed. At this stage of the modeling process, it is no longer possible to model only the longer part of the wall, but also the shorter part of the wall, because the shorter part of the wall will need to be temporarily supported during the printing of the twenty-sixth and thirtieth layers, because of the need to print the wall above the windows, which will then be modeled to analyze the success of the printing.

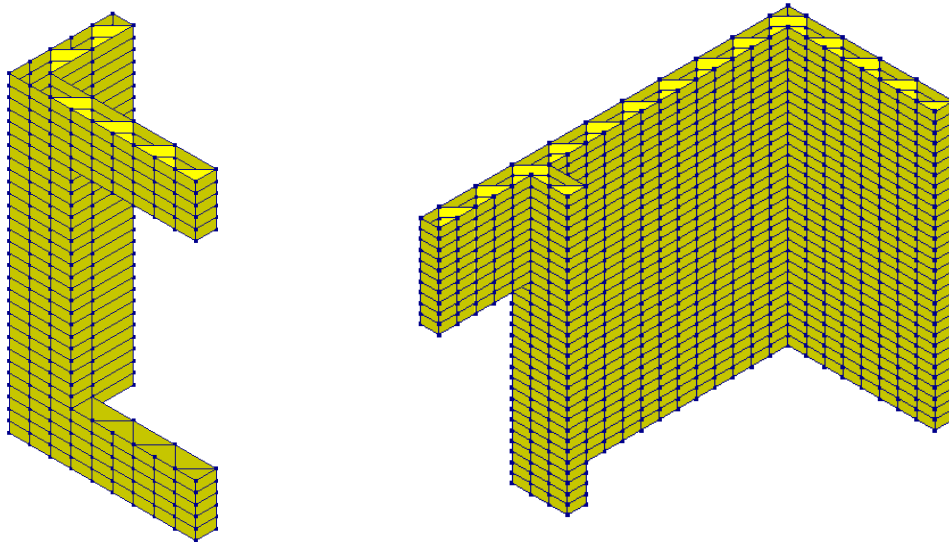


Figure 76: Geometry of 2 structures

The printing process of the longer part of the wall structure is first analyzed. For materials, as in the previous analysis of the first 20 layers, there are still two types of materials, i.e., normal concrete and fiber reinforced concrete. For the boundary conditions, on top of the previous analysis, there is no support since layers 21 to 30 are the wall above the door. Due to the low strength of the freshly pumped concrete, temporary support was used during this phase of the printing process. In the software modeling, the temporary support was set as a spring support because the fixed support would result in the wall above it not being able to deform in the z direction, while the other section of the wall connected to this part of the wall would be displaced in the z direction due to the deformability of the wall below it, resulting in a large displacement difference between the same section of the printed wall in the two parts, which would lead to structural damage.

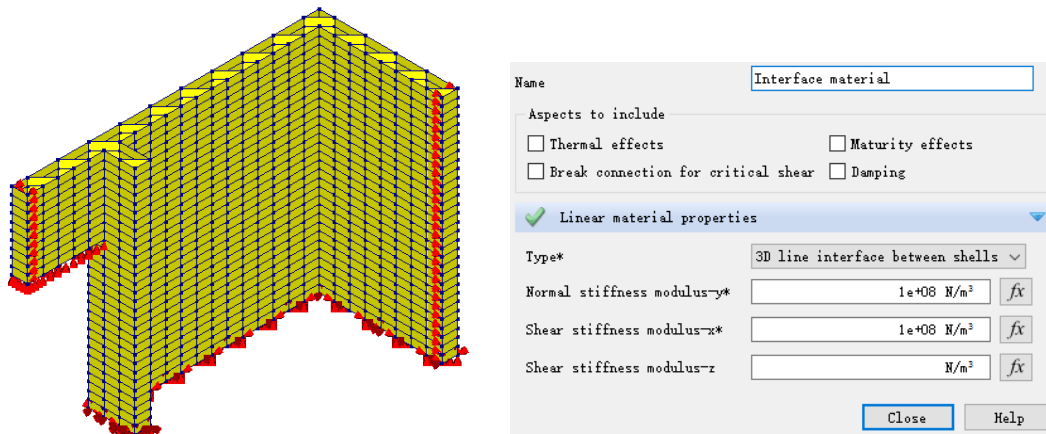


Figure 77: Boundary conditions of the structure and the interface material parameters

In order to implement the spring support, another material, the interface material, needs to be introduced into the modeling to simulate the presence of the spring support. The main parameter of the interface material is the stiffness modulus in the X and Y directions, which is the same as the spring stiffness.

After several adjustments to the distribution and number of fibers, a structural printing solution was finally obtained that could be successfully printed up to the 30th layer. Since the part of the wall printed on the 21st to 30th layers were only temporarily supported underneath, and since the previous analysis of the structure's use phase showed that the wall above the door was subjected to high stresses, fiber reinforced concrete was used for all the walls on the 21st to 30th layers for safety reasons.

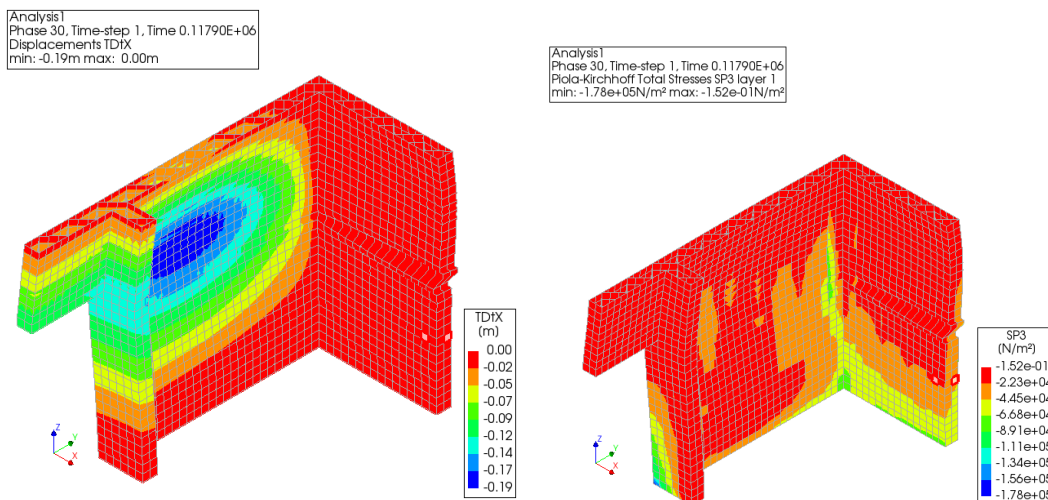


Figure 78: Structural deformation and stress distribution

The results shown above indicate that DIANA predicted structures can be successfully printed up to 30 layers. However, it can still be noticed that the deformation of the structure is large in some places and does not meet the code requirements. The stress distribution of the structure also showed that the largest tensile stresses occur at the corners of the structure. Based on these results, it can be assumed that the longer wall portion of the 30-layer structure can be successfully printed, and subsequent improvements will be made for the larger displacements in the next chapter 'Discussions'.

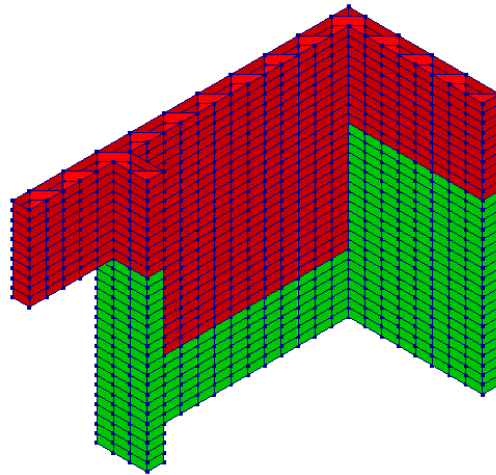


Figure 79: Material distribution of the structure: fiber reinforced concrete (red) and normal concrete (green)

The above is the result of conducting a feedback loop and continually trying to arrive at which part of the entire wall structure needs to be fiber reinforced concrete. The sections on either side of the main wall do not need to be made of the same concrete material as the walls on the same level. In previously tested software modeling, if the same fiber reinforced concrete had been used for the walls on either side, the structure would have collapsed during the printing process and the problem would have been in the walls on either side, not in the expected main wall.

The shorter portion of the wall was analyzed next, shorter length of the wall made this portion of the structure less likely to fail during the printing process, but this portion of the structure was unique in that the printing of the wall above the larger window is the most challenging portion of the structure.

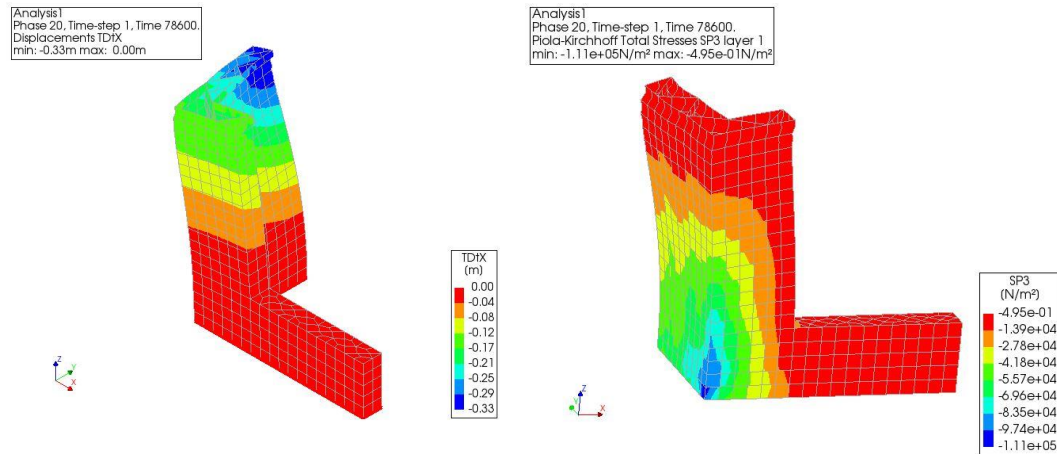


Figure 80: Structural deformation and stress distribution (without fiber reinforced concrete)

When all materials were normal concrete, the structure could only be printed up to the 20th layer and collapsed at the 21st layer due to excessive deformation. From the stress distribution it can be concluded that the maximum stress occurs at the bottom of the structure, so there are two options for adding fibers in the subsequent study. The first one is the same as the previous one, where fibers are added to the weak position of the structure, i.e., the printed layers near the windows, and the second one is to add fibers to the structure where the stresses were the highest, i.e., starting from the bottom, according to the stress distribution.

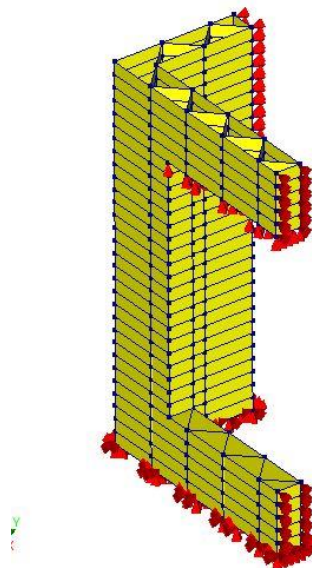


Figure 81: Boundary conditions

As with the previous structure, the wall above the window also required temporary support. The rest of the boundary conditions were similar to those for the longer portion of the wall.

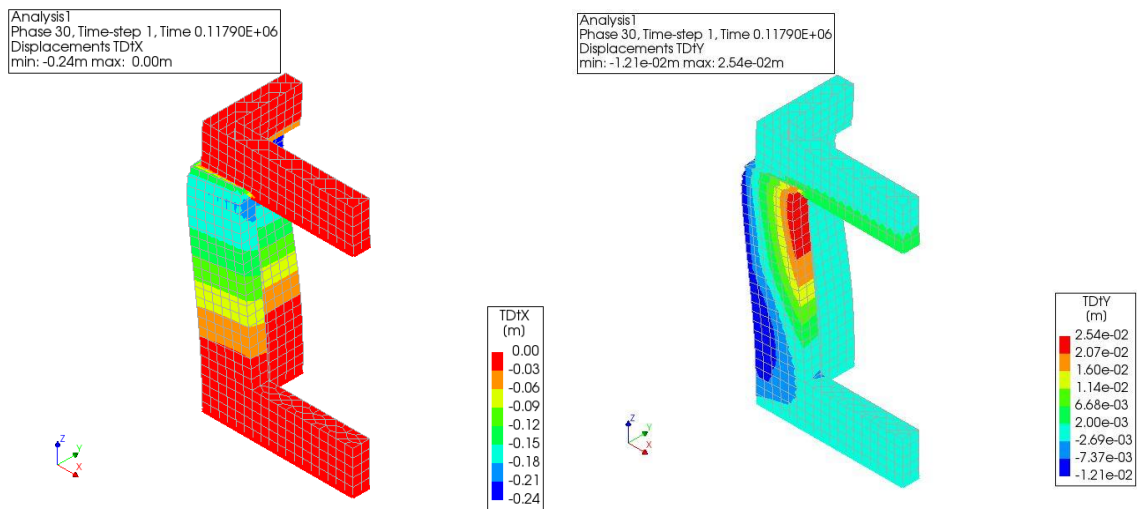


Figure 82: Structural deformation in X and Y direction

Looking at the deformation of the structure, there was a clear discontinuity in the structure at the 25th and 26th layers, which is not consistent with realistic 3D printing. The possible reason for the presence of the discontinuity in the X direction was due to the additional horizontal support (from the adjacent wall) that occurred from the 26th layer onwards, which results in pulling the walls of the 26th to 30th layers back to their original position and thus there was a clear discontinuity with the displacements that were created in the first 25 layers. In contrast, the discontinuity between this portion of the wall without horizontal support in the Y direction and the remaining portion of the wall was less pronounced.

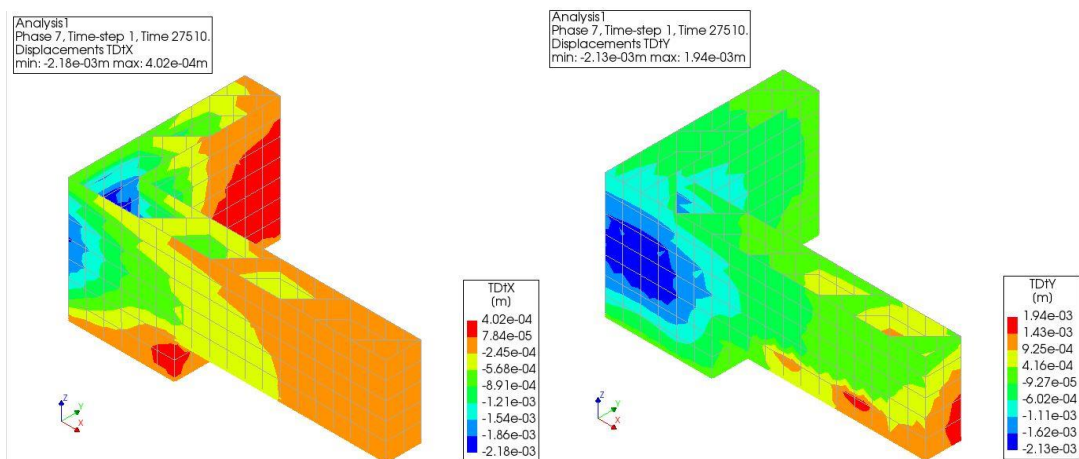


Figure 83: Displacement of remained structure.

Another reason is due to the excessive deformation of the first 25 layers, resulting in what can be clearly seen as a large difference in deformation from the 26th layer with the added horizontal support. In order to demonstrate this, the structure was removed except for the first 23 layers which were used for the analysis and the rest of the parameters were kept the same.

The results are shown above. It can be seen that when the deformation was small, the deformation of the whole structure was more continuous and did not have the above problem.

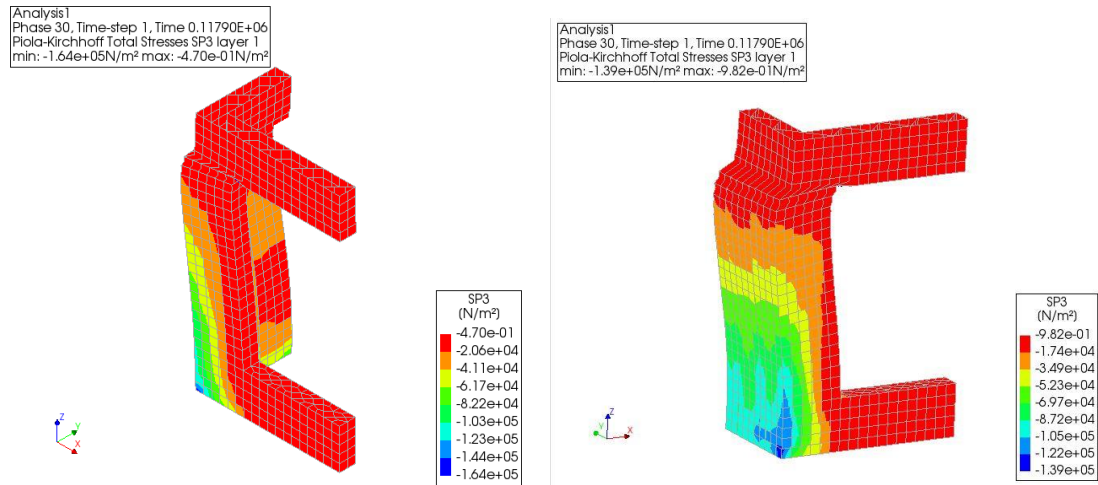


Figure 84: Stress distribution from different view

Based on the structural deformation and stress distribution, it can be noticed that in some parts of the structure the deformation remained high and exceeded the code criteria. This part will also be optimized in the next Chapter 'Discussions'. The highest structural stresses are found at the corners of the structure and at the lower window corners.

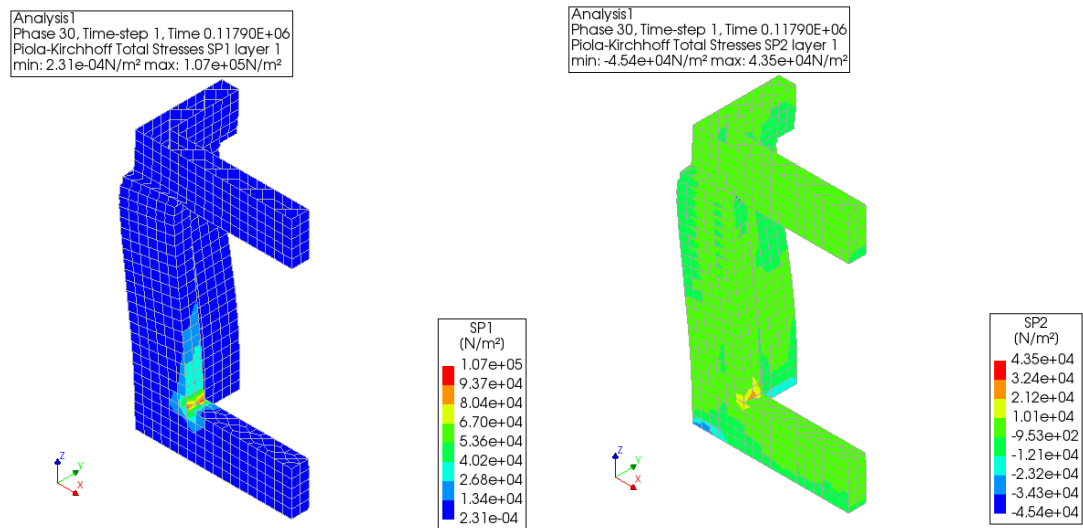


Figure 85: Structural stresses

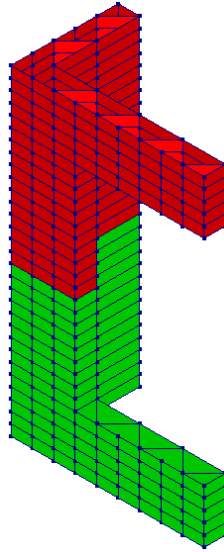


Figure 86: Material distribution of the structure: fiber reinforced concrete (red) and normal concrete (green)

The second strategy for adding fibers is to start at the bottom of the structure, where the stresses were higher.

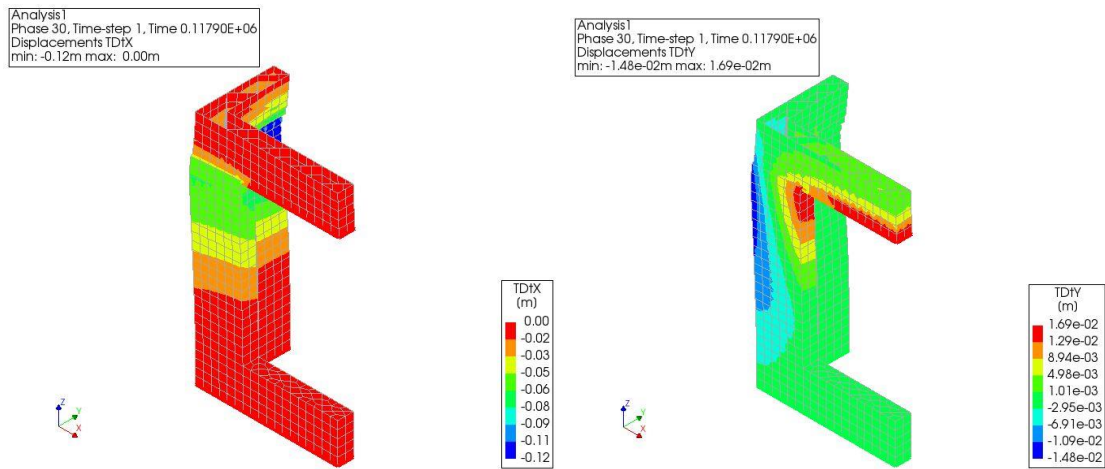


Figure 87: Structural deformation in X and Y direction

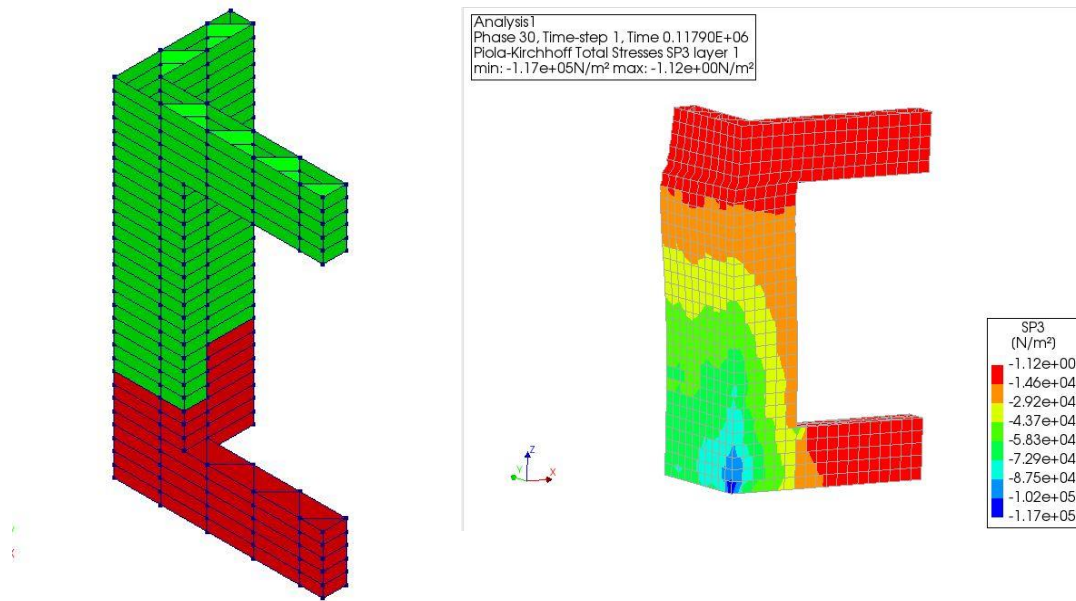


Figure 88: Material distribution and stress distribution

The resultant optimization of the structure using this strategy showed that only the first eight layers of the structure need to be changed to fiber reinforced concrete, and then the entire structure can be printed successfully. The overall deformation of the structure was smaller compared to the first optimization strategy, while the stresses were not reduced much, and the maximum stresses still occur at the bottom of the structure. From the above analysis, it is clear that both optimization strategies can eventually make the structure successfully printed, but the considerations of the two are different.

5.6 Roof printing and connections

After the main structure portion was successfully printed, it was necessary to wait 28 days to allow the concrete of the main structure to fully harden. The roof will then be assembled. The roof will be divided into two parts, which will make it easier to print on site, making the original 5m long assembly become 2.5m.

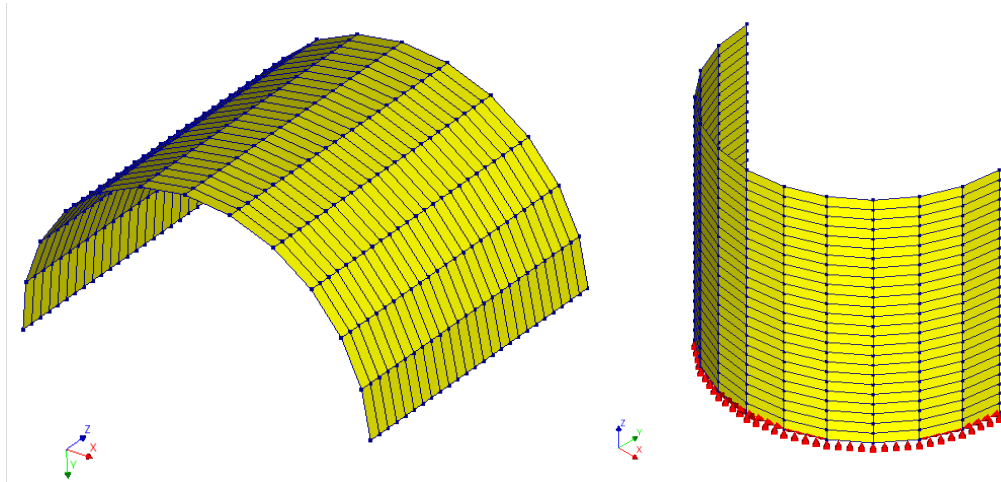


Figure 89: Roof geometry and boundary conditions

The print material used for the roof section was the same as the previously printed wall. For the boundary conditions, the direction of the print was changed, thus making the structure more stable and easier to print successfully, with support only from the bottom of the structure. Since the structure was also in the printing stage, only dead weight was considered.

The printing time of roof for each layer is:

$$T = (3.14 \times 1.5 \times 2 + 0.2 \times 3 \times 3.14 \times 24) \times 2 \times 4 \div 0.07 = 2800 \text{ s}$$

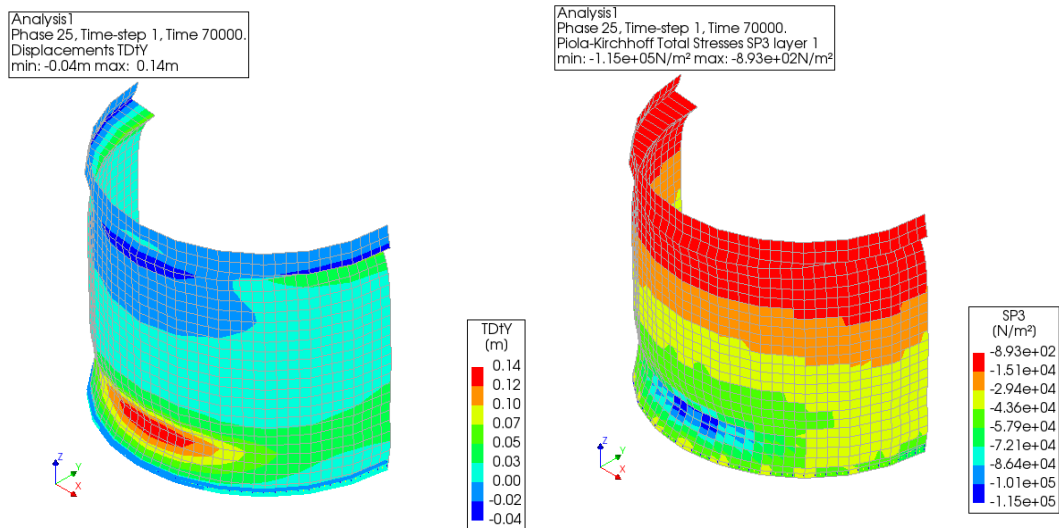


Figure 90: Deformation and Stress Distribution of the Finished Roof Printing

As can be seen from the figure above, even though the roof could be successfully printed, the deformation of part of the structure still exceeded the standard requirements. In terms of stress distribution, the larger stresses were distributed in the middle of the structure from the 4th to

the 7th layer. It can be concluded that the printing process can be successfully completed for the roof members even if all the materials are not used as fiber reinforced concrete.

After the roof has been printed, as with the main part of the structure, a waiting period of about 10 days is required to allow the material to harden sufficiently and become strong enough, after which the connection of the roof to the main body of the structure will begin.

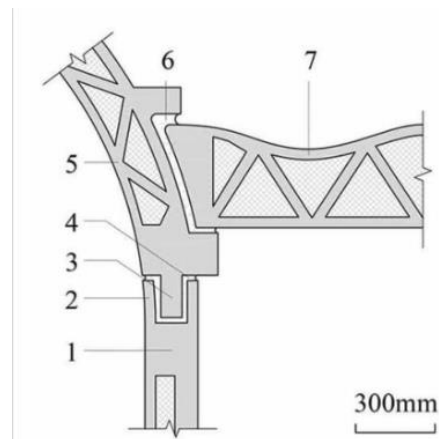


Figure 91: Connection solutions for the roof and the main body of the structure

For the roof and wall connections, the same connections as the Wujiashuang site will be used in this study, as this is not the main issue to be explored in this study. The joining method is shown in the figure, using mortise and tenon joints (2 and 3 in the figure above) and pouring mortar into the gaps after joining to make the joining nodes become a single unit, thus maintaining stability.

6 Discussions

In this chapter, the first step is to revise and optimize the results of the problematic analysis in the previous chapter to meet the needs of the actual situation. Then comes the analysis of possible reasons for the phenomenon of differences in material properties in different literatures. Finally, there is a reflection as well as a discussion of the whole study.

6.1 Optimization of computational results in Chapter 5

From the analysis in Chapter 4, it can be seen that although ultimately all structural components can be successfully printed, the deformation of some of the structures has exceeded the specification requirements, which is unacceptable in the actual printing process. Therefore, the material distribution or material properties need to be optimized. Firstly, the material properties were changed and an initial attempt was made to change the Young's modulus of the fiber reinforced concrete to three times that of normal concrete.

Table 14: Deflection requirements for formwork (STUBECO, 2023)

Deflection requirements

element	additional precondition	eis
contact formwork	class A (standard class) class B from CUR100 (aesthetic requirements from the project specification) class C (no aesthetic requirements)	0.001 m in accordance with project-specific requirements (see contract) n/a
children's beams underlaid	As a result of $Q_{1;rep}$ = eg concrete mortar: at $L_t < 20$ m at $20\text{m} < L_t < 25$ m at $L_t > 25$ m	$1/400 L_t$ $1/400 L_t$ but max 50 mm $1/600 L_t$ but max 50 mm $1/800 L_t$ but max 50 mm
nut beams		$1/600 L_t$

(L_t = center to center distance of the supports)

Based on the code requirements for the displacement of concrete casting forms, this study will use this code as the structural displacement requirement for 3D printed buildings, and with this requirement, the material properties of a portion of the location in the structure will be modified to meet the code requirements.

Based on the table above, the structures printed in this study fall into Class C because there

are no aesthetic requirements for the structures. Therefore, for the main part of the structure, the maximum horizontal displacement allowed is:

$$D_1 = \frac{1}{400} L_t = 5 \div 400 = 1.25 \times 10^{-2} m$$

For the roof of the structure, the maximum displacement allowed is:

$$D_2 = \frac{1}{400} L_t = 2.5 \div 400 = 6.25 \times 10^{-3} m$$

L_t is the center-to-center distance of the supports.

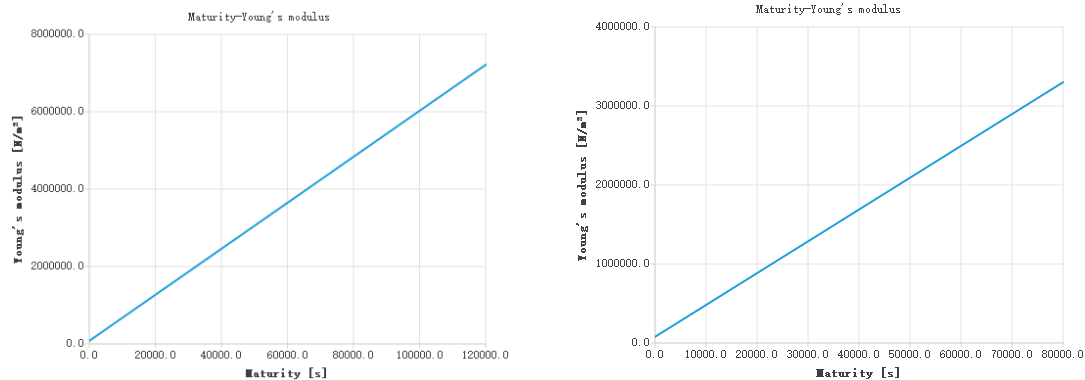


Figure 92: Young's modulus of fiber reinforced concrete before (Right) and after (Left) modification as a function of time.

The above figure shows the difference in the properties of fiber reinforced concrete before and after modification, i.e., the Young's modulus becomes 1.5 times that of the original fiber reinforced concrete. The shorter portion of the wall and roof will be used in the following analyses as an example to test how the deformation of the structure will change after changing the properties of the fiber reinforced concrete.

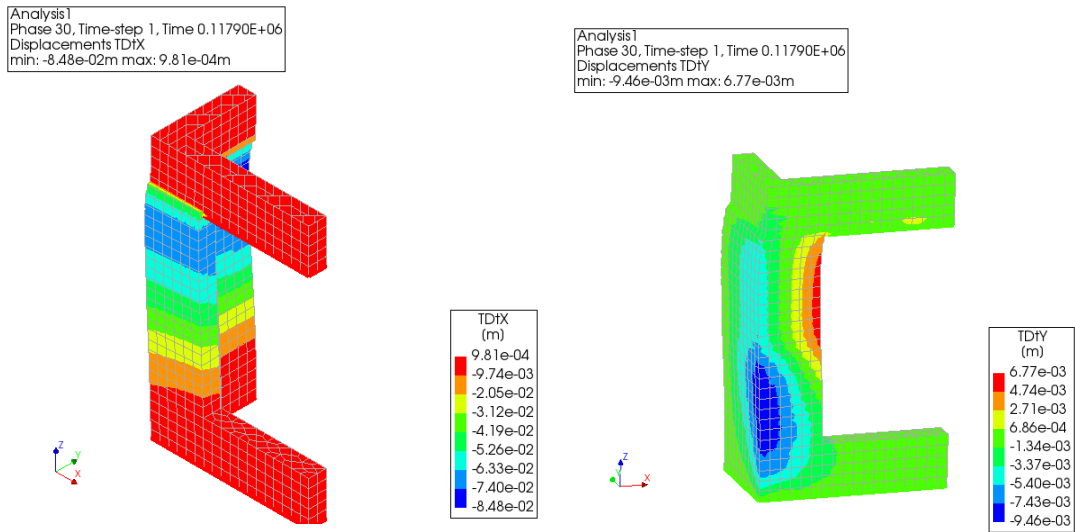


Figure 93: Deformation of the structure in the X and Y directions after changing the material properties.

After adjusting the material properties, it can be seen that the displacement of the structure is significantly reduced. The maximum deformation of the structure in the X direction is about 8.5 cm, which is larger than the 1.25 cm required in the code, but it has been significantly reduced compared to when the material properties were not changed. It can be inferred that if the material properties continue to be increased, the structural deformation will meet the code requirements.

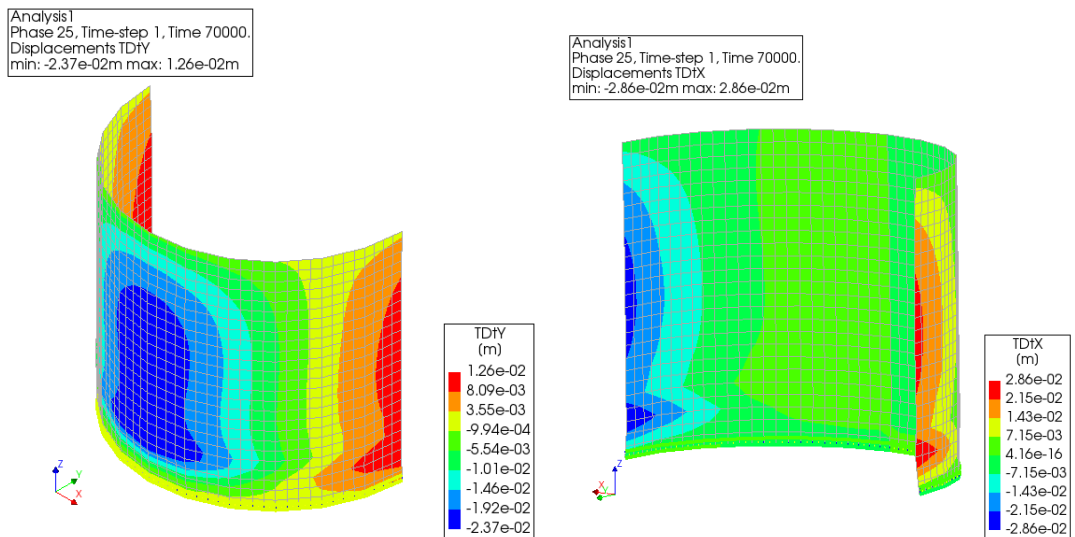


Figure 94: Deformation of the roof in the X and Y directions after changing the material properties.

A similar situation occurs with roof printing. The maximum displacement of the roof structure in

the X direction was 2.9 cm, which is greater than the maximum allowable displacement of 0.63 cm calculated according to the code. However, it is already very close to the code requirements, and if the material properties are made to be greater, then the structural deformation can be made to meet the code requirements.

In order to achieve the reduction of structural displacement, this study provides three optimization ideas. The first one is to change the material properties, i.e., increase the Young's modulus of the material, which will increase faster in a certain time range, thus having a larger Young's modulus, and this material parameter will play a very important role in controlling the structural deformation. The second idea is to increase the printing time, which again will result in a material with a larger Young's modulus when printed to the same number of layers. The third one is to achieve control of structural displacement by changing the geometry of the structure, i.e., increasing the thickness of the wall, which makes the structure more stable. The chart below shows the two material-related methods mentioned, i.e. increasing the strength of the material itself (orange line) or increasing the printing time (blue line).

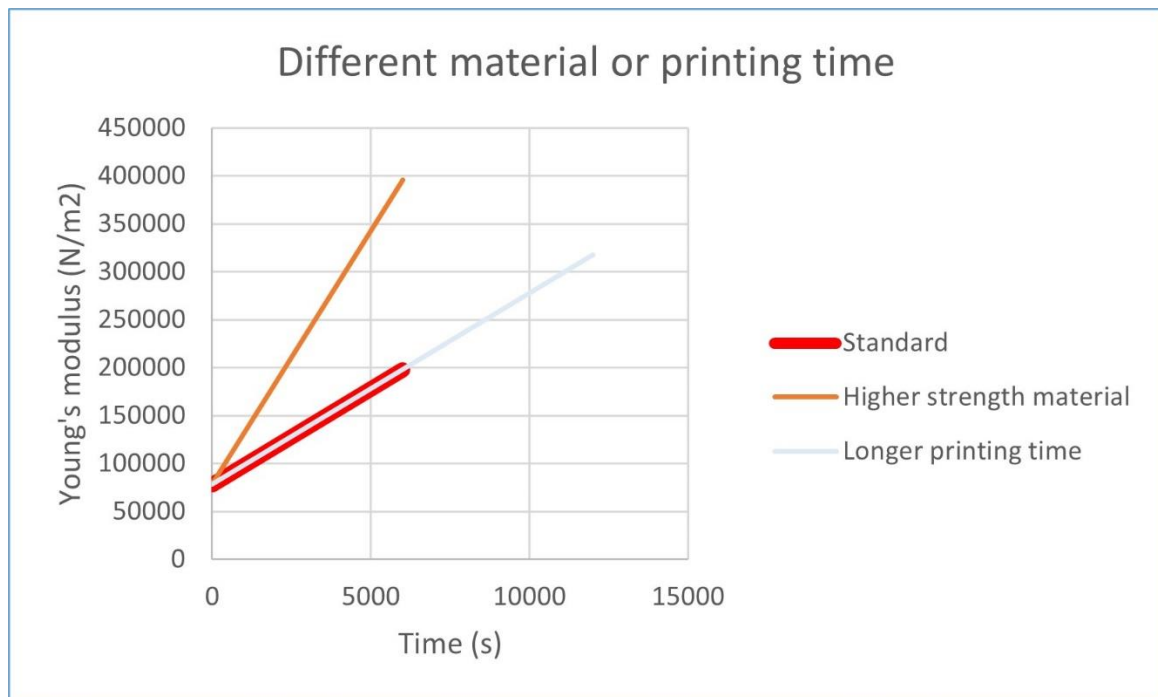


Figure 95: Different options for obtaining materials with better properties.

6.2 Discussions and reflections

The material properties used in this study were primarily derived from the studies of Wolfs et al (2018) and Mink (2019). The two studies give different results for Young's modulus, a parameter that has a significant impact on the 3D printing process. In this study, the magnitude of the Young's modulus of the concrete and its linear relationship with time over 90 minutes after extrusion, as studied by Wolfs et al. and the ratio between the Young's modulus of the fiber reinforced concrete and that of the concrete without fibers, as studied by Mink through experiments conducted in Microlab, were used to obtain all the material parameters needed for this study. Among them, for the measurement of Young's modulus, there is a big difference between the results obtained by the two studies. Possible reasons for this are the different temperatures at which the experiments were carried out, or the different mixtures used and the ratios of the materials they contain, all of which affect the final test results of the specimens.

From the results of the analysis in the previous chapter, it is possible to derive the final printing option and the distribution of fiber reinforced concrete and normal concrete in the structure. The resulting solution has been adjusted and modeled several times, but it is not necessarily the optimal solution, and the location of the added fibers in the structure can still be adjusted and optimized. However, the optimization strategies used in the analysis can be applied in the simulation of actual 3D building printing, and by adding fibers at certain locations in the structure, it does allow the structure to be printed completely successfully.

Through this study, it was found that the most challenging and time-intensive phase of the entire study was the finite element modeling and analysis phase. Also, there is relatively little information and tutorials on 3D printing, a relatively new process. Some parts of the finite element modeling process required the use of embedded Python, in which the code was entered to solve the batch problem, so basic Python knowledge was also learned. In particular, the need to introduce time parameters in the phased and nonlinear analysis required exporting a data file and using Python to enter the relevant commands into the file before it could be done. This process is more prone to errors, which can lead to the printing process not being modeled correctly, and therefore needs to be double-checked.

7 Conclusions & Recommendations

In this study, the whole process of 3D fiber reinforced concrete printing of a simple building has been investigated by means of Finite Element Analysis (FEA), and the following summarizes the conclusions drawn from this study in two main parts and makes recommendations for possible applications of the study results as well as for future follow-up research.

The first part is 3D fiber reinforced concrete printing. Since the performance of fiber reinforced concrete in the early stage after extrusion is significantly enhanced compared to normal concrete, this material can indeed play a role in the process of 3D printing, which is mainly reflected in the fact that the fiber reinforced concrete sets faster, so it can obtain higher Young's modulus, tensile strength, and compressive strength within the same time, which are three material parameters that play a crucial role in the initial stage of 3D printing of structural components. During the analysis of the finite element software, it was found that the material to be changed to fiber reinforced concrete was not only needed at the expected weak positions of the structure (in the case of this study, the weak positions were located near the doors and windows of the structure), but the fiber reinforced concrete needed to be used a few layers prior to the printing of the walls above the doors and windows, which avoids the possibility that the deformation of the structure is already large before the weak positions are printed, which could lead to the collapse of the wall above the window or door when it is printed. The second reinforcement strategy is to add fibers from the bottom upwards, which was done because analysis has concluded that the stresses were greatest at the bottom of the structure. Both strategies were feasible, and both ultimately ensured successful printing of the structure, but the second strategy performed better in controlling the deformation of the structure.

The second part concerns the finite element analysis itself. Since the main work done in this study was done in finite element software, some conclusions have also been drawn about the use of the finite element method to analyze the 3D printing process. In the case where the structure being analyzed is a symmetric structure, it is possible to analyze only half of the structure, but the setting of the boundary conditions is critical, which will affect the analysis of the printing process. When analyzing a model, one should focus on the parameter settings of geometry, material properties, boundary conditions, and loads, which will directly affect the accuracy of the analysis. Phased and structural nonlinear analysis as well as stability analysis are mainly used in the analysis of 3D printing process, while linear static analysis is used to analyze the use state of the structure. Unlike the other two analyses, the stability analysis provides a quicker indication of the buckling value of the structure after each printed layer, which can be used to make preliminary and quick judgments. The parameter study has shown that the thickness of the components, the addition of temporary supports to the structure, the printing time, and the material parameters all have an impact on the 3D printing process. In addition, the use of the shell structure to simulate the truss structure is only applicable when the wall length is short, and once the wall length is long (more than 3 m), the printing results of the two wall structures will largely be different. When simulating temporary supports, spring

supports are preferred to simple fixed supports because fixed supports limit the structural displacement, resulting in a continuous print of the wall with significantly different displacements in the two sections, which can lead to structural failure. Regarding the reduction of computational time, this can be achieved by using larger mesh sizes with guaranteed accuracy or by reducing the number of iterations in the analysis.

Regarding the possible applications of the results of this study, the reinforcement strategy of adding fibers to concrete does have some application within the context of 3D concrete printing. This method can be used to optimize the printing process of the structure and the use of the structure after printing by changing the distribution of the structural material to meet the requirements of the code. However, the application of this method requires modeling in finite element software to analyze the feasibility, i.e., the specific location of the added fibers, which is a more complex process and has higher requirements for the accuracy of the parameters in the analysis. In terms of material properties, it is recommended to use laboratory measured material properties for modeling, since different temperature environments and the proportion of each ingredient in the mixture can lead to very different final material properties.

This study explores optimization strategies for the 3D fiber reinforced concrete printing process, but the accuracy could be higher. For example, the current study results in deciding whether fiber reinforced concrete needs to be used in a particular layer, and future studies could be more refined to the point where certain locations in a layer are used and others are not, which places higher demands on modeling in finite element software. And subsequent research could analyze more complex structures based on the results of this study and draw conclusions that are more applicable to the printing of complex structures with today's shapes.

Bibliography

Ranjit, J. (2022, October 24). Project milestone: 3D-printed home by Houben & Van Mierlo. Parametric Architecture. <https://parametric-architecture.com/project-milestone-3d-printed-home-by-houben-van-mierlo/>

Wolfs, R., Bos, D., & Salet, T. (2023). Lessons learned of Project Milestone: The first 3D printed concrete house in the Netherlands. *Materials Today: Proceedings*. <https://doi.org/10.1016/j.matpr.2023.06.183>

Corazza, L. (2021). Tecla – technology and Clay. Mario Cucinella Architects. <https://www.mcarchitects.it/en/projects/tecla-technology-and-clay>

Buswell, R. A., da Silva, W. R. L., Bos, F. P., Schipper, H. R., Lowke, D., Hack, N., Kloft, H., Mechtcherine, V., Wangler, T., & Roussel, N. (2020). A process classification framework for defining and describing digital fabrication with concrete. *Cement and Concrete Research*, 134, 106068. <https://doi.org/10.1016/j.cemconres.2020.106068>

Regli, W., Rossignac, J., Shapiro, V., & Srinivasan, V. (2016). The New Frontiers in Computational Modeling of Material Structures. <https://doi.org/10.6028/nist.ir.8110>

Wolfs, R. J., & Suiker, A. S. (2019). Structural failure during extrusion-based 3D printing processes. *The International Journal of Advanced Manufacturing Technology*, 104(1–4), 565–584. <https://doi.org/10.1007/s00170-019-03844-6>

Majko, J., Saga, M., Vasko, M., Handrik, M., Barnik, F., & Dorčiak, F. (2019). FEM analysis of long-fibre composite structures created by 3D printing. *Transportation Research Procedia*, 40, 792–799. <https://doi.org/10.1016/j.trpro.2019.07.112>

RILEM, 2021. *Digital Fabrication with Cement-Based Materials*.

Soltan, D. G., & Li, V. C. (2018). A self-reinforced cementitious composite for building-scale 3D printing. *Cement and Concrete Composites*, 90, 1–13. <https://doi.org/10.1016/j.cemconcomp.2018.03.017>

Thholding.com.cn. 2021. *Tsinghua Design Institute Project / Robot 3D printing Wujiazhuang concrete farmhouse* [online] Available at: <https://www.thholding.com.cn/news/show/contentid/3966.html>

Wolfs, R. J. M., Bos, F. P., & Salet, T. A. M. (2018). Early age mechanical behaviour of 3D printed concrete: Numerical Modelling and experimental testing. *Cement and Concrete Research*, 106, 103–116. <https://doi.org/10.1016/j.cemconres.2018.02.001>

J. Mink, "3D Concrete Printing," Delft University of Technology, 2019.

Le, T. T., Austin, S. A., Lim, S., Buswell, R. A., Gibb, A. G., & Thorpe, T. (2012). Mix design and fresh properties for high-performance printing concrete. *Materials and Structures*, 45(8), 1221–1232. <https://doi.org/10.1617/s11527-012-9828-z>

Asakawa, T., Nishiwaki, T., Ohno, K., Yokoyama, S., Okada, Y., Kojima, S., Satake, Y., Miyata, Y., Miyazawa, Y., Ito, Y., & Kajita, H. (2022). Fundamental study on automated interlayer reinforcing system with metal fiber insertion for 3D concrete printer. *RILEM Bookseries*, 411–416. https://doi.org/10.1007/978-3-031-06116-5_61

Awolusi, T. F., Oke, O. L., Akinkulore, O. O., Sojobi, A. O., & Aluko, O. G. (2019). Performance comparison of neural network training algorithms in the modeling properties of steel fiber reinforced concrete. *Heliyon*, 5(1). <https://doi.org/10.1016/j.heliyon.2018.e01115>

Sun, X., Zhou, J., Wang, Q., Shi, J., & Wang, H. (2022). PVA fibre reinforced high-strength cementitious composite for 3D printing: Mechanical properties and durability. *Additive Manufacturing*, 49, 102500. <https://doi.org/10.1016/j.addma.2021.102500>

Yang, Y., Wu, C., Liu, Z., Wang, H., & Ren, Q. (2022). Mechanical anisotropy of ultra-high performance fibre-reinforced concrete for 3D printing. *Cement and Concrete Composites*, 125, 104310. <https://doi.org/10.1016/j.cemconcomp.2021.104310>

Zeina Malaeb, Fatima AlSakka, Farook Hamzeh. (2019). 3D Concrete Printing: Machine Design, Mix Proportioning, and Mix Comparison Between Different Machine Setups. *3D Concrete Printing Technology*, 115-136. <https://doi.org/10.1016/B978-0-12-815481-6.00006-3>

El Cheikh, K., Rémond, S., Khalil, N., & Aouad, G. (2017). Numerical and experimental studies of aggregate blocking in mortar extrusion. *Construction and Building Materials*, 145, 452–463. <https://doi.org/10.1016/j.conbuildmat.2017.04.032>

Roussel, N. (2018). Rheological requirements for printable concretes. *Cement and Concrete Research*, 112, 76–85. <https://doi.org/10.1016/j.cemconres.2018.04.005>

Hou, S., Duan, Z., Xiao, J., & Ye, J. (2021). A review of 3D printed concrete: Performance requirements, testing measurements and mix design. *Construction and Building Materials*, 273, 121745. <https://doi.org/10.1016/j.conbuildmat.2020.121745>

Paul, S. C., van Zijl, G. P. A. G., Tan, M. J., & Gibson, I. (2018). A review of 3D concrete printing systems and materials properties: Current status and Future Research Prospects. *Rapid Prototyping Journal*, 24(4), 784–798. <https://doi.org/10.1108/rpj-09->

[2016-0154](#)

Xu, W., Huang, S., Han, D., Zhang, Z., Gao, Y., Feng, P., & Zhang, D. (2022). Toward automated construction: The design-to-printing workflow for a robotic in-situ 3D printed house. *Case Studies in Construction Materials*, 17. <https://doi.org/10.1016/j.cscm.2022.e01442>

XU, W., GAO, Y., SUN, C., & WANG, Z. (2020). Fabrication and application of 3D-printed concrete structural components in the Baoshan Pedestrian Bridge Project. *Fabricate* 2020, 140–147. <https://doi.org/10.2307/j.ctv13xpsvw.22>

Malaeb, Z., AlSakka, F., & Hamzeh, F. (2019). 3D Concrete Printing: Machine Design, Mix Proportioning, and Mix Comparison Between Different Machine Setups. *3D Concrete Printing Technology*, 115-136. <https://doi.org/10.1016/B978-0-12-815481-6.00006-3>

Xu, J., Ding, L., Cai, L., Zhang, L., Luo, H., & Qin, W. (2019). Volume-forming 3D concrete printing using a variable-size square nozzle. *Automation in Construction*, 104, 95–106. <https://doi.org/10.1016/j.autcon.2019.03.008>

Khan, M. A. (2020). Mix suitable for Concrete 3D printing: A Review. *Materials Today: Proceedings*, 32, 831–837. <https://doi.org/10.1016/j.matpr.2020.03.825>

Arunothayan, A. R., Nematollahi, B., Ranade, R., Bong, S. H., Sanjayan, J. G., & Khayat, K. H. (2021). Fiber orientation effects on ultra-high performance concrete formed by 3D printing. *Cement and Concrete Research*, 143, 106384. <https://doi.org/10.1016/j.cemconres.2021.106384>

Suiker, A. S. J. (2022). Effect of accelerated curing and layer deformations on structural failure during extrusion-based 3D printing. *Cement and Concrete Research*, 151, 106586. <https://doi.org/10.1016/j.cemconres.2021.106586>

Ataalla, C. / M. (2018). Fiber reinforced concrete. LinkedIn. <https://www.linkedin.com/pulse/fiber-reinforced-concrete-mina-ataalla>

SolidWorks Help. (2012). Buckling Load Factor. [https://help.solidworks.com/2012/english/solidworks/cworks/buckling_load_factor.htm#:~:text=The%20buckling%20load%20factor%20\(BLF,Buckling%20Status](https://help.solidworks.com/2012/english/solidworks/cworks/buckling_load_factor.htm#:~:text=The%20buckling%20load%20factor%20(BLF,Buckling%20Status)

RIC Technology. (2022). Wujiazhuang Village. <https://www.rictechnology.com/wujiazhuangvillage>

Nguyen-Van, V., Nguyen-Xuan, H., Panda, B., & Tran, P. (2022). 3D concrete printing modelling of thin-walled structures. *Structures*, 39, 496–511. <https://doi.org/10.1016/j.istruc.2022.03.049>

STUBECO. (2023). 1. Berekeningsaspecten van Hulpconstructies: STUBECO - Studievereniging Uitvoering Betonconstructies. <https://www.stubeco.nl/1-berekeningsaspecten-van-hulpconstructies.html>

Appendix: Python Scripts

```
1  #Supports
2  addSet( "GEOMETRYSUPPORTSET", "Support set 1" )
3  rename( "GEOMETRYSUPPORTSET", "boundary_sup", "boundary sup" )
4  createLineSupport( "boundary sup", "boundary sup" )
5  setParameter( "GEOMETRYSUPPORT", "boundary sup", "AXES", [ 1, 2 ] )
6  setParameter( "GEOMETRYSUPPORT", "boundary sup", "TRANSL", [ 1, 1, 1 ] )
7  setParameter( "GEOMETRYSUPPORT", "boundary sup", "ROTATI", [ 0, 0, 0 ] )
8  attach( "GEOMETRYSUPPORT", "boundary sup", "Wall 1", [ [ 1.5, 0.5, 0 ], [ -1.5, 0.5, 0 ] ] )
9  attach( "GEOMETRYSUPPORT", "boundary sup", "Wall 2", [ [ 1.5, 3.5, 0 ], [ -1.5, 3.5, 0 ],
10 [ 0, 5, 0 ] ] )
11
12 #Materials
13 addMaterial( "concrete_lin", "CONCR", "LEI", [] )
14 setParameter( "MATERIAL", "concrete_lin", "LINEAR/ELASTI/YOUNG", 18000000 )
15 setParameter( "MATERIAL", "concrete_lin", "LINEAR/ELASTI/POISON", 0.3 )
16 setParameter( "MATERIAL", "concrete_lin", "LINEAR/MASS/DENSIT", 2100 )
17
18
19 #Thickness
```

```

20 addGeometry( "Element geometry 1", "SHEET", "FLASHL", [] )
21 rename( "GEOMET", "Element geometry 1", "thk" )
22 setParameter( "GEOMET", "thk", "THICK", 0.1 )
23
24 #Element data
25 addElementData( "Element data 1" )
26 setParameter( DATA, "Element data 1", "./THINTE", [] )
27 setParameter( DATA, "Element data 1", "THINTE", 5 )
28
29 #Element size
30 elem_size=0.025
31 setElementSize( shapes(), elem_size, -1, True )
32
33 #Interface
34 addMaterial( "interf_mat", "INTERF", "ELASTI", [] )
35 setParameter( "MATERIAL", "interf_mat", "LINEAR/IFTYP", "LIN3D" )
36 setParameter( "MATERIAL", "interf_mat", "LINEAR/ELAS4/DSNY", 1e+08 )
37 setParameter( "MATERIAL", "interf_mat", "LINEAR/ELAS4/DSSX", 1000000 )
38
39 addGeometry( "Element geometry 1", "LINE", "SHLLIF", [] )
40 setParameter( "GEOMET", "Element geometry 1", "THICK", thk )
41 setParameter( "GEOMET", "Element geometry 1", "SHAPSH", "CYLIN" )
42 setParameter( "GEOMET", "Element geometry 1", "CYLCEN", [ 0, 0, 0 ] )
43 setParameter( "GEOMET", "Element geometry 1", "CYLAX", [ 0, 0, 1 ] )
44
45 createConnection( "Connection 1", "BOUNDA", "SHAPEEDGE" )

```

```

46 setParameter( "GEOMETRYCONNECTION", "Connection 1", "MODE", "CLOSED" )
47 setElementClassType( "GEOMETRYCONNECTION", "Connection 1", "SHLLIF" )
48 assignMaterial( "interf_mat", "GEOMETRYCONNECTION", "Connection 1" )
49 assignGeometry( "Element geometry 1", "GEOMETRYCONNECTION", "Connection 1" )
50 setParameter( "GEOMETRYCONNECTION", "Connection 1", "FLIP", False )
51 attachTo( "GEOMETRYCONNECTION", "Connection 1", "SOURCE", "Wall 1", [ [ 1.5, 0.5, 0 ] ] )
52 attachTo( "GEOMETRYCONNECTION", "Connection 1", "SOURCE", "Wall 2", [ [ 1.5, 3.5, 0 ] ] )
53 attachTo( "GEOMETRYCONNECTION", "Connection 1", "SOURCE", "Wall 1", [ [ 0, 0, 0 ] ] )
54 attachTo( "GEOMETRYCONNECTION", "Connection 1", "SOURCE", "Wall 1", [ [ -1.5, 0.5, 0 ] ] )
55 attachTo( "GEOMETRYCONNECTION", "Connection 1", "SOURCE", "Wall 2", [ [ -1.5, 3.5, 0 ] ] )
56 attachTo( "GEOMETRYCONNECTION", "Connection 1", "SOURCE", "Wall 2", [ [ 0, 5, 0 ] ] )
57
58 #Mesh
59 generateMesh( [] )
60 hideView( "GEOM" )
61 showView( "MESH" )
62
63 #Analysis
64 addAnalysis( "Analysis1" )
65 addAnalysisCommand( "Analysis1", "PHASE", "Phase" )
66 renameAnalysisCommand( "Analysis1", "Phase", "Phase 1" )
67 setActivePhase( "Analysis1", "Phase 1" )
68 setActiveInPhase( "Analysis1", "SHAPESET", [ "Layer 2" ], [ "Phase 1" ], False )
69 setActiveInPhase( "Analysis1", "SHAPESET", [ "Layer 3" ], [ "Phase 1" ], False )
70 setActiveInPhase( "Analysis1", "SHAPESET", [ "Layer 4" ], [ "Phase 1" ], False )
71 setActiveInPhase( "Analysis1", "SHAPESET", [ "Layer 5" ], [ "Phase 1" ], False )

```

```
72 setActiveInPhase( "Analysis1", "SHAPESET", [ "Layer 6" ], [ "Phase 1" ], False )
73 setActiveInPhase( "Analysis1", "SHAPESET", [ "Layer 7" ], [ "Phase 1" ], False )
74 setActiveInPhase( "Analysis1", "SHAPESET", [ "Layer 8" ], [ "Phase 1" ], False )
75 setActiveInPhase( "Analysis1", "SHAPESET", [ "Layer 9" ], [ "Phase 1" ], False )
76 setActiveInPhase( "Analysis1", "SHAPESET", [ "Layer 10" ], [ "Phase 1" ], False )
77 setActiveInPhase( "Analysis1", "SHAPESET", [ "Layer 11" ], [ "Phase 1" ], False )
78 setActiveInPhase( "Analysis1", "SHAPESET", [ "Layer 12" ], [ "Phase 1" ], False )
79 setActiveInPhase( "Analysis1", "SHAPESET", [ "Layer 13" ], [ "Phase 1" ], False )
80 setActiveInPhase( "Analysis1", "SHAPESET", [ "Layer 14" ], [ "Phase 1" ], False )
81 setActiveInPhase( "Analysis1", "SHAPESET", [ "Layer 15" ], [ "Phase 1" ], False )
82 setActiveInPhase( "Analysis1", "SHAPESET", [ "Layer 16" ], [ "Phase 1" ], False )
83 setActiveInPhase( "Analysis1", "SHAPESET", [ "Layer 17" ], [ "Phase 1" ], False )
84 setActiveInPhase( "Analysis1", "SHAPESET", [ "Layer 18" ], [ "Phase 1" ], False )
85 setActiveInPhase( "Analysis1", "SHAPESET", [ "Layer 19" ], [ "Phase 1" ], False )
86 setActiveInPhase( "Analysis1", "SHAPESET", [ "Layer 20" ], [ "Phase 1" ], False )
87 setActiveInPhase( "Analysis1", "SHAPESET", [ "Layer 21" ], [ "Phase 1" ], False )
88 setActiveInPhase( "Analysis1", "SHAPESET", [ "Layer 22" ], [ "Phase 1" ], False )
89 setActiveInPhase( "Analysis1", "SHAPESET", [ "Layer 23" ], [ "Phase 1" ], False )
90 setActiveInPhase( "Analysis1", "SHAPESET", [ "Layer 24" ], [ "Phase 1" ], False )
91 setActiveInPhase( "Analysis1", "SHAPESET", [ "Layer 25" ], [ "Phase 1" ], False )
92 setActiveInPhase( "Analysis1", "SHAPESET", [ "Layer 26" ], [ "Phase 1" ], False )
93 setActiveInPhase( "Analysis1", "SHAPESET", [ "Layer 27" ], [ "Phase 1" ], False )
94 setActiveInPhase( "Analysis1", "SHAPESET", [ "Layer 28" ], [ "Phase 1" ], False )
95 setActiveInPhase( "Analysis1", "SHAPESET", [ "Layer 29" ], [ "Phase 1" ], False )
96 setActiveInPhase( "Analysis1", "SHAPESET", [ "Layer 30" ], [ "Phase 1" ], False )
97 addAnalysisCommand( "Analysis1", "NONLIN", "Structural nonlinear" )
```



```

98  renameAnalysisCommand( "Analysis1", "Structural nonlinear", "Structural nonlinear 1" )
99  addAnalysisCommandDetail( "Analysis1", "Structural nonlinear 1", "TYPE/GEOMET" )
100 setAnalysisCommandDetail( "Analysis1", "Structural nonlinear 1", "TYPE/GEOMET", True )
101 setAnalysisCommandDetail( "Analysis1", "Structural nonlinear 1", "EXECUT(1)/EXETYP",
    "START" )
102 setAnalysisCommandDetail( "Analysis1", "Structural nonlinear 1", "EXECUT(1)/ITERAT/MAXITE",
    20 )
103 addAnalysisCommandDetail( "Analysis1", "Structural nonlinear 1", "EXECUT(1)/ITERAT/LINESE" )
104 setAnalysisCommandDetail( "Analysis1", "Structural nonlinear 1", "EXECUT(1)/ITERAT/LINESE",
    True )
105 setAnalysisCommandDetail( "Analysis1", "Structural nonlinear 1",
    "EXECUT(1)/ITERAT/CONVER/SIMULT", True )
106 setAnalysisCommandDetail( "Analysis1", "Structural nonlinear 1",
    "EXECUT(1)/ITERAT/CONVER/DISPLA/NOCONV", "CONTIN" )
107 setAnalysisCommandDetail( "Analysis1", "Structural nonlinear 1",
    "EXECUT(1)/ITERAT/CONVER/FORCE/NOCONV", "CONTIN" )
108 setAnalysisCommandDetail( "Analysis1", "Structural nonlinear 1", "OUTPUT(1)/SELTYP", "USER" )
109 addAnalysisCommandDetail( "Analysis1", "Structural nonlinear 1", "OUTPUT(1)/USER" )
110 addAnalysisCommandDetail( "Analysis1", "Structural nonlinear 1", "OUTPUT(1)/USER/DISPLA" )
111 addAnalysisCommandDetail( "Analysis1", "Structural nonlinear 1",
    "OUTPUT(1)/USER/DISPLA(2)/TOTAL/TRANSL/AXIAL" )
112 addAnalysisCommandDetail( "Analysis1", "Structural nonlinear 1",
    "OUTPUT(1)/USER/STRESS(1)/TOTAL/PIOLAK/PRINCI" )
113 setAnalysisCommandDetail( "Analysis1", "Structural nonlinear 1",
    "OUTPUT(1)/USER/STRESS(1)/TOTAL/PIOLAK/PRINCI/LOCATI", "INTPNT" )

```

```

114 addAnalysisCommandDetail( "Analysis1", "Structural nonlinear 1",
    "OUTPUT(1)/USER/STRAIN(1)/TOTAL/GREEN/PRINCI" )
115 setAnalysisCommandDetail( "Analysis1", "Structural nonlinear 1",
    "OUTPUT(1)/USER/STRAIN(1)/TOTAL/GREEN/PRINCI/LOCATI", "INTPNT" )
116 addAnalysisCommandDetail( "Analysis1", "Structural nonlinear 1",
    "OUTPUT(1)/USER/STRESS(2)/TOTAL/TRACTI/LOCAL" )
117 addAnalysisCommandDetail( "Analysis1", "Structural nonlinear 1",
    "OUTPUT(1)/USER/STRAIN(2)/TOTAL/TRACTI/LOCAL" )
118
119 for i in range(1,30):
120     copyAnalysisCommand( "Analysis1", "Phase "+str(i), "Phase "+str(i+1) )
121     setActiveInPhase( "Analysis1", SHAPESET, [ "Layer "+str(i+1) ], [ "Phase "+str(i+1) ],
122     True )
123     copyAnalysisCommand( "Analysis1", "Structural nonlinear "+str(i), "Structural nonlinear
124     "+str(i+1) )
125
126 setAnalysisCommandDetail( "Analysis1", "Structural nonlinear 1", "EXECUT(1)/EXETYP", "LOAD" )
127 addAnalysisCommandDetail( "Analysis1", "Structural nonlinear 1", "EXECUT(1)/LOAD/LOADNR" )
128 setAnalysisCommandDetail( "Analysis1", "Structural nonlinear 1", "EXECUT(1)/LOAD/LOADNR", 1 )
129
130 addAnalysis( "Analysis2" )
131 addAnalysisCommand( "Analysis2", "PHASE", "Phase" )
132 renameAnalysisCommand( "Analysis2", "Phase", "Phase 1" )
133 setActiveInPhase( "Analysis2", "SHAPESET", [ "Layer 2" ], [ "Phase 1" ], False )
134 setActiveInPhase( "Analysis2", "SHAPESET", [ "Layer 3" ], [ "Phase 1" ], False )
135 setActiveInPhase( "Analysis2", "SHAPESET", [ "Layer 4" ], [ "Phase 1" ], False )

```

```
134 setActiveInPhase( "Analysis2", "SHAPESET", [ "Layer 5" ], [ "Phase 1" ], False )
135 setActiveInPhase( "Analysis2", "SHAPESET", [ "Layer 6" ], [ "Phase 1" ], False )
136 setActiveInPhase( "Analysis2", "SHAPESET", [ "Layer 7" ], [ "Phase 1" ], False )
137 setActiveInPhase( "Analysis2", "SHAPESET", [ "Layer 8" ], [ "Phase 1" ], False )
138 setActiveInPhase( "Analysis2", "SHAPESET", [ "Layer 9" ], [ "Phase 1" ], False )
139 setActiveInPhase( "Analysis2", "SHAPESET", [ "Layer 10" ], [ "Phase 1" ], False )
140 setActiveInPhase( "Analysis2", "SHAPESET", [ "Layer 11" ], [ "Phase 1" ], False )
141 setActiveInPhase( "Analysis2", "SHAPESET", [ "Layer 12" ], [ "Phase 1" ], False )
142 setActiveInPhase( "Analysis2", "SHAPESET", [ "Layer 13" ], [ "Phase 1" ], False )
143 setActiveInPhase( "Analysis2", "SHAPESET", [ "Layer 14" ], [ "Phase 1" ], False )
144 setActiveInPhase( "Analysis2", "SHAPESET", [ "Layer 15" ], [ "Phase 1" ], False )
145 setActiveInPhase( "Analysis2", "SHAPESET", [ "Layer 16" ], [ "Phase 1" ], False )
146 setActiveInPhase( "Analysis2", "SHAPESET", [ "Layer 17" ], [ "Phase 1" ], False )
147 setActiveInPhase( "Analysis2", "SHAPESET", [ "Layer 18" ], [ "Phase 1" ], False )
148 setActiveInPhase( "Analysis2", "SHAPESET", [ "Layer 19" ], [ "Phase 1" ], False )
149 setActiveInPhase( "Analysis2", "SHAPESET", [ "Layer 20" ], [ "Phase 1" ], False )
150 setActiveInPhase( "Analysis2", "SHAPESET", [ "Layer 21" ], [ "Phase 1" ], False )
151 setActiveInPhase( "Analysis2", "SHAPESET", [ "Layer 22" ], [ "Phase 1" ], False )
152 setActiveInPhase( "Analysis2", "SHAPESET", [ "Layer 23" ], [ "Phase 1" ], False )
153 setActiveInPhase( "Analysis2", "SHAPESET", [ "Layer 24" ], [ "Phase 1" ], False )
154 setActiveInPhase( "Analysis2", "SHAPESET", [ "Layer 25" ], [ "Phase 1" ], False )
155 setActiveInPhase( "Analysis2", "SHAPESET", [ "Layer 26" ], [ "Phase 1" ], False )
156 setActiveInPhase( "Analysis2", "SHAPESET", [ "Layer 27" ], [ "Phase 1" ], False )
157 setActiveInPhase( "Analysis2", "SHAPESET", [ "Layer 28" ], [ "Phase 1" ], False )
158 setActiveInPhase( "Analysis2", "SHAPESET", [ "Layer 29" ], [ "Phase 1" ], False )
159 setActiveInPhase( "Analysis2", "SHAPESET", [ "Layer 30" ], [ "Phase 1" ], False )
```

```

160 addAnalysisCommand( "Analysis2", "NONLIN", "Structural nonlinear" )
161 renameAnalysisCommand( "Analysis2", "Structural nonlinear", "Structural nonlinear 1" )
162 addAnalysisCommandDetail( "Analysis2", "Structural nonlinear 1", "TYPE/GEOMET" )
163 setAnalysisCommandDetail( "Analysis2", "Structural nonlinear 1", "TYPE/GEOMET", True )
164 setAnalysisCommandDetail( "Analysis2", "Structural nonlinear 1", "EXECUT(1)/EXETYP",
"START" )
165 setAnalysisCommandDetail( "Analysis2", "Structural nonlinear 1", "EXECUT(1)/START/STEPS",
False )
166 setAnalysisCommandDetail( "Analysis2", "Structural nonlinear 1", "EXECUT/EXETYP", "TIME" )
167 setAnalysisCommandDetail( "Analysis2", "Structural nonlinear 1", "EXECUT(2)/ITERAT/MAXITE",
10 )
168 setAnalysisCommandDetail( "Analysis2", "Structural nonlinear 1", "EXECUT(2)/ITERAT/MAXITE",
10 )
169 setAnalysisCommandDetail( "Analysis2", "Structural nonlinear 1",
"EXECUT(2)/TIME/STEPS/EXPLIC/SIZES", "3930.00000" )
170 setAnalysisCommandDetail( "Analysis2", "Structural nonlinear 1", "EXECUT(2)/ITERAT/MAXITE",
50 )
171 addAnalysisCommandDetail( "Analysis2", "Structural nonlinear 1", "EXECUT(2)/ITERAT/LINESE" )
172 setAnalysisCommandDetail( "Analysis2", "Structural nonlinear 1", "EXECUT(2)/ITERAT/LINESE",
True )
173 setAnalysisCommandDetail( "Analysis2", "Structural nonlinear 1",
"EXECUT(2)/ITERAT/CONVER/SIMULT", True )
174 setAnalysisCommandDetail( "Analysis2", "Structural nonlinear 1",
"EXECUT(2)/ITERAT/CONVER/DISPLA/NOCONV", "CONTIN" )
175 setAnalysisCommandDetail( "Analysis2", "Structural nonlinear 1",
"EXECUT(2)/ITERAT/CONVER/FORCE/NOCONV", "TERMIN" )

```

```
176 setAnalysisCommandDetail( "Analysis2", "Structural nonlinear 1",  
    "EXECUT(2)/ITERAT/CONVER/FORCE/NOCONV", "CONTIN" )  
177 setAnalysisCommandDetail( "Analysis2", "Structural nonlinear 1", "OUTPUT(1)/SELTYP", "USER" )  
178 addAnalysisCommandDetail( "Analysis2", "Structural nonlinear 1", "OUTPUT(1)/USER" )  
179 addAnalysisCommandDetail( "Analysis2", "Structural nonlinear 1", "OUTPUT(1)/USER/DISPLA" )  
180 addAnalysisCommandDetail( "Analysis2", "Structural nonlinear 1",  
    "OUTPUT(1)/USER/DISPLA(2)/TOTAL/TRANSL/AXIAL" )  
181 addAnalysisCommandDetail( "Analysis2", "Structural nonlinear 1",  
    "OUTPUT(1)/USER/MATURI(1)/TOTAL" )  
182 addAnalysisCommandDetail( "Analysis2", "Structural nonlinear 1",  
    "OUTPUT(1)/USER/PARAME(1)/YOUNG" )  
183 addAnalysisCommandDetail( "Analysis2", "Structural nonlinear 1",  
    "OUTPUT(1)/USER/PARAME(2)/COMSTR" )  
184 addAnalysisCommandDetail( "Analysis2", "Structural nonlinear 1",  
    "OUTPUT(1)/USER/STRESS(1)/TOTAL/PIOLAK/PRINCI" )  
185 setAnalysisCommandDetail( "Analysis2", "Structural nonlinear 1",  
    "OUTPUT(1)/USER/STRESS(1)/TOTAL/PIOLAK/PRINCI/LOCATI", "INTPNT" )  
186 addAnalysisCommandDetail( "Analysis2", "Structural nonlinear 1",  
    "OUTPUT(1)/USER/STRAIN(1)/TOTAL/GREEN/PRINCI" )  
187 setAnalysisCommandDetail( "Analysis2", "Structural nonlinear 1",  
    "OUTPUT(1)/USER/STRAIN(1)/TOTAL/GREEN/PRINCI/LOCATI", "INTPNT" )  
188 addAnalysisCommandDetail( "Analysis2", "Structural nonlinear 1",  
    "OUTPUT(1)/USER/STRESS(2)/TOTAL/TRACTI/LOCAL" )  
189 addAnalysisCommandDetail( "Analysis2", "Structural nonlinear 1",  
    "OUTPUT(1)/USER/STRAIN(2)/TOTAL/TRACTI/LOCAL" )
```

```

190 addAnalysisCommandDetail( "Analysis2", "Structural nonlinear 1",
    "OUTPUT(1)/USER/STRAIN(3)/CRKWDT/GREEN/PRINCI" )
191 setAnalysisCommandDetail( "Analysis2", "Structural nonlinear 1",
    "OUTPUT(1)/USER/STRAIN(3)/CRKWDT/GREEN/PRINCI/LOCATI", "INTPNT" )
192
193 for i in range(1,20):
194     copyAnalysisCommand( "Analysis2", "Phase "+str(i), "Phase "+str(i+1) )
195     setActiveInPhase( "Analysis2", SHAPESET, [ "Layer "+str(i+1) ], [ "Phase "+str(i+1) ],
    True )
196     copyAnalysisCommand( "Analysis2", "Structural nonlinear "+str(i), "Structural nonlinear
    "+str(i+1) )
197     setAnalysisCommandDetail( "Analysis2", "Structural nonlinear "+str(i+1),
    "EXECUT(1)/START/TIME", i*3930 )
198
199 setAnalysisCommandDetail( "Analysis2", "Structural nonlinear 1",
    "EXECUT(1)/START/LOAD/PREVIO", False )
200 addAnalysisCommandDetail( "Analysis2", "Structural nonlinear 1", "EXECUT(1)/START/LOAD/ADD" )
201 setAnalysisCommandDetail( "Analysis2", "Structural nonlinear 1", "EXECUT(1)/START/LOAD/ADD",
    True )
202 setAnalysisCommandDetail( "Analysis2", "Structural nonlinear 1",
    "EXECUT(1)/START/LOAD/ADD/LOADNR", 1 )
203
204 n_start = 1
205 runSolver( [ "Analysis3" ] )
206 fcr = float(resultCases( "Analysis3" )[0].split()[-1])
207 n = n_start

```

```

208 print( "printing layer "+str(n) +" buckling value = "+str(fcr) )
209 while abs (fcr) > 1.0 and n != 30:
210     n1=n+1
211     n = min(n1, 30)
212     setActiveInPhase( "Analysis3", SHAPESET, [ "Layer "+str(n) ], [ "Phase 1" ], True )
213     runSolver( [ "Analysis3" ] )
214     fcr = float(resultCases( "Analysis3" )[0].split()[-1])
215     print( "printing layer "+str(n) +" buckling value = "+str(fcr) )
216 if abs (fcr) < 1.0:
217     print( "Structure fails when printing layer "+str(n) )
218 else:
219     print( "Structure is stable" )
220
221 for i in range(4,20):
222     addSet( "SHAPESET", "Shapes 1" )
223     rename( "SHAPESET", "Shapes 1", "Layer "+str(i) )
224     setCurrentShapeSet( "Layer "+str(i) )
225     moveToShapeSet( [ "Truss "+str(i) , "Wall "+str(i) ], "Layer "+str(i) )
226
227 for i in range(1,20):
228     copyAnalysisCommand( "Analysis2", "Phase "+str(i), "Phase "+str(i+1) )
229     setActiveInPhase( "Analysis2", SHAPESET, [ "Layer "+str(i+1) ], [ "Phase "+str(i+1) ],
True )
230     copyAnalysisCommand( "Analysis2", "Structural nonlinear "+str(i), "Structural nonlinear
"+str(i+1) )

```

```

231     setAnalysisCommandDetail( "Analysis2", "Structural nonlinear "+str(i+1),
"EXECUT(1)/START/TIME", i*60 )
232
233     for i in range(1,20):
234         healAndSew( [ "Wall "+str(i), "Sheet "+str(i) ], 1e-05, {} )
235
236     for i in range(1,20):
237         healAndSew( [ "Truss "+str(i), "Truss "+str(i+20) ], 1e-05, {} )
238
239
240     for i in range(1,20):
241         copyAnalysisCommand( "Analysis2", "Phase "+str(i), "Phase "+str(i+1) )
242         setActiveInPhase( "Analysis2", SHAPESET, [ "Layer "+str(i+1) ], [ "Phase "+str(i+1) ],
True )
243         copyAnalysisCommand( "Analysis2", "Structural nonlinear "+str(i), "Structural nonlinear
"+str(i+1) )
244         setAnalysisCommandDetail( "Analysis2", "Structural nonlinear "+str(i+1),
"EXECUT(1)/START/TIME", i*60 )
245
246     for i in range(1,n_layers+1):
247         f.write("/ \\"Layer "+str(i)+"\\" /\n")
248         f.write("      0("+str(i)+") "+str(time_per_layer)+"-"+str((full_time*2+time_per_layer)-
i*time_per_layer)+"("+str(time_per_layer)+")\n")
249         f.write("      0("+str(n_layers*2+1)+")\n")
250
251

```



```

252 time_per_layer=3930
253 n_layers=30
254 full_time = time_per_layer*n_layers
255 exportModel( "print_wall_analysis2.dat", 6 )
256 saveAnalysisCommands( "Analysis2", "print_wall_analysis2.dcf", 6 )
257
258 f=open("print_wall_analysis2.dat","r")
259 lines = f.readlines()
260 lines[-1] = lines[-1].replace("'END'", "'MATURI'")
261 f.close()
262
263 f=open("print_wall_analysis2.dat","w")
264 f.writelines(lines)
265 f.close()
266
267 f=open("print_wall_analysis2.dat","a")
268 # f.write("'MATURI'\n")
269 f.write("ELEMEN\n")
270 f.write("      0-"+str(full_time*2)+"("+str(time_per_layer)+")\n")
271
272 for i in range(1,n_layers+1):
273     f.write("/ \"Truss "+str(i)+"\" /\n")
274     f.write("      0("+str(i)+") "+str(time_per_layer)+"-"+str((full_time*2+time_per_layer)-
i*time_per_layer)+"("+str(time_per_layer)+")\n")
275     f.write("      0("+str(n_layers*2+1)+")\n")
276

```

```

277 for i in range(21,n_layers+1):
278     f.write("/ \"Wall "+str(i)+"\" , \"Truss "+str(i)+"\", \"Truss "+str(i+10)+"\" /\n")
279     f.write("      0("+str(i)+") "+str(time_per_layer)+"-"+str((full_time*2+time_per_layer)-
i*time_per_layer)+"("+str(time_per_layer)+")\n")
280     f.write("      0("+str(n_layers*2+1)+")\n")
281
282 f.write("'END'\n")
283 f.close()
284
285 f=open("print_wall_analysis2.dcf","r")
286 oline=f.readlines()
287
288 fline="*FILOS\nINITIA\n*INPUT\n\n"
289 oline.insert(0,fline)
290 f.close()
291
292 f=open("print_wall_analysis2.dcf","w")
293 f.writelines(oline)
294 f.close()
295
296 time_per_layer=2800
297 n_layers=25
298 full_time = time_per_layer*n_layers
299 f.write("      0-"+str(full_time*2)+"("+str(time_per_layer)+")\n")
300
301 for i in range(1,n_layers+1):

```

```

302     f.write("/ \"Layer "+str(i)+"\" /\n")
303     f.write("          0("+str(i)+") "+str(time_per_layer)+"-"+str((full_time*2+time_per_layer)-
i*time_per_layer)+"("+str(time_per_layer)+")\n")
304     f.write("          0("+str(n_layers*2+1)+")\n")
305
306     for i in range(2,40):
307         renameShape( "Circle " + str (i), "Layer " + str (i))
308
309     for i in range(1,n_layers+1):
310         f.write("/ \"Layer "+str(i)+"\" /\n")
311         f.write("          0("+str(i)+") "+str(time_per_layer)+"-"+str((full_time*2+time_per_layer)-
i*time_per_layer)+"("+str(time_per_layer)+")\n")
312         f.write("          0("+str(n_layers*2+1)+")\n")
313
314     f.write("'END'\n")
315     f.close()
316
317     newProject( "D:/DIANA/New 1-30 short wall", 100, {} )
318     setModelAnalysisAspects( [ "STRUCT" ] )
319     setModelDimension( "3D" )
320     setDefaultMeshOrder( "QUADRATIC" )
321     setDefaultMesherType( "HEXQUAD" )
322     setDefaultMidSideNodeLocation( "ONSHAP" )
323     saveProject( )
324     createPolyline( "polygon 1", [ [ 0, 0, 0 ], [ 1.8, 0, 0 ], [ 1.8, 0.2, 0 ], [ 0.2, 0.2, 0 ],
[ 0.2, 1, 0 ], [ 0, 1, 0 ] ], True )

```

```

325 saveProject( )
326 createLine( "Line 1", [ 0.2, 1, 0 ], [ 0, 0.8, 0 ] )
327 duplicateShape( "Line 1", "Line 2" )
328 translate( [ "Line 2" ], [ 0, -0.4, 0 ] )
329 createLine( "Line 3", [ 0, 0.8, 0 ], [ 0.2, 0.6, 0 ] )
330 duplicateShape( "Line 3", "Line 4" )
331 translate( [ "Line 4" ], [ 0, -0.4, 0 ] )
332 createLine( "Line 5", [ 0.2, 0.2, 0 ], [ 0.4, 0, 0 ] )
333 arrayCopy( [ "Line 5" ], [ 0.4, 0, 0 ], [ 0, 0, 0 ], [ 0, 0, 0 ], 3 )
334 createLine( "Line 9", [ 0.4, 0, 0 ], [ 0.6, 0.2, 0 ] )
335 createLine( "Line 10", [ 0.8, 0, 0 ], [ 1, 0.2, 0 ] )
336 createLine( "Line 11", [ 1.2, 0, 0 ], [ 1.4, 0.2, 0 ] )
337 createLine( "Line 12", [ 1.6, 0, 0 ], [ 1.8, 0.2, 0 ] )
338 saveProject( )
339 extrudeProfile( "SHAPEEDGE", "polygon 1", [ [ 0.9, 0, 0 ], [ 1.8, 0.1, 0 ], [ 1, 0.2, 0 ],
[ 0.2, 0.6, 0 ], [ 0.1, 1, 0 ], [ 0, 0.5, 0 ] ], [ [ 0, 0, 0.1 ] ] )
340 extrudeProfile( "SHAPEEDGE", "Line 1", [ [ 0.1, 0.9, 0 ] ], [ [ 0, 0, 0.1 ] ] )
341 extrudeProfile( "SHAPEEDGE", "Line 2", [ [ 0.1, 0.5, 0 ] ], [ [ 0, 0, 0.1 ] ] )
342 extrudeProfile( "SHAPEEDGE", "Line 3", [ [ 0.1, 0.7, 0 ] ], [ [ 0, 0, 0.1 ] ] )
343 extrudeProfile( "SHAPEEDGE", "Line 4", [ [ 0.1, 0.3, 0 ] ], [ [ 0, 0, 0.1 ] ] )
344 extrudeProfile( "SHAPEEDGE", "Line 5", [ [ 0.3, 0.1, 0 ] ], [ [ 0, 0, 0.1 ] ] )
345 extrudeProfile( "SHAPEEDGE", "Line 6", [ [ 0.7, 0.1, 0 ] ], [ [ 0, 0, 0.1 ] ] )
346 extrudeProfile( "SHAPEEDGE", "Line 7", [ [ 1.1, 0.1, 0 ] ], [ [ 0, 0, 0.1 ] ] )
347 extrudeProfile( "SHAPEEDGE", "Line 8", [ [ 1.5, 0.1, 0 ] ], [ [ 0, 0, 0.1 ] ] )
348 extrudeProfile( "SHAPEEDGE", "Line 9", [ [ 0.5, 0.1, 0 ] ], [ [ 0, 0, 0.1 ] ] )
349 extrudeProfile( "SHAPEEDGE", "Line 10", [ [ 0.9, 0.1, 0 ] ], [ [ 0, 0, 0.1 ] ] )

```

```

350 extrudeProfile( "SHAPEEDGE", "Line 11", [ [ 1.3, 0.1, 0 ] ], [ [ 0, 0, 0.1 ] ] )
351 extrudeProfile( "SHAPEEDGE", "Line 12", [ [ 1.7, 0.1, 0 ] ], [ [ 0, 0, 0.1 ] ] )
352 healAndSew( [ "Sheet 13", "Sheet 17", "Sheet 15", "Sheet 19", "Sheet 21", "Sheet 29", "Sheet
    23", "Sheet 31", "Sheet 25", "Sheet 33", "Sheet 27", "Sheet 35" ], 1e-05, {} )
353 healAndSew( [ "Sheet 1", "Sheet 2", "Sheet 3", "Sheet 4", "Sheet 5", "Sheet 6" ], 1e-05, {} )
354 removeShape( [ "polygon 1", "Line 1", "Line 2", "Line 3", "Line 4", "Line 5", "Line 6", "Line
    7", "Line 8", "Line 9", "Line 10", "Line 11", "Line 12" ] )
355 saveProject( )
356 setViewPoint( "ISO1" )
357 rename( "SHAPESET", "Shapes", "Layer 1" )
358 renameShape( "Sheet 1", "Wall 1" )
359 renameShape( "Sheet 13", "Truss 1" )
360 saveProject( )
361 arrayCopy( [ "Wall 1", "Truss 1" ], [ 0, 0, 0.1 ], [ 0, 0, 0 ], [ 0, 0, 0 ], 29 )
362 addSet( "SHAPESET", "Shapes 1" )
363 rename( "SHAPESET", "Shapes 1", "Layer 2" )
364 setCurrentShapeSet( "Layer 1" )
365 moveToShapeSet( [ "Truss 2", "Wall 2" ], "Layer 2" )
366
367 for i in range(3,31):
368     addSet( "SHAPESET", "Shapes 1" )
369     rename( "SHAPESET", "Shapes 1", "Layer "+str(i) )
370     setCurrentShapeSet( "Layer "+str(i) )
371     moveToShapeSet( [ "Truss "+str(i), "Wall "+str(i) ], "Layer "+str(i) )
372

```

```
373 createSheet( "Sheet 1", [ [ 0.6, 0, 0.5 ], [ 0.6, 0.2, 0.5 ], [ 0.6, 0.2, 2.5 ], [ 0.6, 0,
    2.5 ] ] )
374 setCurrentShapeSet( "Layer 6" )
375 setCurrentShapeSet( "Layer 25" )
376 setCurrentShapeSet( "Layer 1" )
377 cut( "Wall 6", [ "Sheet 1" ], True, True )
378 cut( "Truss 6", [ "Sheet 1" ], True, True )
379 cut( "Wall 7", [ "Sheet 1" ], True, True )
380 cut( "Truss 7", [ "Sheet 1" ], True, True )
381 cut( "Wall 8", [ "Sheet 1" ], True, True )
382 cut( "Truss 8", [ "Sheet 1" ], True, True )
383 cut( "Wall 9", [ "Sheet 1" ], True, True )
384 cut( "Truss 9", [ "Sheet 1" ], True, True )
385 cut( "Wall 10", [ "Sheet 1" ], True, True )
386 cut( "Truss 10", [ "Sheet 1" ], True, True )
387 cut( "Wall 11", [ "Sheet 1" ], True, True )
388 cut( "Truss 11", [ "Sheet 1" ], True, True )
389 cut( "Wall 12", [ "Sheet 1" ], True, True )
390 cut( "Truss 12", [ "Sheet 1" ], True, True )
391 cut( "Wall 13", [ "Sheet 1" ], True, True )
392 cut( "Truss 13", [ "Sheet 1" ], True, True )
393 cut( "Wall 14", [ "Sheet 1" ], True, True )
394 cut( "Truss 14", [ "Sheet 1" ], True, True )
395 cut( "Wall 15", [ "Sheet 1" ], True, True )
396 cut( "Truss 15", [ "Sheet 1" ], True, True )
397 cut( "Wall 16", [ "Sheet 1" ], True, True )
```

```
398 cut( "Truss 16", [ "Sheet 1" ], True, True )
399 cut( "Wall 17", [ "Sheet 1" ], True, True )
400 cut( "Truss 17", [ "Sheet 1" ], True, True )
401 cut( "Wall 18", [ "Sheet 1" ], True, True )
402 cut( "Truss 18", [ "Sheet 1" ], True, True )
403 cut( "Wall 19", [ "Sheet 1" ], True, True )
404 cut( "Truss 19", [ "Sheet 1" ], True, True )
405 cut( "Wall 20", [ "Sheet 1" ], True, True )
406 cut( "Truss 20", [ "Sheet 1" ], True, True )
407 cut( "Wall 21", [ "Sheet 1" ], True, True )
408 cut( "Truss 21", [ "Sheet 1" ], True, True )
409 cut( "Wall 22", [ "Sheet 1" ], True, True )
410 cut( "Truss 22", [ "Sheet 1" ], True, True )
411 cut( "Wall 23", [ "Sheet 1" ], True, True )
412 cut( "Truss 23", [ "Sheet 1" ], True, True )
413 cut( "Wall 24", [ "Sheet 1" ], True, True )
414 cut( "Truss 24", [ "Sheet 1" ], True, True )
415 cut( "Wall 25", [ "Sheet 1" ], True, True )
416 cut( "Truss 25", [ "Sheet 1" ], True, True )
417 removeShape( [ "Wall 25", "Wall 21", "Wall 22", "Wall 14", "Wall 12", "Wall 18" ] )
418 removeShape( [ "Wall 23" ] )
419 removeShape( [ "Truss 22_1" ] )
420 removeShape( [ "Truss 21_1" ] )
421 removeShape( [ "Wall 20" ] )
422 removeShape( [ "Wall 19" ] )
423 removeShape( [ "Wall 17" ] )
```

```
424 removeShape( [ "Wall 16" ] )
425 removeShape( [ "Wall 15", "Truss 12_1", "Wall 13" ] )
426 removeShape( [ "Wall 11", "Wall 10" ] )
427 removeShape( [ "Wall 8", "Wall 7" ] )
428 removeShape( [ "Wall 6" ] )
429 removeShape( [ "Truss 6_1" ] )
430 removeShape( [ "Truss 7_1" ] )
431 removeShape( [ "Wall 9" ] )
432 removeShape( [ "Truss 8_1" ] )
433 removeShape( [ "Truss 9_1", "Truss 10_1", "Truss 11_1", "Truss 14_1", "Truss 13_1", "Truss
    16_1", "Truss 18_1", "Truss 19_1" ] )
434 removeShape( [ "Truss 15_1", "Truss 17_1" ] )
435 removeShape( [ "Truss 20_1" ] )
436 removeShape( [ "Truss 23_1" ] )
437 removeShape( [ "Wall 24" ] )
438 removeShape( [ "Truss 24_1" ] )
439 removeShape( [ "Truss 25_1" ] )
440 removeShape( [ "Sheet 1" ] )
441 createSheet( "Sheet 1", [ [ 0.6, 0, 0.5 ], [ 0.6, 0.2, 0.5 ], [ 0.6, 0.2, 0.6 ], [ 0.6, 0,
    0.6 ] ] )
442 renameShape( "Sheet 1", "Wall 6" )
443 moveToShapeSet( [ "Wall 6" ], "Layer 6" )
444 setCurrentShapeSet( "Layer 6" )
445 arrayCopy( [ "Wall 6" ], [ 0, 0, 0.1 ], [ 0, 0, 0 ], [ 0, 0, 0 ], 19 )
446 saveProject( )
447 moveToShapeSet( [ "Wall 7" ], "Layer 7" )
```



```

448
449 for i in range(8,26):
450     moveToShapeSet( [ "Wall "+str(i) ], "Layer "+str(i) )
451
452 healAndSew( [ "Wall 6", "Wall 6_1" ], 1e-05, {} )
453
454 for i in range(7,26):
455     healAndSew( [ "Wall "+str(i), "Wall "+str(i)+"_"+"1" ], 1e-05, {} )
456
457 createSheet( "Sheet 1", [ [ 0.6, 0.2, 0.5 ], [ 0.6, 0, 0.5 ], [ 1.8, 0, 0.5 ], [ 1.8, 0.2,
458     0.5 ] ] )
459 moveToShapeSet( [ "Sheet 1" ], "Layer 5" )
460 setCurrentShapeSet( "Layer 5" )
461 healAndSew( [ "Wall 5", "Sheet 1" ], 1e-05, {} )
462 setCurrentShapeSet( "Layer 4" )
463 setCurrentShapeSet( "Layer 25" )
464 setCurrentShapeSet( "Layer 26" )
465 createSheet( "Sheet 1", [ [ 0.6, 0, 2.5 ], [ 0.6, 0.2, 2.5 ], [ 1.8, 0.2, 2.5 ], [ 1.8, 0,
466     2.5 ] ] )
467 healAndSew( [ "Wall 26", "Sheet 1" ], 1e-05, {} )
468
469 addMaterial( "concrete_nonlin", "CONCR", "TSCR", [ "MATURI" ] )
470 setParameter( "MATERIAL", "concrete_nonlin", "LINEAR/ELASTI/YOUNG", 18000000 )
471 setParameter( "MATERIAL", "concrete_nonlin", "LINEAR/ELASTI/POISON", 0.3 )
472 setParameter( "MATERIAL", "concrete_nonlin", "LINEAR/MASS/DENSIT", 2100 )

```

```

471 setParameter( "MATERIAL", "concrete_nonlin", "LINEAR/MATURI/MATYOU", [ 0, 77900, 120000,
    2477900 ] )
472 setParameter( "MATERIAL", "concrete_nonlin", "MODTYP/TOTCRK", "ROTATE" )
473 setParameter( "MATERIAL", "concrete_nonlin", "TENSIL/TENCRV", "CONSTA" )
474 setParameter( "MATERIAL", "concrete_nonlin", "TENSIL/TENSTR", 3000 )
475 setParameter( "MATERIAL", "concrete_nonlin", "TENSIL/MATURI/MATTST", "[]" )
476 setParameter( "MATERIAL", "concrete_nonlin", "TENSIL/MATURI/MATTST", [ 0, 3067, 120000,
    132267 ] )
477 setParameter( "MATERIAL", "concrete_nonlin", "COMPRS/COMCRV", "CONSTA" )
478 setParameter( "MATERIAL", "concrete_nonlin", "COMPRS/COMSTR", 6000 )
479 setParameter( "MATERIAL", "concrete_nonlin", "COMPRS/COMSTR", 6000 )
480 setParameter( "MATERIAL", "concrete_nonlin", "COMPRS/MATURI/MATCST", "[]" )
481 setParameter( "MATERIAL", "concrete_nonlin", "COMPRS/MATURI/MATCST", [ 0, 5984, 120000,
    299984 ] )
482 setParameter( "MATERIAL", "concrete_nonlin", "COMPRS/CONFIN/CNFCRV", "VECCHI" )
483
484 addMaterial( "concrete_nonlin2", "CONCR", "TSCR", [ "MATURI" ] )
485 setParameter( "MATERIAL", "concrete_nonlin2", "LINEAR/ELASTI/YOUNG", 18000000 )
486 setParameter( "MATERIAL", "concrete_nonlin2", "LINEAR/ELASTI/POISON", 0.3 )
    setParameter( "MATERIAL", "concrete_nonlin2", "LINEAR/MASS/DENSIT", 2100 )
487 setParameter( "MATERIAL", "concrete_nonlin2", "LINEAR/MATURI/MATYOU", [ 0, 77900, 120000,
488 4911050 ] )
489 setParameter( "MATERIAL", "concrete_nonlin2", "MODTYP/TOTCRK", "ROTATE" )
490 setParameter( "MATERIAL", "concrete_nonlin2", "TENSIL/TENCRV", "CONSTA" )
491 setParameter( "MATERIAL", "concrete_nonlin2", "TENSIL/TENSTR", 3000 )
492 setParameter( "MATERIAL", "concrete_nonlin2", "TENSIL/MATURI/MATTST", "[]" )

```

```

493 setParameter( "MATERIAL", "concrete_nonlin2", "TENSIL/MATURI/MATTST", [ 0, 3067, 120000,
    5998470 ] )
494 setParameter( "MATERIAL", "concrete_nonlin2", "COMPRS/COMCRV", "CONSTA" )
495 setParameter( "MATERIAL", "concrete_nonlin2", "COMPRS/COMSTR", 6000 )
496 setParameter( "MATERIAL", "concrete_nonlin2", "COMPRS/COMSTR", 6000 )
497 setParameter( "MATERIAL", "concrete_nonlin2", "COMPRS/MATURI/MATCST", "[]" )
498 setParameter( "MATERIAL", "concrete_nonlin2", "COMPRS/MATURI/MATCST", [ 0, 5984, 120000,
    60000000 ] )
499 setParameter( "MATERIAL", "concrete_nonlin2", "COMPRS/CONFIN/CNFCRV", "VECCHI" )
500
501 addMaterial( "interf_mat", "INTERF", "ELASTI", [] )
502 setParameter( "MATERIAL", "interf_mat", "LINEAR/IFTYP", "LIN3D" )
503 setParameter( "MATERIAL", "interf_mat", "LINEAR/ELAS4/DSNY", 1e+08 )
504 setParameter( "MATERIAL", "interf_mat", "LINEAR/ELAS4/DSSX", 1e+08 )
505
506 addGeometry( "Thickness", "SHEET", "CURSHL", [] )
507 setParameter( "GEOMET", "Thickness", "THICK", 0.05 )
508 addGeometry( "Element geometry 1", "LINE", "SHLLIF", [] )
509 setParameter( "GEOMET", "Element geometry 1", "THICK", 0.05 )
510 setParameter( "GEOMET", "Element geometry 1", "ZAXIS", [ 0, 0, 1 ] )
511
512 addElementData( "Element data 1" )
513 setParameter( "DATA", "Element data 1", "THINTE", 5 )
514
515 addSet( "GEOMETRYSUPPORTSET", "Support set 1" )
516 createSurfaceSupport( "Support 1", "Support set 1" )

```

```

517 setParameter( "GEOMETRY SUPPORT", "Support 1", "AXES", [ 1, 2 ] )
518 setParameter( "GEOMETRY SUPPORT", "Support 1", "TRANSL", [ 0, 1, 0 ] )
519 setParameter( "GEOMETRY SUPPORT", "Support 1", "ROTATI", [ 0, 0, 0 ] )
520 attach( "GEOMETRY SUPPORT", "Support 1", "Wall 26", [ [ 0.1147146, 1, 2.5573573 ] ] )
521 attach( "GEOMETRY SUPPORT", "Support 1", "Wall 27", [ [ 0.1147146, 1, 2.6573573 ] ] )
522 attach( "GEOMETRY SUPPORT", "Support 1", "Wall 28", [ [ 0.1147146, 1, 2.7573573 ] ] )
523 attach( "GEOMETRY SUPPORT", "Support 1", "Wall 29", [ [ 0.1147146, 1, 2.8573573 ] ] )
524 attach( "GEOMETRY SUPPORT", "Support 1", "Wall 30", [ [ 0.1147146, 1, 2.9573573 ] ] )
525 attach( "GEOMETRY SUPPORT", "Support 1", "Wall 21", [ [ 0.1147146, 1, 2.0573573 ] ] )
526 attach( "GEOMETRY SUPPORT", "Support 1", "Wall 22", [ [ 0.1147146, 1, 2.1573573 ] ] )
527 attach( "GEOMETRY SUPPORT", "Support 1", "Wall 23", [ [ 0.1147146, 1, 2.2573573 ] ] )
528 attach( "GEOMETRY SUPPORT", "Support 1", "Wall 24", [ [ 0.1147146, 1, 2.3573573 ] ] )
529 attach( "GEOMETRY SUPPORT", "Support 1", "Wall 25", [ [ 0.1147146, 1, 2.4573573 ] ] )
530
531 addSet( "GEOMETRY SUPPORT SET", "Support set 2" )
532 createSurfaceSupport( "Support 2", "Support set 2" )
533 setParameter( "GEOMETRY SUPPORT", "Support 2", "AXES", [ 1, 2 ] )
534 setParameter( "GEOMETRY SUPPORT", "Support 2", "TRANSL", [ 1, 0, 0 ] )
535 setParameter( "GEOMETRY SUPPORT", "Support 2", "ROTATI", [ 0, 0, 0 ] )
536 attach( "GEOMETRY SUPPORT", "Support 2", "Wall 26", [ [ 1.8, 0.1147146, 2.5426427 ] ] )
537 attach( "GEOMETRY SUPPORT", "Support 2", "Wall 27", [ [ 1.8, 0.1147146, 2.6426427 ] ] )
538 attach( "GEOMETRY SUPPORT", "Support 2", "Wall 28", [ [ 1.8, 0.1147146, 2.7426427 ] ] )
539 attach( "GEOMETRY SUPPORT", "Support 2", "Wall 29", [ [ 1.8, 0.1147146, 2.8426427 ] ] )
540 attach( "GEOMETRY SUPPORT", "Support 2", "Wall 30", [ [ 1.8, 0.1147146, 2.9426427 ] ] )
541 createLineSupport( "Support 3", "Support set 2" )
542 setParameter( "GEOMETRY SUPPORT", "Support 3", "AXES", [ 1, 2 ] )

```

```

543 setParameter( "GEOMETRY SUPPORT", "Support 3", "TRANSL", [ 0, 0, 1 ] )
544 setParameter( "GEOMETRY SUPPORT", "Support 3", "ROTATI", [ 0, 0, 0 ] )
545 attach( "GEOMETRY SUPPORT", "Support 3", "Wall 26", [ [ 1.2, 0, 2.5 ], [ 1.8, 0.1, 2.5 ],
[ 1.2, 0.2, 2.5 ] ] )
546 attach( "GEOMETRY SUPPORT", "Support 3", "Truss 26", [ [ 1.7, 0.1, 2.5 ], [ 1.5, 0.1, 2.5 ],
[ 1.3, 0.1, 2.5 ], [ 1.1, 0.1, 2.5 ], [ 0.9, 0.1, 2.5 ], [ 0.7, 0.1, 2.5 ] ] )
547
548 addSet( "GEOMETRY SUPPORT SET", "Support set 3" )
549 createSurfaceSupport( "Support 4", "Support set 3" )
550 setParameter( "GEOMETRY SUPPORT", "Support 4", "AXES", [ 1, 2 ] )
551 setParameter( "GEOMETRY SUPPORT", "Support 4", "TRANSL", [ 1, 0, 0 ] )
552 setParameter( "GEOMETRY SUPPORT", "Support 4", "ROTATI", [ 0, 0, 0 ] )
553 attach( "GEOMETRY SUPPORT", "Support 4", "Wall 1", [ [ 1.8, 0.1147146, 0.0426427 ] ] )
554 attach( "GEOMETRY SUPPORT", "Support 4", "Wall 2", [ [ 1.8, 0.1147146, 0.1426427 ] ] )
555 attach( "GEOMETRY SUPPORT", "Support 4", "Wall 3", [ [ 1.8, 0.1147146, 0.2426427 ] ] )
556 attach( "GEOMETRY SUPPORT", "Support 4", "Wall 4", [ [ 1.8, 0.1147146, 0.3426427 ] ] )
557 attach( "GEOMETRY SUPPORT", "Support 4", "Wall 5", [ [ 1.8, 0.1147146, 0.4426427 ] ] )
558
559 createSheet( "Sheet 1", [ [ 0, 0, 0 ], [ 1.8, 0, 0 ], [ 1.8, 0.2, 0 ], [ 0, 0.2, 0 ] ] )
560 createSheet( "Sheet 2", [ [ 0, 0.2, 0 ], [ 0.2, 0.2, 0 ], [ 0.2, 1, 0 ], [ 0, 1, 0 ] ] )
561 healAndSew( [ "Wall 1", "Sheet 1", "Sheet 2" ], 1e-05, {} )
562
563 createSurfaceSupport( "Support 5", "Support set 3" )
564 setParameter( "GEOMETRY SUPPORT", "Support 5", "AXES", [ 1, 2 ] )
565 setParameter( "GEOMETRY SUPPORT", "Support 5", "TRANSL", [ 1, 1, 1 ] )
566 setParameter( "GEOMETRY SUPPORT", "Support 5", "ROTATI", [ 0, 0, 0 ] )

```

```

567 attach( "GEOMETRYSUPPORT", "Support 5", "Wall 1", [ [ 1.0324314, 0.1147146, 0 ], [ 0.1147146,
0.6588584, 0 ] ] )
568
569 createLineSupport( "Support 6", "Support set 3" )
570 setParameter( "GEOMETRYSUPPORT", "Support 6", "AXES", [ 1, 2 ] )
571 setParameter( "GEOMETRYSUPPORT", "Support 6", "TRANSL", [ 1, 1, 1 ] )
572 setParameter( "GEOMETRYSUPPORT", "Support 6", "ROTATI", [ 0, 0, 0 ] )
573 attach( "GEOMETRYSUPPORT", "Support 6", "Wall 1", [ [ 1.8, 0.1, 0 ], [ 0.9, 0, 0 ], [ 1, 0.2,
0 ], [ 0, 0.1, 0 ], [ 0, 0.6, 0 ], [ 0.1, 1, 0 ], [ 0.2, 0.6, 0 ] ] )
574 attach( "GEOMETRYSUPPORT", "Support 6", "Truss 1", [ [ 0.1, 0.9, 0 ], [ 0.1, 0.7, 0 ], [ 0.1,
0.5, 0 ], [ 0.1, 0.3, 0 ], [ 0.3, 0.1, 0 ], [ 0.5, 0.1, 0 ], [ 0.7, 0.1, 0 ], [ 0.9, 0.1,
0 ], [ 1.1, 0.1, 0 ], [ 1.3, 0.1, 0 ], [ 1.5, 0.1, 0 ], [ 1.7, 0.1, 0 ] ] )
575
576 createConnection( "Connection 1", "BOUNDA", "SHAPEEDGE" )
577 setParameter( "GEOMETRYCONNECTION", "Connection 1", "MODE", "CLOSED" )
578 setElementClassType( "GEOMETRYCONNECTION", "Connection 1", "SHLLIF" )
579 assignMaterial( "interf_mat", "GEOMETRYCONNECTION", "Connection 1" )
580 assignGeometry( "Element geometry 1", "GEOMETRYCONNECTION", "Connection 1" )
581 assignElementData( "Element data 1", "GEOMETRYCONNECTION", "Connection 1" )
582 setParameter( "GEOMETRYCONNECTION", "Connection 1", "FLIP", False )
583 attach( "GEOMETRYSUPPORT", "Support 3", "Wall 26", [ [ 1.2, 0, 2.5 ], [ 1.8, 0.1, 2.5 ],
[ 1.2, 0.2, 2.5 ] ] )
584 attach( "GEOMETRYSUPPORT", "Support 3", "Truss 26", [ [ 1.7, 0.1, 2.5 ], [ 1.5, 0.1, 2.5 ],
[ 1.3, 0.1, 2.5 ], [ 1.1, 0.1, 2.5 ], [ 0.9, 0.1, 2.5 ], [ 0.7, 0.1, 2.5 ] ] )
585 attachTo( "GEOMETRYCONNECTION", "Connection 1", "SOURCE", "Wall 26", [ [ 1.2, 0, 2.5 ] ] )
586 attachTo( "GEOMETRYCONNECTION", "Connection 1", "SOURCE", "Wall 26", [ [ 1.8, 0.1, 2.5 ] ] )

```

```

587 attachTo( "GEOMETRYCONNECTION", "Connection 1", "SOURCE", "Wall 26", [ [ 1.2, 0.2, 2.5 ] ] )
588 attachTo( "GEOMETRYCONNECTION", "Connection 1", "SOURCE", "Truss 26", [ [ 1.7, 0.1, 2.5 ] ] )
589 attachTo( "GEOMETRYCONNECTION", "Connection 1", "SOURCE", "Truss 26", [ [ 1.5, 0.1, 2.5 ] ] )
590 attachTo( "GEOMETRYCONNECTION", "Connection 1", "SOURCE", "Truss 26", [ [ 1.3, 0.1, 2.5 ] ] )
591 attachTo( "GEOMETRYCONNECTION", "Connection 1", "SOURCE", "Truss 26", [ [ 1.1, 0.1, 2.5 ] ] )
592 attachTo( "GEOMETRYCONNECTION", "Connection 1", "SOURCE", "Truss 26", [ [ 0.9, 0.1, 2.5 ] ] )
593 attachTo( "GEOMETRYCONNECTION", "Connection 1", "SOURCE", "Truss 26", [ [ 0.7, 0.1, 2.5 ] ] )
594 rename( "GEOMETRYCONNECTION", "Connection 1", "Connection 2" )
595
596 createConnection( "Connection 1", "BOUNDARY", "SHAPEEDGE" )
597 setParameter( "GEOMETRYCONNECTION", "Connection 1", "MODE", "CLOSED" )
598 setElementClassType( "GEOMETRYCONNECTION", "Connection 1", "SHLLIF" )
599 assignMaterial( "interf_mat", "GEOMETRYCONNECTION", "Connection 1" )
600 assignGeometry( "Element geometry 1", "GEOMETRYCONNECTION", "Connection 1" )
601 assignElementData( "Element data 1", "GEOMETRYCONNECTION", "Connection 1" )
602 setParameter( "GEOMETRYCONNECTION", "Connection 1", "FLIP", False )
603 attach( "GEOMETRYSUPPORT", "Support 6", "Wall 1", [ [ 1, 0.2, 0 ], [ 0.2, 0.6, 0 ], [ 0.1, 1,
0 ], [ 0, 0.6, 0 ], [ 0, 0.1, 0 ], [ 0.9, 0, 0 ], [ 1.8, 0.1, 0 ] ] )
604 attach( "GEOMETRYSUPPORT", "Support 6", "Truss 1", [ [ 1.7, 0.1, 0 ], [ 1.5, 0.1, 0 ], [ 1.3,
0.1, 0 ], [ 1.1, 0.1, 0 ], [ 0.9, 0.1, 0 ], [ 0.7, 0.1, 0 ], [ 0.5, 0.1, 0 ], [ 0.3, 0.1,
0 ], [ 0.1, 0.3, 0 ], [ 0.1, 0.5, 0 ], [ 0.1, 0.7, 0 ], [ 0.1, 0.9, 0 ] ] )
605 attachTo( "GEOMETRYCONNECTION", "Connection 1", "SOURCE", "Wall 1", [ [ 1, 0.2, 0 ] ] )
606 attachTo( "GEOMETRYCONNECTION", "Connection 1", "SOURCE", "Wall 1", [ [ 0.2, 0.6, 0 ] ] )
607 attachTo( "GEOMETRYCONNECTION", "Connection 1", "SOURCE", "Wall 1", [ [ 0.1, 1, 0 ] ] )
608 attachTo( "GEOMETRYCONNECTION", "Connection 1", "SOURCE", "Wall 1", [ [ 0, 0.6, 0 ] ] )
609 attachTo( "GEOMETRYCONNECTION", "Connection 1", "SOURCE", "Wall 1", [ [ 0, 0.1, 0 ] ] )

```

```

610 attachTo( "GEOMETRYCONNECTION", "Connection 1", "SOURCE", "Wall 1", [ [ 0.9, 0, 0 ] ] )
611 attachTo( "GEOMETRYCONNECTION", "Connection 1", "SOURCE", "Wall 1", [ [ 1.8, 0.1, 0 ] ] )
612 attachTo( "GEOMETRYCONNECTION", "Connection 1", "SOURCE", "Truss 1", [ [ 1.7, 0.1, 0 ] ] )
613 attachTo( "GEOMETRYCONNECTION", "Connection 1", "SOURCE", "Truss 1", [ [ 1.5, 0.1, 0 ] ] )
614 attachTo( "GEOMETRYCONNECTION", "Connection 1", "SOURCE", "Truss 1", [ [ 1.3, 0.1, 0 ] ] )
615 attachTo( "GEOMETRYCONNECTION", "Connection 1", "SOURCE", "Truss 1", [ [ 1.1, 0.1, 0 ] ] )
616 attachTo( "GEOMETRYCONNECTION", "Connection 1", "SOURCE", "Truss 1", [ [ 0.9, 0.1, 0 ] ] )
617 attachTo( "GEOMETRYCONNECTION", "Connection 1", "SOURCE", "Truss 1", [ [ 0.7, 0.1, 0 ] ] )
618 attachTo( "GEOMETRYCONNECTION", "Connection 1", "SOURCE", "Truss 1", [ [ 0.5, 0.1, 0 ] ] )
619 attachTo( "GEOMETRYCONNECTION", "Connection 1", "SOURCE", "Truss 1", [ [ 0.3, 0.1, 0 ] ] )
620 attachTo( "GEOMETRYCONNECTION", "Connection 1", "SOURCE", "Truss 1", [ [ 0.1, 0.3, 0 ] ] )
621 attachTo( "GEOMETRYCONNECTION", "Connection 1", "SOURCE", "Truss 1", [ [ 0.1, 0.5, 0 ] ] )
622 attachTo( "GEOMETRYCONNECTION", "Connection 1", "SOURCE", "Truss 1", [ [ 0.1, 0.7, 0 ] ] )
623 attachTo( "GEOMETRYCONNECTION", "Connection 1", "SOURCE", "Truss 1", [ [ 0.1, 0.9, 0 ] ] )
624
625 addSet( "GEOMETRYLOADSET", "Load case 1" )
626 createModelLoad( "Global Load 1", "Load case 1" )
627
628 setElementSize( [ "Wall 1", "Truss 1", "Wall 2", "Truss 2", "Wall 3", "Truss 3", "Wall 4",
    "Truss 4", "Wall 5", "Truss 5", "Truss 6", "Truss 7", "Truss 8", "Truss 9", "Truss 10",
    "Truss 11", "Truss 12", "Truss 13", "Truss 14", "Truss 15", "Truss 16", "Truss 17", "Truss
    18", "Truss 19", "Truss 20", "Truss 21", "Truss 22", "Truss 23", "Truss 24", "Truss 25",
    "Wall 26", "Truss 26", "Wall 27", "Truss 27", "Wall 28", "Truss 28", "Wall 29", "Truss 29",
    "Wall 30", "Truss 30", "Wall 6", "Wall 7", "Wall 8", "Wall 9", "Wall 10", "Wall 11", "Wall
    12", "Wall 13", "Wall 14", "Wall 15", "Wall 16", "Wall 17", "Wall 18", "Wall 19", "Wall 20",
    "Wall 21", "Wall 22", "Wall 23", "Wall 24", "Wall 25" ], 0.1, 0.5, True )

```



```

629 clearMesherType( [ "Wall 1", "Truss 1", "Wall 2", "Truss 2", "Wall 3", "Truss 3", "Wall 4",
"Truss 4", "Wall 5", "Truss 5", "Truss 6", "Truss 7", "Truss 8", "Truss 9", "Truss 10",
"Truss 11", "Truss 12", "Truss 13", "Truss 14", "Truss 15", "Truss 16", "Truss 17", "Truss
18", "Truss 19", "Truss 20", "Truss 21", "Truss 22", "Truss 23", "Truss 24", "Truss 25",
"Wall 26", "Truss 26", "Wall 27", "Truss 27", "Wall 28", "Truss 28", "Wall 29", "Truss 29",
"Wall 30", "Truss 30", "Wall 6", "Wall 7", "Wall 8", "Wall 9", "Wall 10", "Wall 11", "Wall
12", "Wall 13", "Wall 14", "Wall 15", "Wall 16", "Wall 17", "Wall 18", "Wall 19", "Wall 20",
"Wall 21", "Wall 22", "Wall 23", "Wall 24", "Wall 25" ] )
630 clearMidSideNodeLocation( [ "Wall 1", "Truss 1", "Wall 2", "Truss 2", "Wall 3", "Truss 3",
"Wall 4", "Truss 4", "Wall 5", "Truss 5", "Truss 6", "Truss 7", "Truss 8", "Truss 9", "Truss
10", "Truss 11", "Truss 12", "Truss 13", "Truss 14", "Truss 15", "Truss 16", "Truss 17",
"Truss 18", "Truss 19", "Truss 20", "Truss 21", "Truss 22", "Truss 23", "Truss 24", "Truss
25", "Wall 26", "Truss 26", "Wall 27", "Truss 27", "Wall 28", "Truss 28", "Wall 29", "Truss
29", "Wall 30", "Truss 30", "Wall 6", "Wall 7", "Wall 8", "Wall 9", "Wall 10", "Wall 11",
"Wall 12", "Wall 13", "Wall 14", "Wall 15", "Wall 16", "Wall 17", "Wall 18", "Wall 19", "Wall
20", "Wall 21", "Wall 22", "Wall 23", "Wall 24", "Wall 25" ] )
631 setCurrentShapeSet( "Layer 30" )
632 setElementClassType( "SHAPE", [ "Wall 1", "Truss 1", "Truss 27", "Wall 27", "Truss 11", "Wall
2", "Truss 7", "Truss 2", "Wall 3", "Truss 3", "Wall 4", "Truss 8", "Wall 5", "Truss 4",
"Wall 28", "Wall 24", "Truss 5", "Truss 6", "Wall 6", "Truss 21", "Wall 7", "Wall 20", "Wall
8", "Truss 9", "Wall 9", "Truss 25", "Truss 10", "Wall 22", "Wall 13", "Wall 10", "Wall 23",
"Wall 11", "Truss 12", "Wall 26", "Wall 12", "Truss 13", "Wall 19", "Wall 16", "Truss 14",
"Wall 14", "Wall 18", "Truss 15", "Wall 15", "Truss 29", "Truss 23", "Truss 16", "Truss 30",
"Truss 17", "Truss 19", "Wall 17", "Truss 20", "Truss 18", "Truss 22", "Wall 21", "Truss 24",
"Wall 25", "Truss 26", "Truss 28", "Wall 29", "Wall 30" ], "CURSHL" )

```

```

633 assignMaterial( "concrete_nonlin", "SHAPE", [ "Wall 1", "Truss 1", "Truss 27", "Wall 27",
"Truss 11", "Wall 2", "Truss 7", "Truss 2", "Wall 3", "Truss 3", "Wall 4", "Truss 8", "Wall
5", "Truss 4", "Wall 28", "Wall 24", "Truss 5", "Truss 6", "Wall 6", "Truss 21", "Wall 7",
"Wall 20", "Wall 8", "Truss 9", "Wall 9", "Truss 25", "Truss 10", "Wall 22", "Wall 13", "Wall
10", "Wall 23", "Wall 11", "Truss 12", "Wall 26", "Wall 12", "Truss 13", "Wall 19", "Wall
16", "Truss 14", "Wall 14", "Wall 18", "Truss 15", "Wall 15", "Truss 29", "Truss 23", "Truss
16", "Truss 30", "Truss 17", "Truss 19", "Wall 17", "Truss 20", "Truss 18", "Truss 22", "Wall
21", "Truss 24", "Wall 25", "Truss 26", "Truss 28", "Wall 29", "Wall 30" ] )
634 assignGeometry( "Thickness", "SHAPE", [ "Wall 1", "Truss 1", "Truss 27", "Wall 27", "Truss
11", "Wall 2", "Truss 7", "Truss 2", "Wall 3", "Truss 3", "Wall 4", "Truss 8", "Wall 5",
"Truss 4", "Wall 28", "Wall 24", "Truss 5", "Truss 6", "Wall 6", "Truss 21", "Wall 7", "Wall
20", "Wall 8", "Truss 9", "Wall 9", "Truss 25", "Truss 10", "Wall 22", "Wall 13", "Wall 10",
"Wall 23", "Wall 11", "Truss 12", "Wall 26", "Wall 12", "Truss 13", "Wall 19", "Wall 16",
"Truss 14", "Wall 14", "Wall 18", "Truss 15", "Wall 15", "Truss 29", "Truss 23", "Truss 16",
"Truss 30", "Truss 17", "Truss 19", "Wall 17", "Truss 20", "Truss 18", "Truss 22", "Wall 21",
"Truss 24", "Wall 25", "Truss 26", "Truss 28", "Wall 29", "Wall 30" ] )
635 assignElementData( "Element data 1", "SHAPE", [ "Wall 1", "Truss 1", "Truss 27", "Wall 27",
"Truss 11", "Wall 2", "Truss 7", "Truss 2", "Wall 3", "Truss 3", "Wall 4", "Truss 8", "Wall
5", "Truss 4", "Wall 28", "Wall 24", "Truss 5", "Truss 6", "Wall 6", "Truss 21", "Wall 7",
"Wall 20", "Wall 8", "Truss 9", "Wall 9", "Truss 25", "Truss 10", "Wall 22", "Wall 13", "Wall
10", "Wall 23", "Wall 11", "Truss 12", "Wall 26", "Wall 12", "Truss 13", "Wall 19", "Wall
16", "Truss 14", "Wall 14", "Wall 18", "Truss 15", "Wall 15", "Truss 29", "Truss 23", "Truss
16", "Truss 30", "Truss 17", "Truss 19", "Wall 17", "Truss 20", "Truss 18", "Truss 22", "Wall
21", "Truss 24", "Wall 25", "Truss 26", "Truss 28", "Wall 29", "Wall 30" ] )
636
637 addAnalysis( "Analysis2" )

```

```
638 addAnalysisCommand( "Analysis2", "PHASE", "Phase" )
639 renameAnalysisCommand( "Analysis2", "Phase", "Phase 1" )
640 setActiveInPhase( "Analysis2", "SHAPESET", [ "Layer 2" ], [ "Phase 1" ], False )
641 setActiveInPhase( "Analysis2", "SHAPESET", [ "Layer 3" ], [ "Phase 1" ], False )
642 setActiveInPhase( "Analysis2", "SHAPESET", [ "Layer 4" ], [ "Phase 1" ], False )
643 setActiveInPhase( "Analysis2", "SHAPESET", [ "Layer 5" ], [ "Phase 1" ], False )
644 setActiveInPhase( "Analysis2", "SHAPESET", [ "Layer 6" ], [ "Phase 1" ], False )
645 setActiveInPhase( "Analysis2", "SHAPESET", [ "Layer 7" ], [ "Phase 1" ], False )
646 setActiveInPhase( "Analysis2", "SHAPESET", [ "Layer 8" ], [ "Phase 1" ], False )
647 setActiveInPhase( "Analysis2", "SHAPESET", [ "Layer 9" ], [ "Phase 1" ], False )
648 setActiveInPhase( "Analysis2", "SHAPESET", [ "Layer 10" ], [ "Phase 1" ], False )
649 setActiveInPhase( "Analysis2", "SHAPESET", [ "Layer 11" ], [ "Phase 1" ], False )
650 setActiveInPhase( "Analysis2", "SHAPESET", [ "Layer 12" ], [ "Phase 1" ], False )
651 setActiveInPhase( "Analysis2", "SHAPESET", [ "Layer 13" ], [ "Phase 1" ], False )
652 setActiveInPhase( "Analysis2", "SHAPESET", [ "Layer 14" ], [ "Phase 1" ], False )
653 setActiveInPhase( "Analysis2", "SHAPESET", [ "Layer 15" ], [ "Phase 1" ], False )
654 setActiveInPhase( "Analysis2", "SHAPESET", [ "Layer 16" ], [ "Phase 1" ], False )
655 setActiveInPhase( "Analysis2", "SHAPESET", [ "Layer 17" ], [ "Phase 1" ], False )
656 setActiveInPhase( "Analysis2", "SHAPESET", [ "Layer 18" ], [ "Phase 1" ], False )
657 setActiveInPhase( "Analysis2", "SHAPESET", [ "Layer 19" ], [ "Phase 1" ], False )
658 setActiveInPhase( "Analysis2", "SHAPESET", [ "Layer 20" ], [ "Phase 1" ], False )
659 setActiveInPhase( "Analysis2", "SHAPESET", [ "Layer 21" ], [ "Phase 1" ], False )
660 setActiveInPhase( "Analysis2", "SHAPESET", [ "Layer 22" ], [ "Phase 1" ], False )
661 setActiveInPhase( "Analysis2", "SHAPESET", [ "Layer 23" ], [ "Phase 1" ], False )
662 setActiveInPhase( "Analysis2", "SHAPESET", [ "Layer 24" ], [ "Phase 1" ], False )
663 setActiveInPhase( "Analysis2", "SHAPESET", [ "Layer 25" ], [ "Phase 1" ], False )
```

```

664 setActiveInPhase( "Analysis2", "SHAPESET", [ "Layer 26" ], [ "Phase 1" ], False )
665 setActiveInPhase( "Analysis2", "SHAPESET", [ "Layer 27" ], [ "Phase 1" ], False )
666 setActiveInPhase( "Analysis2", "SHAPESET", [ "Layer 28" ], [ "Phase 1" ], False )
667 setActiveInPhase( "Analysis2", "SHAPESET", [ "Layer 29" ], [ "Phase 1" ], False )
668 setActiveInPhase( "Analysis2", "SHAPESET", [ "Layer 30" ], [ "Phase 1" ], False )
669 addAnalysisCommand( "Analysis2", "NONLIN", "Structural nonlinear" )
670 renameAnalysisCommand( "Analysis2", "Structural nonlinear", "Structural nonlinear 1" )
671 addAnalysisCommandDetail( "Analysis2", "Structural nonlinear 1", "TYPE/GEOMET" )
672 setAnalysisCommandDetail( "Analysis2", "Structural nonlinear 1", "TYPE/GEOMET", True )
673 setAnalysisCommandDetail( "Analysis2", "Structural nonlinear 1", "EXECUT(1)/EXETYP",
"START" )
674 setAnalysisCommandDetail( "Analysis2", "Structural nonlinear 1", "EXECUT(1)/START/STEPS",
False )
675 setAnalysisCommandDetail( "Analysis2", "Structural nonlinear 1", "EXECUT/EXETYP", "TIME" )
676 setAnalysisCommandDetail( "Analysis2", "Structural nonlinear 1", "EXECUT(2)/ITERAT/MAXITE",
10 )
677 setAnalysisCommandDetail( "Analysis2", "Structural nonlinear 1", "EXECUT(2)/ITERAT/MAXITE",
10 )
678 setAnalysisCommandDetail( "Analysis2", "Structural nonlinear 1",
"EXECUT(2)/TIME/STEPS/EXPLICIT/SIZES", "3930.00000" )
679 setAnalysisCommandDetail( "Analysis2", "Structural nonlinear 1", "EXECUT(2)/ITERAT/MAXITE",
50 )
680 addAnalysisCommandDetail( "Analysis2", "Structural nonlinear 1", "EXECUT(2)/ITERAT/LINESE" )
681 setAnalysisCommandDetail( "Analysis2", "Structural nonlinear 1", "EXECUT(2)/ITERAT/LINESE",
True )

```

```
682 setAnalysisCommandDetail( "Analysis2", "Structural nonlinear 1",  
    "EXECUT(2)/ITERAT/CONVER/SIMULT", True )  
683 setAnalysisCommandDetail( "Analysis2", "Structural nonlinear 1",  
    "EXECUT(2)/ITERAT/CONVER/DISPLA/NOCONV", "CONTIN" )  
684 setAnalysisCommandDetail( "Analysis2", "Structural nonlinear 1",  
    "EXECUT(2)/ITERAT/CONVER/FORCE/NOCONV", "TERMIN" )  
685 setAnalysisCommandDetail( "Analysis2", "Structural nonlinear 1",  
    "EXECUT(2)/ITERAT/CONVER/FORCE/NOCONV", "CONTIN" )  
686 setAnalysisCommandDetail( "Analysis2", "Structural nonlinear 1", "OUTPUT(1)/SELTYP", "USER" )  
687 addAnalysisCommandDetail( "Analysis2", "Structural nonlinear 1", "OUTPUT(1)/USER" )  
688 addAnalysisCommandDetail( "Analysis2", "Structural nonlinear 1", "OUTPUT(1)/USER/DISPLA" )  
689 addAnalysisCommandDetail( "Analysis2", "Structural nonlinear 1",  
    "OUTPUT(1)/USER/DISPLA(2)/TOTAL/TRANSL/AXIAL" )  
690 addAnalysisCommandDetail( "Analysis2", "Structural nonlinear 1",  
    "OUTPUT(1)/USER/MATURI(1)/TOTAL" )  
691 addAnalysisCommandDetail( "Analysis2", "Structural nonlinear 1",  
    "OUTPUT(1)/USER/PARAME(1)/YOUNG" )  
692 addAnalysisCommandDetail( "Analysis2", "Structural nonlinear 1",  
    "OUTPUT(1)/USER/PARAME(2)/COMSTR" )  
693 addAnalysisCommandDetail( "Analysis2", "Structural nonlinear 1",  
    "OUTPUT(1)/USER/STRESS(1)/TOTAL/PIOLAK/PRINCI" )  
694 setAnalysisCommandDetail( "Analysis2", "Structural nonlinear 1",  
    "OUTPUT(1)/USER/STRESS(1)/TOTAL/PIOLAK/PRINCI/LOCATI", "INTPNT" )  
695 addAnalysisCommandDetail( "Analysis2", "Structural nonlinear 1",  
    "OUTPUT(1)/USER/STRAIN(1)/TOTAL/GREEN/PRINCI" )
```

```

696 setAnalysisCommandDetail( "Analysis2", "Structural nonlinear 1",
    "OUTPUT(1)/USER/STRAIN(1)/TOTAL/GREEN/PRINCI/LOCATI", "INTPNT" )
697 addAnalysisCommandDetail( "Analysis2", "Structural nonlinear 1",
    "OUTPUT(1)/USER/STRESS(2)/TOTAL/TRACTI/LOCAL" )
698 addAnalysisCommandDetail( "Analysis2", "Structural nonlinear 1",
    "OUTPUT(1)/USER/STRAIN(2)/TOTAL/TRACTI/LOCAL" )
699 addAnalysisCommandDetail( "Analysis2", "Structural nonlinear 1",
    "OUTPUT(1)/USER/STRAIN(3)/CRKWDT/GREEN/PRINCI" )
700 setAnalysisCommandDetail( "Analysis2", "Structural nonlinear 1",
    "OUTPUT(1)/USER/STRAIN(3)/CRKWDT/GREEN/PRINCI/LOCATI", "INTPNT" )
701 setActivePhase( "Analysis2", "Phase 1" )
702 setActivePhase( "Analysis2", "" )
703 setActivePhase( "Analysis2", "Phase 1" )
704 setActiveInPhase( "Analysis2", "GEOMETRYSUPPORTSET", [ "Support set 1" ], [ "Phase 1" ],
    False )
705 setActiveInPhase( "Analysis2", "GEOMETRYSUPPORTSET", [ "Support set 2" ], [ "Phase 1" ],
    False )
706 setActiveInPhase( "Analysis2", "GEOMETRYCONNECTION", [ "Connection 2" ], [ "Phase 1" ],
    False )
707 copyAnalysisCommand( "Analysis2", "Phase 1", "Phase 2" )
708 setActiveInPhase( "Analysis2", "SHAPESET", [ "Layer 2" ], [ "Phase 2" ], True )
709 copyAnalysisCommand( "Analysis2", "Structural nonlinear 1", "Structural nonlinear 2" )
710 setAnalysisCommandDetail( "Analysis2", "Structural nonlinear 2", "EXECUT(1)/START/TIME",
    3930 )
711 copyAnalysisCommand( "Analysis2", "Phase 2", "Phase 3" )
712 setActiveInPhase( "Analysis2", "SHAPESET", [ "Layer 3" ], [ "Phase 3" ], True )

```

```
713 copyAnalysisCommand( "Analysis2", "Structural nonlinear 2", "Structural nonlinear 3" )
714 setAnalysisCommandDetail( "Analysis2", "Structural nonlinear 3", "EXECUT(1)/START/TIME",
715 7860 )
716 copyAnalysisCommand( "Analysis2", "Phase 3", "Phase 4" )
717 setActiveInPhase( "Analysis2", "SHAPESET", [ "Layer 4" ], [ "Phase 4" ], True )
718 copyAnalysisCommand( "Analysis2", "Structural nonlinear 3", "Structural nonlinear 4" )
719 setAnalysisCommandDetail( "Analysis2", "Structural nonlinear 4", "EXECUT(1)/START/TIME",
720 11790 )
721 copyAnalysisCommand( "Analysis2", "Phase 4", "Phase 5" )
722 setActiveInPhase( "Analysis2", "SHAPESET", [ "Layer 5" ], [ "Phase 5" ], True )
723 copyAnalysisCommand( "Analysis2", "Structural nonlinear 4", "Structural nonlinear 5" )
724 setAnalysisCommandDetail( "Analysis2", "Structural nonlinear 5", "EXECUT(1)/START/TIME",
725 15720 )
726 copyAnalysisCommand( "Analysis2", "Phase 5", "Phase 6" )
727 setActiveInPhase( "Analysis2", "SHAPESET", [ "Layer 6" ], [ "Phase 6" ], True )
728 copyAnalysisCommand( "Analysis2", "Structural nonlinear 5", "Structural nonlinear 6" )
729 setAnalysisCommandDetail( "Analysis2", "Structural nonlinear 6", "EXECUT(1)/START/TIME",
730 19650 )
731 copyAnalysisCommand( "Analysis2", "Phase 6", "Phase 7" )
732 setActiveInPhase( "Analysis2", "SHAPESET", [ "Layer 7" ], [ "Phase 7" ], True )
733 copyAnalysisCommand( "Analysis2", "Structural nonlinear 6", "Structural nonlinear 7" )
734 setAnalysisCommandDetail( "Analysis2", "Structural nonlinear 7", "EXECUT(1)/START/TIME",
735 23580 )
736 copyAnalysisCommand( "Analysis2", "Phase 7", "Phase 8" )
737 setActiveInPhase( "Analysis2", "SHAPESET", [ "Layer 8" ], [ "Phase 8" ], True )
738 copyAnalysisCommand( "Analysis2", "Structural nonlinear 7", "Structural nonlinear 8" )
```

```
734 setAnalysisCommandDetail( "Analysis2", "Structural nonlinear 8", "EXECUT(1)/START/TIME",
    27510 )
735 copyAnalysisCommand( "Analysis2", "Phase 8", "Phase 9" )
736 setActiveInPhase( "Analysis2", "SHAPESET", [ "Layer 9" ], [ "Phase 9" ], True )
737 copyAnalysisCommand( "Analysis2", "Structural nonlinear 8", "Structural nonlinear 9" )
738 setAnalysisCommandDetail( "Analysis2", "Structural nonlinear 9", "EXECUT(1)/START/TIME",
    31440 )
739 copyAnalysisCommand( "Analysis2", "Phase 9", "Phase 10" )
740 setActiveInPhase( "Analysis2", "SHAPESET", [ "Layer 10" ], [ "Phase 10" ], True )
741 copyAnalysisCommand( "Analysis2", "Structural nonlinear 9", "Structural nonlinear 10" )
742 setAnalysisCommandDetail( "Analysis2", "Structural nonlinear 10", "EXECUT(1)/START/TIME",
    35370 )
743 copyAnalysisCommand( "Analysis2", "Phase 10", "Phase 11" )
744 setActiveInPhase( "Analysis2", "SHAPESET", [ "Layer 11" ], [ "Phase 11" ], True )
745 copyAnalysisCommand( "Analysis2", "Structural nonlinear 10", "Structural nonlinear 11" )
746 setAnalysisCommandDetail( "Analysis2", "Structural nonlinear 11", "EXECUT(1)/START/TIME",
    39300 )
747 copyAnalysisCommand( "Analysis2", "Phase 11", "Phase 12" )
748 setActiveInPhase( "Analysis2", "SHAPESET", [ "Layer 12" ], [ "Phase 12" ], True )
749 copyAnalysisCommand( "Analysis2", "Structural nonlinear 11", "Structural nonlinear 12" )
750 setAnalysisCommandDetail( "Analysis2", "Structural nonlinear 12", "EXECUT(1)/START/TIME",
    43230 )
751 copyAnalysisCommand( "Analysis2", "Phase 12", "Phase 13" )
752 setActiveInPhase( "Analysis2", "SHAPESET", [ "Layer 13" ], [ "Phase 13" ], True )
753 copyAnalysisCommand( "Analysis2", "Structural nonlinear 12", "Structural nonlinear 13" )
```



```
754 setAnalysisCommandDetail( "Analysis2", "Structural nonlinear 13", "EXECUT(1)/START/TIME",
47160 )
755 copyAnalysisCommand( "Analysis2", "Phase 13", "Phase 14" )
756 setActiveInPhase( "Analysis2", "SHAPESET", [ "Layer 14" ], [ "Phase 14" ], True )
757 copyAnalysisCommand( "Analysis2", "Structural nonlinear 13", "Structural nonlinear 14" )
758 setAnalysisCommandDetail( "Analysis2", "Structural nonlinear 14", "EXECUT(1)/START/TIME",
51090 )
759 copyAnalysisCommand( "Analysis2", "Phase 14", "Phase 15" )
760 setActiveInPhase( "Analysis2", "SHAPESET", [ "Layer 15" ], [ "Phase 15" ], True )
761 copyAnalysisCommand( "Analysis2", "Structural nonlinear 14", "Structural nonlinear 15" )
762 setAnalysisCommandDetail( "Analysis2", "Structural nonlinear 15", "EXECUT(1)/START/TIME",
55020 )
763 copyAnalysisCommand( "Analysis2", "Phase 15", "Phase 16" )
764 setActiveInPhase( "Analysis2", "SHAPESET", [ "Layer 16" ], [ "Phase 16" ], True )
765 copyAnalysisCommand( "Analysis2", "Structural nonlinear 15", "Structural nonlinear 16" )
766 setAnalysisCommandDetail( "Analysis2", "Structural nonlinear 16", "EXECUT(1)/START/TIME",
58950 )
767 copyAnalysisCommand( "Analysis2", "Phase 16", "Phase 17" )
768 setActiveInPhase( "Analysis2", "SHAPESET", [ "Layer 17" ], [ "Phase 17" ], True )
769 copyAnalysisCommand( "Analysis2", "Structural nonlinear 16", "Structural nonlinear 17" )
770 setAnalysisCommandDetail( "Analysis2", "Structural nonlinear 17", "EXECUT(1)/START/TIME",
62880 )
771 copyAnalysisCommand( "Analysis2", "Phase 17", "Phase 18" )
772 setActiveInPhase( "Analysis2", "SHAPESET", [ "Layer 18" ], [ "Phase 18" ], True )
773 copyAnalysisCommand( "Analysis2", "Structural nonlinear 17", "Structural nonlinear 18" )
```

```
774 setAnalysisCommandDetail( "Analysis2", "Structural nonlinear 18", "EXECUT(1)/START/TIME",
66810 )
775 copyAnalysisCommand( "Analysis2", "Phase 18", "Phase 19" )
776 setActiveInPhase( "Analysis2", "SHAPESET", [ "Layer 19" ], [ "Phase 19" ], True )
777 copyAnalysisCommand( "Analysis2", "Structural nonlinear 18", "Structural nonlinear 19" )
778 setAnalysisCommandDetail( "Analysis2", "Structural nonlinear 19", "EXECUT(1)/START/TIME",
70740 )
779 copyAnalysisCommand( "Analysis2", "Phase 19", "Phase 20" )
780 setActiveInPhase( "Analysis2", "SHAPESET", [ "Layer 20" ], [ "Phase 20" ], True )
781 copyAnalysisCommand( "Analysis2", "Structural nonlinear 19", "Structural nonlinear 20" )
782 setAnalysisCommandDetail( "Analysis2", "Structural nonlinear 20", "EXECUT(1)/START/TIME",
74670 )
783 copyAnalysisCommand( "Analysis2", "Phase 20", "Phase 21" )
784 setActiveInPhase( "Analysis2", "SHAPESET", [ "Layer 21" ], [ "Phase 21" ], True )
785 copyAnalysisCommand( "Analysis2", "Structural nonlinear 20", "Structural nonlinear 21" )
786 setAnalysisCommandDetail( "Analysis2", "Structural nonlinear 21", "EXECUT(1)/START/TIME",
78600 )
787 copyAnalysisCommand( "Analysis2", "Phase 21", "Phase 22" )
788 setActiveInPhase( "Analysis2", "SHAPESET", [ "Layer 22" ], [ "Phase 22" ], True )
789 copyAnalysisCommand( "Analysis2", "Structural nonlinear 21", "Structural nonlinear 22" )
790 setAnalysisCommandDetail( "Analysis2", "Structural nonlinear 22", "EXECUT(1)/START/TIME",
82530 )
791 copyAnalysisCommand( "Analysis2", "Phase 22", "Phase 23" )
792 setActiveInPhase( "Analysis2", "SHAPESET", [ "Layer 23" ], [ "Phase 23" ], True )
793 copyAnalysisCommand( "Analysis2", "Structural nonlinear 22", "Structural nonlinear 23" )
```

```
794 setAnalysisCommandDetail( "Analysis2", "Structural nonlinear 23", "EXECUT(1)/START/TIME",  
86460 )  
795 copyAnalysisCommand( "Analysis2", "Phase 23", "Phase 24" )  
796 setActiveInPhase( "Analysis2", "SHAPESET", [ "Layer 24" ], [ "Phase 24" ], True )  
797 copyAnalysisCommand( "Analysis2", "Structural nonlinear 23", "Structural nonlinear 24" )  
798 setAnalysisCommandDetail( "Analysis2", "Structural nonlinear 24", "EXECUT(1)/START/TIME",  
90390 )  
799 copyAnalysisCommand( "Analysis2", "Phase 24", "Phase 25" )  
800 setActiveInPhase( "Analysis2", "SHAPESET", [ "Layer 25" ], [ "Phase 25" ], True )  
801 copyAnalysisCommand( "Analysis2", "Structural nonlinear 24", "Structural nonlinear 25" )  
802 setAnalysisCommandDetail( "Analysis2", "Structural nonlinear 25", "EXECUT(1)/START/TIME",  
94320 )  
803 copyAnalysisCommand( "Analysis2", "Phase 25", "Phase 26" )  
804 setActiveInPhase( "Analysis2", "SHAPESET", [ "Layer 26" ], [ "Phase 26" ], True )  
805 copyAnalysisCommand( "Analysis2", "Structural nonlinear 25", "Structural nonlinear 26" )  
806 setAnalysisCommandDetail( "Analysis2", "Structural nonlinear 26", "EXECUT(1)/START/TIME",  
98250 )  
807 copyAnalysisCommand( "Analysis2", "Phase 26", "Phase 27" )  
808 setActiveInPhase( "Analysis2", "SHAPESET", [ "Layer 27" ], [ "Phase 27" ], True )  
809 copyAnalysisCommand( "Analysis2", "Structural nonlinear 26", "Structural nonlinear 27" )  
810 setAnalysisCommandDetail( "Analysis2", "Structural nonlinear 27", "EXECUT(1)/START/TIME",  
102180 )  
811 copyAnalysisCommand( "Analysis2", "Phase 27", "Phase 28" )  
812 setActiveInPhase( "Analysis2", "SHAPESET", [ "Layer 28" ], [ "Phase 28" ], True )  
813 copyAnalysisCommand( "Analysis2", "Structural nonlinear 27", "Structural nonlinear 28" )
```

```

814 setAnalysisCommandDetail( "Analysis2", "Structural nonlinear 28", "EXECUT(1)/START/TIME",
    106110 )
815 copyAnalysisCommand( "Analysis2", "Phase 28", "Phase 29" )
816 setActiveInPhase( "Analysis2", "SHAPESET", [ "Layer 29" ], [ "Phase 29" ], True )
817 copyAnalysisCommand( "Analysis2", "Structural nonlinear 28", "Structural nonlinear 29" )
818 setAnalysisCommandDetail( "Analysis2", "Structural nonlinear 29", "EXECUT(1)/START/TIME",
    110040 )
819 copyAnalysisCommand( "Analysis2", "Phase 29", "Phase 30" )
820 setActiveInPhase( "Analysis2", "SHAPESET", [ "Layer 30" ], [ "Phase 30" ], True )
821 copyAnalysisCommand( "Analysis2", "Structural nonlinear 29", "Structural nonlinear 30" )
822 setAnalysisCommandDetail( "Analysis2", "Structural nonlinear 30", "EXECUT(1)/START/TIME",
    113970 )
823
824 setAnalysisCommandDetail( "Analysis2", "Structural nonlinear 1",
    "EXECUT(1)/START/LOAD/PREVIO", False )
825 addAnalysisCommandDetail( "Analysis2", "Structural nonlinear 1", "EXECUT(1)/START/LOAD/ADD" )
826 setAnalysisCommandDetail( "Analysis2", "Structural nonlinear 1", "EXECUT(1)/START/LOAD/ADD",
    True )
827 setAnalysisCommandDetail( "Analysis2", "Structural nonlinear 1",
    "EXECUT(1)/START/LOAD/ADD/LOADNR", 1 )
828
829 setActiveInPhase( "Analysis2", "GEOMETRYSUPPORTSET", [ "Support set 1" ], [ "Phase 21" ],
    True )
830 setActivePhase( "Analysis2", "Phase 22" )
831 setActiveInPhase( "Analysis2", "GEOMETRYSUPPORTSET", [ "Support set 1" ], [ "Phase 22" ],
    True )

```

```
832 setActivePhase( "Analysis2", "Phase 23" )
833 setActiveInPhase( "Analysis2", "GEOMETRYSUPPORTSET", [ "Support set 1" ], [ "Phase 23" ],
True )
834 setActivePhase( "Analysis2", "Phase 24" )
835 setActiveInPhase( "Analysis2", "GEOMETRYSUPPORTSET", [ "Support set 1" ], [ "Phase 24" ],
True )
836 setActivePhase( "Analysis2", "Phase 25" )
837 setActiveInPhase( "Analysis2", "GEOMETRYSUPPORTSET", [ "Support set 1" ], [ "Phase 25" ],
True )
838 setActivePhase( "Analysis2", "Phase 26" )
839 setActiveInPhase( "Analysis2", "GEOMETRYSUPPORTSET", [ "Support set 1" ], [ "Phase 26" ],
True )
840 setActiveInPhase( "Analysis2", "GEOMETRYSUPPORTSET", [ "Support set 2" ], [ "Phase 26" ],
True )
841 setActiveInPhase( "Analysis2", "GEOMETRYCONNECTION", [ "Connection 2" ], [ "Phase 26" ],
True )
842 setActivePhase( "Analysis2", "Phase 27" )
843 setActiveInPhase( "Analysis2", "GEOMETRYSUPPORTSET", [ "Support set 1" ], [ "Phase 27" ],
True )
844 setActiveInPhase( "Analysis2", "GEOMETRYSUPPORTSET", [ "Support set 2" ], [ "Phase 27" ],
True )
845 setActiveInPhase( "Analysis2", "GEOMETRYCONNECTION", [ "Connection 2" ], [ "Phase 27" ],
True )
846 setActivePhase( "Analysis2", "Phase 28" )
847 setActiveInPhase( "Analysis2", "GEOMETRYSUPPORTSET", [ "Support set 2" ], [ "Phase 28" ],
True )
```

```

848 setActiveInPhase( "Analysis2", "GEOMETRYSUPPORTSET", [ "Support set 1" ], [ "Phase 28" ],
True )
849 setActiveInPhase( "Analysis2", "GEOMETRYCONNECTION", [ "Connection 2" ], [ "Phase 28" ],
True )
850 setActivePhase( "Analysis2", "Phase 29" )
851 setActiveInPhase( "Analysis2", "GEOMETRYSUPPORTSET", [ "Support set 1" ], [ "Phase 29" ],
True )
852 setActiveInPhase( "Analysis2", "GEOMETRYSUPPORTSET", [ "Support set 2" ], [ "Phase 29" ],
True )
853 setActiveInPhase( "Analysis2", "GEOMETRYCONNECTION", [ "Connection 2" ], [ "Phase 29" ],
True )
854 setActivePhase( "Analysis2", "Phase 30" )
855 setActiveInPhase( "Analysis2", "GEOMETRYSUPPORTSET", [ "Support set 1" ], [ "Phase 30" ],
True )
856 setActiveInPhase( "Analysis2", "GEOMETRYSUPPORTSET", [ "Support set 2" ], [ "Phase 30" ],
True )
857 setActiveInPhase( "Analysis2", "GEOMETRYCONNECTION", [ "Connection 2" ], [ "Phase 30" ],
True )
858
859 saveAnalysisCommands( "Analysis2", "D:/DIANA/New 1-30 short Analysis2.dcf", 6 )
860
861 exportModel( "D:/DIANA/New 1-30 short wall.dat", 15 )
862 time_per_layer=3930
863 n_layers=30
864 full_time = time_per_layer*n_layers
865 f=open("New 1-30 short wall.dat","a")

```

```

866 f.write("      0-"+str(full_time*2)+"("+str(time_per_layer)+")\n")
867 for i in range(1,n_layers+1):
868     f.write("/ \"Wall "+str(i)+"\" , \"Truss "+str(i)+"\" /\n")
869     f.write("      0("+str(i)+") "+str(time_per_layer)+"-"+str((full_time*2+time_per_layer)-
i*time_per_layer)+"("+str(time_per_layer)+")\n")
870     f.write("      0("+str(n_layers*2+1)+")\n")
871 f.write("'END'\n")
872 f.close()
873
874
875
876 openProject( "D:/DIANA/Test1 short wall.dpf" )
877 remove( "SHAPESET", [ "Layer 1", "Layer 2", "Layer 3", "Layer 4", "Layer 5", "Layer 6",
"Layer 7", "Layer 8", "Layer 9", "Layer 10", "Layer 11", "Layer 12", "Layer 13", "Layer 14",
"Layer 15", "Layer 16", "Layer 17", "Layer 18", "Layer 19", "Layer 20", "Layer 21", "Layer
22", "Layer 23" ] )
878 setCurrentShapeSet( "Layer 24" )
879 removeAnalysis( "Analysis2" )
880 rename( "SHAPESET", "Layer 24", "Layer 1" )
881 setCurrentShapeSet( "Layer 25" )
882 rename( "SHAPESET", "Layer 25", "Layer 2" )
883 setCurrentShapeSet( "Layer 26" )
884 rename( "SHAPESET", "Layer 26", "Layer 3" )
885 setCurrentShapeSet( "Layer 27" )
886 rename( "SHAPESET", "Layer 27", "Layer 4" )
887 setCurrentShapeSet( "Layer 28" )

```

```

888 rename( "SHAPESET", "Layer 28", "Layer 5" )
889 setCurrentShapeSet( "Layer 29" )
890 rename( "SHAPESET", "Layer 29", "Layer 6" )
891 setCurrentShapeSet( "Layer 30" )
892 rename( "SHAPESET", "Layer 30", "Layer 7" )
893 createSheet( "Sheet 1", [ [ 0, 0, 2.3 ], [ 0.6, 0, 2.3 ], [ 0.6, 0.2, 2.3 ], [ 0, 0.2,
2.3 ] ] )
894 createSheet( "Sheet 2", [ [ 0, 0.2, 2.3 ], [ 0.2, 0.2, 2.3 ], [ 0.2, 1, 2.3 ], [ 0, 1,
2.3 ] ] )
895 healAndSew( [ "Sheet 1", "Sheet 2" ], 1e-05, {} )
896 moveToShapeSet( [ "Sheet 1" ], "Layer 1" )
897 setCurrentShapeSet( "Layer 1" )
898 healAndSew( [ "Wall 24", "Sheet 1" ], 1e-05, {} )
899 remove( "GEOMETRYSUPPORT", [ "Support 4" ] )
900 remove( "GEOMETRYSUPPORT", "Support 5" )
901 createSurfaceSupport( "Support 5", "Support set 3" )
902 setParameter( "GEOMETRYSUPPORT", "Support 5", "AXES", [ 1, 2 ] )
903 setParameter( "GEOMETRYSUPPORT", "Support 5", "TRANSL", [ 1, 1, 1 ] )
904 setParameter( "GEOMETRYSUPPORT", "Support 5", "ROTATI", [ 0, 0, 0 ] )
905 attach( "GEOMETRYSUPPORT", "Support 5", "Wall 24", [ [ 0.3441438, 0.1147146, 2.3 ],
[ 0.1147146, 0.6588584, 2.3 ] ] )
906 remove( "GEOMETRYSUPPORT", "Support 6" )
907 createLineSupport( "Support 6", "Support set 3" )
908 setParameter( "GEOMETRYSUPPORT", "Support 6", "AXES", [ 1, 2 ] )
909 setParameter( "GEOMETRYSUPPORT", "Support 6", "TRANSL", [ 1, 1, 1 ] )
910 setParameter( "GEOMETRYSUPPORT", "Support 6", "ROTATI", [ 0, 0, 0 ] )

```



```

911 attach( "GEOMETRYSUPPORT", "Support 6", "Truss 24", [ [ 0.5, 0.1, 2.3 ], [ 0.3, 0.1, 2.3 ],
    [ 0.1, 0.3, 2.3 ], [ 0.1, 0.5, 2.3 ], [ 0.1, 0.7, 2.3 ], [ 0.1, 0.9, 2.3 ] ] )
912 attach( "GEOMETRYSUPPORT", "Support 6", "Wall 24", [ [ 0.1, 1, 2.3 ], [ 0, 0.6, 2.3 ], [ 0.2,
    0.6, 2.3 ], [ 0, 0.1, 2.3 ], [ 0.3, 0, 2.3 ], [ 0.4, 0.2, 2.3 ], [ 0.6, 0.1, 2.3 ] ] )
913 rename( "GEOMETRYSUPPORT", "Support 5", "Support 4" )
914 rename( "GEOMETRYSUPPORT", "Support 6", "Support 5" )
915 show( "GEOMETRYCONNECTION", [ "Connection 2" ] )
916 hide( "GEOMETRYCONNECTION", [ "Connection 2" ] )
917 showLocalAxes( "GEOMETRYCONNECTION", True )
918 showLocalAxes( "GEOMETRYCONNECTION", False )
919 createConnection( "Connection 1", "BOUNDARY", "SHAPEEDGE" )
920 setParameter( "GEOMETRYCONNECTION", "Connection 1", "MODE", "CLOSED" )
921 setElementClassType( "GEOMETRYCONNECTION", "Connection 1", "SHLLIF" )
922 assignMaterial( "interf_mat", "GEOMETRYCONNECTION", "Connection 1" )
923 assignGeometry( "Element geometry 1", "GEOMETRYCONNECTION", "Connection 1" )
924 assignElementData( "Element data 1", "GEOMETRYCONNECTION", "Connection 1" )
925 setParameter( "GEOMETRYCONNECTION", "Connection 1", "FLIP", False )
926 attach( "GEOMETRYSUPPORT", "Support 5", "Truss 24", [ [ 0.5, 0.1, 2.3 ], [ 0.3, 0.1, 2.3 ],
    [ 0.1, 0.3, 2.3 ], [ 0.1, 0.5, 2.3 ], [ 0.1, 0.7, 2.3 ], [ 0.1, 0.9, 2.3 ] ] )
927 attach( "GEOMETRYSUPPORT", "Support 5", "Wall 24", [ [ 0.3, 0, 2.3 ], [ 0.6, 0.1, 2.3 ],
    [ 0.4, 0.2, 2.3 ], [ 0, 0.1, 2.3 ], [ 0, 0.6, 2.3 ], [ 0.1, 1, 2.3 ], [ 0.2, 0.6, 2.3 ] ] )
928 attachTo( "GEOMETRYCONNECTION", "Connection 1", "SOURCE", "Truss 24", [ [ 0.5, 0.1, 2.3 ] ] )
929 attachTo( "GEOMETRYCONNECTION", "Connection 1", "SOURCE", "Truss 24", [ [ 0.3, 0.1, 2.3 ] ] )
930 attachTo( "GEOMETRYCONNECTION", "Connection 1", "SOURCE", "Truss 24", [ [ 0.1, 0.3, 2.3 ] ] )
931 attachTo( "GEOMETRYCONNECTION", "Connection 1", "SOURCE", "Truss 24", [ [ 0.1, 0.5, 2.3 ] ] )
932 attachTo( "GEOMETRYCONNECTION", "Connection 1", "SOURCE", "Truss 24", [ [ 0.1, 0.7, 2.3 ] ] )

```

```

933 attachTo( "GEOMETRYCONNECTION", "Connection 1", "SOURCE", "Truss 24", [ [ 0.1, 0.9, 2.3 ] ] )
934 attachTo( "GEOMETRYCONNECTION", "Connection 1", "SOURCE", "Wall 24", [ [ 0.3, 0, 2.3 ] ] )
935 attachTo( "GEOMETRYCONNECTION", "Connection 1", "SOURCE", "Wall 24", [ [ 0.6, 0.1, 2.3 ] ] )
936 attachTo( "GEOMETRYCONNECTION", "Connection 1", "SOURCE", "Wall 24", [ [ 0.4, 0.2, 2.3 ] ] )
937 attachTo( "GEOMETRYCONNECTION", "Connection 1", "SOURCE", "Wall 24", [ [ 0, 0.1, 2.3 ] ] )
938 attachTo( "GEOMETRYCONNECTION", "Connection 1", "SOURCE", "Wall 24", [ [ 0, 0.6, 2.3 ] ] )
939 attachTo( "GEOMETRYCONNECTION", "Connection 1", "SOURCE", "Wall 24", [ [ 0.1, 1, 2.3 ] ] )
940 attachTo( "GEOMETRYCONNECTION", "Connection 1", "SOURCE", "Wall 24", [ [ 0.2, 0.6, 2.3 ] ] )
941 hide( "GEOMETRYCONNECTION", [ "Connection 1" ] )
942 generateMesh( [] )
943 addAnalysis( "Analysis2" )
944 addAnalysisCommand( "Analysis2", "PHASE", "Phase" )
945 renameAnalysisCommand( "Analysis2", "Phase", "Phase 1" )
946 setActiveInPhase( "Analysis2", "SHAPESET", [ "Layer 2" ], [ "Phase 1" ], False )
947 setActiveInPhase( "Analysis2", "SHAPESET", [ "Layer 3" ], [ "Phase 1" ], False )
948 setActiveInPhase( "Analysis2", "SHAPESET", [ "Layer 4" ], [ "Phase 1" ], False )
949 setActiveInPhase( "Analysis2", "SHAPESET", [ "Layer 5" ], [ "Phase 1" ], False )
950 setActiveInPhase( "Analysis2", "SHAPESET", [ "Layer 6" ], [ "Phase 1" ], False )
951 setActiveInPhase( "Analysis2", "SHAPESET", [ "Layer 7" ], [ "Phase 1" ], False )
952 addAnalysisCommand( "Analysis2", "NONLIN", "Structural nonlinear" )
953 renameAnalysisCommand( "Analysis2", "Structural nonlinear", "Structural nonlinear 1" )
954 addAnalysisCommandDetail( "Analysis2", "Structural nonlinear 1", "TYPE/GEOMET" )
955 setAnalysisCommandDetail( "Analysis2", "Structural nonlinear 1", "TYPE/GEOMET", True )
956 setAnalysisCommandDetail( "Analysis2", "Structural nonlinear 1", "EXECUT(1)/EXETYP",
"START" )

```

```

957 setAnalysisCommandDetail( "Analysis2", "Structural nonlinear 1", "EXECUT(1)/START/STEPS",
    False )
958 setAnalysisCommandDetail( "Analysis2", "Structural nonlinear 1", "EXECUT/EXETYP", "TIME" )
959 setAnalysisCommandDetail( "Analysis2", "Structural nonlinear 1", "EXECUT(2)/ITERAT/MAXITE",
    10 )
960 setAnalysisCommandDetail( "Analysis2", "Structural nonlinear 1", "EXECUT(2)/ITERAT/MAXITE",
    10 )
961 setAnalysisCommandDetail( "Analysis2", "Structural nonlinear 1",
    "EXECUT(2)/TIME/STEPS/EXPLIC/SIZES", "3930.00000" )
962 setAnalysisCommandDetail( "Analysis2", "Structural nonlinear 1", "EXECUT(2)/ITERAT/MAXITE",
    50 )
963 addAnalysisCommandDetail( "Analysis2", "Structural nonlinear 1", "EXECUT(2)/ITERAT/LINESE" )
964 setAnalysisCommandDetail( "Analysis2", "Structural nonlinear 1", "EXECUT(2)/ITERAT/LINESE",
    True )
965 setAnalysisCommandDetail( "Analysis2", "Structural nonlinear 1",
    "EXECUT(2)/ITERAT/CONVER/SIMULT", True )
966 setAnalysisCommandDetail( "Analysis2", "Structural nonlinear 1",
    "EXECUT(2)/ITERAT/CONVER/DISPLA/NOCONV", "CONTIN" )
967 setAnalysisCommandDetail( "Analysis2", "Structural nonlinear 1",
    "EXECUT(2)/ITERAT/CONVER/FORCE/NOCONV", "TERMIN" )
968 setAnalysisCommandDetail( "Analysis2", "Structural nonlinear 1",
    "EXECUT(2)/ITERAT/CONVER/FORCE/NOCONV", "CONTIN" )
969 setAnalysisCommandDetail( "Analysis2", "Structural nonlinear 1", "OUTPUT(1)/SELTYP", "USER" )
970 addAnalysisCommandDetail( "Analysis2", "Structural nonlinear 1", "OUTPUT(1)/USER" )
971 addAnalysisCommandDetail( "Analysis2", "Structural nonlinear 1", "OUTPUT(1)/USER/DISPLA" )

```

```
972 addAnalysisCommandDetail( "Analysis2", "Structural nonlinear 1",  
"OUTPUT (1) /USER/DISPLA (2) /TOTAL/TRANSL/AXIAL" )  
973 addAnalysisCommandDetail( "Analysis2", "Structural nonlinear 1",  
"OUTPUT (1) /USER/MATURI (1) /TOTAL" )  
974 addAnalysisCommandDetail( "Analysis2", "Structural nonlinear 1",  
"OUTPUT (1) /USER/PARAME (1) /YOUNG" )  
975 addAnalysisCommandDetail( "Analysis2", "Structural nonlinear 1",  
"OUTPUT (1) /USER/PARAME (2) /COMSTR" )  
976 addAnalysisCommandDetail( "Analysis2", "Structural nonlinear 1",  
"OUTPUT (1) /USER/STRESS (1) /TOTAL/PIOLAK/PRINCI" )  
977 setAnalysisCommandDetail( "Analysis2", "Structural nonlinear 1",  
"OUTPUT (1) /USER/STRESS (1) /TOTAL/PIOLAK/PRINCI/LOCATI", "INTPNT" )  
978 addAnalysisCommandDetail( "Analysis2", "Structural nonlinear 1",  
"OUTPUT (1) /USER/STRAIN (1) /TOTAL/GREEN/PRINCI" )  
979 setAnalysisCommandDetail( "Analysis2", "Structural nonlinear 1",  
"OUTPUT (1) /USER/STRAIN (1) /TOTAL/GREEN/PRINCI/LOCATI", "INTPNT" )  
980 addAnalysisCommandDetail( "Analysis2", "Structural nonlinear 1",  
"OUTPUT (1) /USER/STRESS (2) /TOTAL/TRACTI/LOCAL" )  
981 addAnalysisCommandDetail( "Analysis2", "Structural nonlinear 1",  
"OUTPUT (1) /USER/STRAIN (2) /TOTAL/TRACTI/LOCAL" )  
982 addAnalysisCommandDetail( "Analysis2", "Structural nonlinear 1",  
"OUTPUT (1) /USER/STRAIN (3) /CRKWDT/GREEN/PRINCI" )  
983 setAnalysisCommandDetail( "Analysis2", "Structural nonlinear 1",  
"OUTPUT (1) /USER/STRAIN (3) /CRKWDT/GREEN/PRINCI/LOCATI", "INTPNT" )  
984 setActivePhase( "Analysis2", "Phase 1" )  
985 copyAnalysisCommand( "Analysis2", "Phase 1", "Phase 2" )
```

```
986 setActiveInPhase( "Analysis2", "SHAPESET", [ "Layer 2" ], [ "Phase 2" ], True )
987 copyAnalysisCommand( "Analysis2", "Structural nonlinear 1", "Structural nonlinear 2" )
988 setAnalysisCommandDetail( "Analysis2", "Structural nonlinear 2", "EXECUT(1)/START/TIME",
3930 )
989 copyAnalysisCommand( "Analysis2", "Phase 2", "Phase 3" )
990 setActiveInPhase( "Analysis2", "SHAPESET", [ "Layer 3" ], [ "Phase 3" ], True )
991 copyAnalysisCommand( "Analysis2", "Structural nonlinear 2", "Structural nonlinear 3" )
992 setAnalysisCommandDetail( "Analysis2", "Structural nonlinear 3", "EXECUT(1)/START/TIME",
7860 )
993 copyAnalysisCommand( "Analysis2", "Phase 3", "Phase 4" )
994 setActiveInPhase( "Analysis2", "SHAPESET", [ "Layer 4" ], [ "Phase 4" ], True )
995 copyAnalysisCommand( "Analysis2", "Structural nonlinear 3", "Structural nonlinear 4" )
996 setAnalysisCommandDetail( "Analysis2", "Structural nonlinear 4", "EXECUT(1)/START/TIME",
11790 )
997 copyAnalysisCommand( "Analysis2", "Phase 4", "Phase 5" )
998 setActiveInPhase( "Analysis2", "SHAPESET", [ "Layer 5" ], [ "Phase 5" ], True )
999 copyAnalysisCommand( "Analysis2", "Structural nonlinear 4", "Structural nonlinear 5" )
1000 setAnalysisCommandDetail( "Analysis2", "Structural nonlinear 5", "EXECUT(1)/START/TIME",
15720 )
1001 copyAnalysisCommand( "Analysis2", "Phase 5", "Phase 6" )
1002 setActiveInPhase( "Analysis2", "SHAPESET", [ "Layer 6" ], [ "Phase 6" ], True )
1003 copyAnalysisCommand( "Analysis2", "Structural nonlinear 5", "Structural nonlinear 6" )
1004 setAnalysisCommandDetail( "Analysis2", "Structural nonlinear 6", "EXECUT(1)/START/TIME",
19650 )
1005 copyAnalysisCommand( "Analysis2", "Phase 6", "Phase 7" )
1006 setActiveInPhase( "Analysis2", "SHAPESET", [ "Layer 7" ], [ "Phase 7" ], True )
```

```

1007 copyAnalysisCommand( "Analysis2", "Structural nonlinear 6", "Structural nonlinear 7" )
1008 setAnalysisCommandDetail( "Analysis2", "Structural nonlinear 7", "EXECUT(1)/START/TIME",
23580 )
1009 setAnalysisCommandDetail( "Analysis2", "Structural nonlinear 1",
"EXECUT(1)/START/LOAD/PREVI", False )
1010 addAnalysisCommandDetail( "Analysis2", "Structural nonlinear 1", "EXECUT(1)/START/LOAD/ADD" )
1011 setAnalysisCommandDetail( "Analysis2", "Structural nonlinear 1", "EXECUT(1)/START/LOAD/ADD",
True )
1012 setAnalysisCommandDetail( "Analysis2", "Structural nonlinear 1",
"EXECUT(1)/START/LOAD/ADD/LOADNR", 1 )
1013 setActivePhase( "Analysis2", "" )
1014 setActivePhase( "Analysis2", "Phase 1" )
1015 setActiveInPhase( "Analysis2", "GEOMETRY SUPPORTSET", [ "Support set 2" ], [ "Phase 1" ],
False )
1016 setActiveInPhase( "Analysis2", "GEOMETRY SUPPORTSET", [ "Support set 1" ], [ "Phase 1" ],
False )
1017 setActivePhase( "Analysis2", "Phase 2" )
1018 setActiveInPhase( "Analysis2", "GEOMETRY SUPPORTSET", [ "Support set 1" ], [ "Phase 2" ],
False )
1019 setActiveInPhase( "Analysis2", "GEOMETRY SUPPORTSET", [ "Support set 2" ], [ "Phase 2" ],
False )
1020 setActivePhase( "Analysis2", "Phase 1" )
1021 setActivePhase( "Analysis2", "Phase 2" )
1022 setActivePhase( "Analysis2", "Phase 3" )
1023 setActivePhase( "Analysis2", "Phase 1" )

```

```
1024 setActiveInPhase( "Analysis2", "GEOMETRYCONNECTION", [ "Connection 2" ], [ "Phase 1" ],  
    False )  
1025 setActivePhase( "Analysis2", "Phase 2" )  
1026 setActiveInPhase( "Analysis2", "GEOMETRYCONNECTION", [ "Connection 2" ], [ "Phase 2" ],  
    False )  
1027 setActivePhase( "Analysis2", "Phase 3" )  
1028 setActivePhase( "Analysis2", "Phase 2" )  
1029 setActivePhase( "Analysis2", "" )  
1030 saveAnalysisCommands( "Analysis2", "D:/DIANA/Test1 short wall Analysis2.dcf", 6 )  
1031 exportModel( "D:/DIANA/Test1 short wall.dat", 15 )  
1032 closeProject( )
```